Design and Synthesis of Safer Chemicals by Benign Green Routes

Thesis submitted to

INSTITUTE OF CHEMICAL TECHNOLOGY, MUMBAI

for the award of the degree of

DOCTOR OF PHILOSOPHY (SCIENCE)

In the

CHEMISTRY

by

Jayaram Molleti

under the supervision of

Professor (Dr.) Ganapati D. Yadav,

FTWAS, FNA,FNASc, FRSC (UK), FIChemE (UK)

Department of Chemical Engineering
Institute of Chemical Technology, Mumbai
(University under Section 3 of UGC Act 1956;
Elite Status and Centre of Excellence, Government of Maharashtra)
Maharashtra, India

July 2017

DECLARATION BY THE CADIDATE AS PER ORDINANCE…..

I hereby declare, as per Ordinance relating to the Degree of Doctor of Philosophy, that –

(1) The thesis entitled "**Design and Synthesis of Safer Chemicals by Benign Green routes**" submitted by me for the degree of Doctor of Philosophy (Science) is the record of the research work carried out by me during the period from September 2011 to April 2017 under the guidance of my research guide Professor (Dr.) Ganapati D. Yadav.

(2) The work is original and whenever I have used materials (data, theoretical analyses, figures, text, etc.) from other sources, I have given due credit to them by citing them in the text of the thesis. Further, I have taken permission from the copyright owners of the sources, whenever necessary.

(3) The work embodied in the thesis has not been submitted to this or any other University or Institute for the award of any degree, diploma, or certificate.

(4) I have followed the guidelines of the Institute in preparing the thesis. I have conformed to the norms and guidelines given in the Ethical Code of Conduct of the Institute, including the policy of plagiarism.

(5) I hereby grant to the university and its agents the non-exclusive license to archive and make accessible, my thesis, in whole in all forms of media, now or hereafter known.

(6) I have followed all safety norms and labelled all the chemicals synthesized in the laboratory which have been either consumed or stored in appropriate place with the knowledge of research supervisor/guide and mentioned in the inventory of chemicals.

(7) I had no accident, major or minor, during laboratory work. If any incident had taken place, whether in my work place or adjacent laboratory, it was properly reported to the supervisor and safety committee to prevent occurrence of incident/accident of that kind.

Date: 22/06/2017 **Jayaram Molleti**
(Registration No. 11CHY4011)

Date: 22/06/2017 **Prof. (Dr.) Ganapati D. Yadav**

CERTIFICATE OF RESEARCH GUIDE

This is to certify that the thesis titled "*Design and Synthesis of Safer Chemicals by Benign Green routes*" submitted by *Mr. Jayaram Molleti* to the Institute of Chemical Technology, Mumbai, for the degree of "*Doctor of Philosophy (Science) in Chemistry*" is a bonafide record of the research work carried out by him in the Department of Chemical Engineering, Institute of Chemical Technology, Mumbai, under my supervision. *Mr. Jayaram Molleti* has worked under my guidance on this topic from September 2011 till April 2017.

a. The results embodied in this thesis have not been submitted to any other University or Institute for the award of any degree, diploma, or certificate.
b. The thesis has resulted in to 3 publications which have been cited in this thesis and a few are likely to be published where a citation will be given to this thesis and it will be mentioned in the cover letter to the editor to avoid charges of plagiarism of my own work.

The thesis, in my opinion, is worthy of consideration for the award of the degree "Doctor of Philosophy (Science) in Chemistry "in accordance with the Rules and Regulations of this University.

Date : 22/06/2017
Research Supervisor: Professor (Dr.) Ganapati D. Yadav
Affiliation : Institute of Chemical Technology, Mumbai,
Maharashtra, India.

ACKNOWLEDGEMENT

I would like to sincerely acknowledge the following for their valuable help during my research work:

- Professor (Dr.) Ganapati D. Yadav for his belief in me, constant support, advice and crucial contribution towards this research work.
- Professor (Dr.) Ganapati D. Yadav (Vice Chancellor, ICT, Mumbai) for providing all the facilities to work.
- UGC-NET, India for providing financial assistance.
- I pay my due respect and sincere regards to my family, my labmates, whose love, blessing, encouragement and belief are always with me for the accomplishments that I had so far and going to have in future.

JAYARAM MOLLETI

CONTENTS

List of Figures

List of Tables

List of Abbreviations

GC	Gas Chromatography
GC-MS	Gas Chromatography-Mass Spectrometry
FT-IR	Fourier Transform Infra-Red
BET	Brunauer-Emmett-Teller Surface area analyzer
XRD	X-ray Diffraction
EDXS	Energy Dispersive X-ray Spectroscopy
FEG-SEM	Field Emission Gun-Scanning Electron Microscopy
TPD	Temperature-programmed desorption
TEM	Transmission Electron Microscopy
ICP-AES	Inductively Coupled Plasma Atomic Emission Spectroscopy
TGA	Thermo Gravimetric Analysis
DSC	Differential Scanning Colorimeter
HT	Hydrotalcite
CHT	Calcined Hydrotalcite
MEGPE	Mono-Ethylene Glycol Phenyl Ether
LDH	Layered Double Hydroxide
LA	Levulinic Acid
GVL	γ-Valerolactone
OMS-2	Octahedral Molecular Sieves
PAN	Phenyl Acetonitrile
DMC	Dimethyl Carbonate
2-PPN	2-Phenylpropionitrile
PTC	Phase Transfer Catalysts
SZ	Sulfated Zirconia
SFZ	Sulfated Iron Zirconia
LHHW	Langmuir-Hinshelwood-Hougen-Watson

Nomenclature

$\mathbf{A}_S$	Chemisorbed reactant A
B_S	Chemisorbed reactant B
C	product species
S	Vacant site
C_A	Concentration of reactant A, in mol/cm^3
C_B	Concentration of reactant B, mol/cm^3
C_{A0}	initial concentration of reactant A in bulk liquid phase, mol/cm^3
C_{B0}	initial concentration of reactant B in bulk liquid phase, mol/cm^3
C_{BS}	concentration of reactant B at solid surface, mol/cm^3
C_c	concentration of product, mol/cm^3
C_{CS}	concentration of product at solid surface, mol/cm^3
C_S	concentration of vacant sites, mol/cm^3
C_T	total concentration of sites, mol/cm^3
k_{R2}	reaction rate constant, cm^6 g-cat mol^{-1}s^{-1}
k_1	pseudo-first-order rate constant, s^{-1}
K_i	adsorption equilibrium constant for species i, cm_3/mol
W	product species, methanol
w	catalyst loading g/cm^3 of the liquid volume
X_A	fractional conversion of reactant A
$-r_A$	rate of reaction of A, mol cm^{-3} s^{-1}

Abstract

Catalysis is one of the principles of green chemistry which is in combination with other principles can be used to develop the atom economical green processes. It plays a vital role in the production of wide variety of products, which are having applications in drugs, plastics, agrochemicals, perfumery, detergents, food, clothing, fuels etc. In addition to these, it plays an important role in the balance of ecology and environment by providing cleaner alternative routes to stoichiometric technologies. The present work aims at a selective synthesis of the organic molecules used as intermediates in various industries by using various solid acid and metal catalysts. Different catalysts were synthesized by using methods developed in our laboratory method and reported elsewhere in the literature. Hydroxyalkoxylation of phenol and ethylene carbonate was catalyzed by calcined hydrotalcite. γ-valerolactone was synthesized from levulinic acid catalyzed by Ru supported on octahedral molecular sieves. Potassium promoted La-Mg catalyzed synthesis of 2-phenyl propionitrile from phenylacetonitrile was studied. Veratraldehyde was synthesized from vanillin and dimethyl carbonate catalyzed by potassium promoted La-Mg. Sulfated iron zirconia was used as catalyst for esterification of salicylic acid.

Classification: Heterogeneous catalysis, Sustainability, Green Chemistry

Keywords: Esterification, Catalyst support, Kinetics, O-methylation, Hydrotalcite, Fine chemicals

CHAPTER 1

INTRODUCTION

1.1 Preamble

Catalysis is an important interdisciplinary scientific and technological area for the development of environmentally benign chemical processes. Homogeneous catalysts are difficult to recover, reuse and generally require neutralization process. To overcome drawbacks of homogeneous catalysts heterogeneous catalysts have been used to develop green processes [1,2]. Considering the new environmental regulations and amendments, the Green chemistry and engineering concepts were introduced in order to define exactly what the needs of future industries and processes are [3,4]. It consists of 12 different principles which can easily be found in several articles. Amongst the 12 different principles such as catalysis, process intensification, atom efficient process, waste minimization, use of renewable resources etc. are few well-practiced principles.

Green Chemistry comprises designing, development and execution of chemical products and processes to decrease or remove the use and generation of hazardous substances. It is an innovative, non–regulatory, economically driven approach toward sustainability. Sustainable development is now accepted by governments, industry and the public as a necessary goal of achieving the desired combination of environmental, economic and societal objectives. The release of harmful chemicals into the environment must be minimized or, preferably, completely eliminated. It should be an endeavor to use renewable resources and extend the strength and recyclability of products in an economical way [3].

In recent years, classical organic transformations using solid acid-base catalysts continue to attract considerable attention in both industrial and academic laboratories because of the potential of such technologies to simplify processing and improving the economics of such reactions, thus converting them into green processes [5].

1.2 Research Strategy

Owing to the growing importance of heterogeneous catalysts in organic synthesis, it was thought worthwhile to study synthesize various heterogeneous catalysts and their suitable applications in fine chemical and intermediates synthesis. Therefore, the synthesis and characterization of catalysts, both reported and new, was considered to be an area of immense potential.

Thus, a general theme with the following specific objectives was planned, under the aegis of the current work. The following reaction systems were planned:

1. Selectivity engineering in hydroxyalkoxylation of phenol by ethylene carbonate using calcined hydrotalcite
2. Novel synthesis of Ru supported on OMS by solvent-free method: Highly active catalyst for selective hydrogenation of levulinic acid to γ-valerolactone in aqueous medium
3. Potassium modified La-Mg mixed oxide: selective mono-methylation of phenylacetonitrile with dimethyl carbonate
4. Green synthesis of veratraldehyde using potassium promoted lanthanum-magnesium mixed oxide catalyst
5. Solvent-free synthesis of methyl salicylate using combustion synthesized novel sulfated iron-zirconia catalyst

1.3 Organization of Thesis

Chapter 1 is the introduction to the thesis depicting plan.

Chapter 2 gives a glimpse of some of the useful trends and application of various forms of catalysts for the selective synthesis. Also, it includes the literature related to acid, base and metal catalysts designing and synthesis.

Chapter 3 is about the application of calcined hydrotalcite as a heterogeneous catalyst for the selective hydroxyalkoxylation of phenol by ethylene carbonate. It also accounts the different characterization method to understand the nature of the catalyst and systematic study of various reaction parameters to derive a mathematical model useful for kinetic data analysis.

Chapter 4 consists of the selective hydrogenation levulinic acid to γ-valerolactone in an aqueous medium over novel synthesis of Ru supported on OMS by the solvent-free method. The catalyst was characterized by different techniques. Also, a mathematical model was developed to understand the kinetics of the reaction**.**

Chapter 5 describes the synthesis of novel potassium modified La-Mg mixed oxide catalyst and its application to the selective mono-methylation of phenylacetonitrile with dimethyl carbonate. The catalyst was characterized by using different methods and a mathematical model was developed based on experimental data.

Chapter 6 deals with the green synthesis of veratraldehyde using potassium promoted lanthanum-magnesium mixed oxide catalyst and its characterization by using different methods. The catalyst is highly active and selective.

Chapter 7 covers the esterification of salicylic acid with dimethyl carbonate under solvent free condition. A novel combustion synthesized sulfated iron-zirconia catalyst was developed to get better activity and selectivity as compared to reported literature**.**

Chapter 8 presents a summary of significant contributions made under the aegis of present dissertation followed by the scope of future work and outlook.

1.4 Summary

This work dealt with the synthesis, characterization and application of novel catalysts such as ruthenium supported on octahedral molecular sieves (OMS), potassium supported on La-Mg mixed oxide, and sulfated ferrous zirconia. Several catalysts were synthesized and evaluated in each reaction studied. The catalysts were fully characterized and used in the synthesis of value-added products. For the synthesis phenoxyethanol from phenol and ethylene carbonate, calcined hydrotalcite catalyst was found to be highly active and robust. γ-Valerolactone was synthesized by the aqueous phase hydrogenation of biomass-derived levulinic acid using Ru supported on OMS. Selective mono-methylation of phenylacetonitrile was catalyzed by potassium modified La-Mg mixed oxide. Veratraldehyde was synthesized from vanillin and dimethyl carbonate catalyzed by potassium modified La-Mg mixed oxide. Sulfated iron-zirconia catalyst was used as a catalyst for esterification of salicylic acid. These reactions are of great industrial importance. Detailed mechanistic and kinetic aspects have been discussed in all cases.

CHAPTER 2

GENERAL LITERATURE SEARCH

2.1 Introduction

Synthesis of safer chemicals using catalytic systems is the ultimate goal of present thesis. It includes the use of heterogeneous acid, metal and combination of both to make a multifunctional catalytic system. There are various types of catalysts that have been employed to get a selective and efficient synthesis of various products. In this chapter attempts have been made to cover the difference between homogeneous and heterogeneous catalysis, use of acid catalysts, basically sulfated iron-zirconia mixed oxide, use of metal catalysts in the hydrogenation reaction, use of base catalysts.

2.2 Homogeneous vs. Heterogeneous Catalysis

In the chemical industry, use of catalysts has resulted to get the most from available resources in different areas such as pharmaceutical, polymer, petroleum, etc. [6]. Based on the phase of catalyst present in the reaction mixture, they are classified as a homogeneous and heterogeneous catalyst. Homogeneous catalysts are present in the same phase as that of reaction mixture which is generally liquid. Various chemicals and fine chemical industries are based on the use of homogeneous catalysis as it gives a very selective product and is cheaper. However, it has a drawback such as product contamination and separation difficulties from the reaction mixture. Homogeneous catalysts are used in stoichiometric quantities and are at times difficult to handle, corrosive in nature, which increases the capital and processing cost and decreases the process equipment life [7]. There is no control of the reaction, by-product formation; also, reusability and regeneration of catalyst are major concerns. It decreases the process efficacy. The effluent stream containing harmful acids need neutralization and presence of heavy metals make post processing difficult, cumbersome and costly. A possible answer is immobilization of the catalytic material and efforts are being taken to heterogenize the homogeneous catalysts.

Heterogeneous catalysis, in particular, addresses the goals of Green Chemistry by providing the ease of separation of product and catalyst, thereby eliminating the need for separation through distillation or extraction of the catalyst. Indeed, several different modes of operation and reactor configuration to increase process efficiency and intensification become possible. Solid acid catalyst is such an example which replaces homogeneous catalyst like H_2SO_4, HF, $AlCl_3$, etc. completely from petrochemical industry and is beginning to impact non-petrochemical industries [6]. The use of heterogeneous solid catalysts being in a different phase than the reagents and products has an obvious advantage in terms of easy separation from the reaction mixture, allowing the recovery of the solid

and eventually its reuse, provided that the solid catalyst is not deactivated during the course of the reaction. The development of selective and reusable solid catalysts for organic reactions has been a very active area of research [8]. Thus, in addition to easy separation [9–11], the use of insoluble solid catalysts has the extra bonus of minimizing wastes derived from catalyst separation and disposal, fulfilling the principle of recyclability. In addition, solid catalysts allow the design of continuous flow processes that are economically very attractive at the industrial scale. A scientifically rewarding methodology could, therefore, be to transform a successful homogeneous catalyst into a heterogeneous solid catalyst. The simplest strategy to perform this task is by supporting the soluble metallic complex on the surface of an insoluble solid [12–15]. Our lab has been instrumental in developing various heterogeneous catalysts including UDCaT series of novel solid acid catalysts which can be employed in many industrially important chemical processes [16–21].

2.3 Solid Acid Catalyst

A general trend in catalysis is to transform a successful homogeneous catalyst into a heterogeneous catalytic system [22,23]. Solid acids and, in particular, zeolites have contributed immensely to the development of cost-effective refinery processes such as cracking, isomerization, oligomerization, cyclization, etc., [7–9] but their commercial applications in organic synthesis are rather limited. Some important solids such as heteropoly acid, clays, ion exchange resins, modified metal oxides, mesoporous materials (MCM-41, SBA-15, HMS) etc. have been studied vociferously in a number of industrial reactions [7,24]. However, the main focus was given on the application of sulfated iron-zirconia as a solid acid catalyst for synthesis.

2.3.1 Sulfated iron-zirconia mixed oxide as super acid

Metal oxides exhibit super acidity when they are modified or promoted with sulfate ions. Thus, there has been a rapid progress on the development of sulfate promoted metal oxides such as ZrO_2, TiO_2, SnO_2, Fe_2O_3, HfO_2, etc. [20,25]. Amongst them, surface of zirconium oxide is known to possess all these catalytic activities. Zirconium oxide or zirconia when modified with anions, such as sulfate ions, forms a solid super acid catalyst exhibiting a high activity to catalyze many reactions [25,26]. It has been widely used to catalyze reactions such as hydrocarbon isomerization, alkylation, acylation, esterification, etherification, condensation, etc. [26–30] . Thus, sulfated zirconia (S-ZrO_2) and its variants

form an important class of catalysts as is evident from the voluminous research that has appeared in the last decade. Moreover, these catalysts show a promising future in that they can provide environmentally clean processes for the chemical industry of this eco-friendly era.

The S-ZrO_2 behaves as a solid super acid, depending on its method of preparation and activation. A considerable amount of debate is centered on the application of the term super acid to the S-ZrO_2 catalysts. Umansky et al.[27] suggested that S-ZrO_2 does not fall in the family of super acids since its acidity is not stronger than that of 100% H_2SO_4. S-ZrO_2, however, is known to catalyze reactions such as *n*-butane isomerization even at low temperatures [28,29] . The fact that this isomerization requires highly acidic catalysts when coupled with the above observation, suggests that S-ZrO_2 is super acidic. Keogh et al. [30] have observed that the activated S-ZrO_2 catalyst appears to eliminate the measurable catalytic activity even in the presence of 100% sulfuric acid, implying that, based on the competition of water, it is a stronger acid. It is also suggestive of the super acidity of S-ZrO_2 since 100% H_2SO_4 is itself a strong dehydrating agent. Moreover, S-ZrO_2 exhibits a Hammett acid strength of $Ho = -16.04$, whereas for 100% sulfuric acid it is only −11.99. The catalytic properties of sulfated zirconia significantly depend upon the preparation methods and the activation treatments [26,27] . Although S-ZrO_2 shows higher strength, it suffers from deactivation due to coke formation at high temperature. The deactivation of S-ZrO_2 has, to a large extent, been overcome by modifying it with various transition metals, like platinum, nickel, palladium, gallium and tungstate of which platinum-promoted S-ZrO_2 has been widely studied for alkane transformations. Yadav and Nair [25] have reviewed all pertinent aspects of S-ZrO_2.

2.3.2 Combustion synthesis

Combustion synthesis (CS) or self-propagating high-temperature synthesis is an effective, low-cost method for production of various industrially useful materials. The combustion synthesis method explores an exothermic, generally very fast and self-sustaining chemical reaction between the desired metal salts and a suitable organic fuel, which is ignited at a temperature much lower than the actual phase formation temperature. Its key feature is that the heat required to drive the chemical reaction and accomplish the compound synthesis is supplied by the reaction itself and not by an external source. Recently, the combustion synthesis of nanoscale oxides has been gaining a reputation as a straightforward preparation process to produce homogeneous, very fine, crystalline and

unagglomerated powders, without the intermediate decomposition and or calcining steps. These are the characteristics required of a catalyst and suggest the possibility of producing, in a single stage, the oxide precursor of a supported catalyst. Although this method appears to be a breaking down (destructive) process, is in fact, a building up process as the product nuclei are formed initially and grow.

2.3.3 Advantages of combustion synthesis:

- Simple and fast (explosion type)
- Low power requirement
- Low operating temperature (<400 ^{o}C) and high combustion temperature (up to 3500 ^{o}C)
- Front propagation velocities (~ 25 cm / second)
- Pure product with better catalytic properties (mesoporous, meta-stable phases with unique Structures and surface defects)
- Very high-temperature gradients (~105 K cm^{-1}) and fast reaction rates
- Elimination of volatile impurity powders (self-cleaning)
- Potential for industrial application.

2.4 Base Catalyst

The studies on the catalysis by solid acids are enormous. Though a little attention is devoted to solid base catalysts in comparison with solid acid catalysts, high activities and selectivities are often attained only by solid bases for many kinds of reactions. Actually, numerous reactions such as isomerization, addition, alkylation and cyclization are carried out industrially by using liquid bases as catalysts. Furthermore, many organic reactions require a stoichiometric amount of liquid bases. The replacement of liquid bases by solid base catalysts would have the advantages of decreasing corrosion and environmental problems while allowing easier separation and recovery of the catalysts. Excellent reviews by Hattori on the catalysis by solid bases have been published [31,32]. The main topics will be hydrotalcite as solid bases and solid superbases, namely, potassium promoted lanthanum-magnesium mixed oxide.

2.4.1 Hydrotalcite and calcined hydrotalcite

Hydrotalcite has the ideal unit cell formula, $Mg_6Al_2(OH)_{16}(CO_3^{2-})$ $4H_2O$; the ratio of Mg/Al ratio can be variable (1.7-4) in synthetic samples. By synthesis, Mg can be replaced by Zn, Fe, Ni and Co, and Al can be replaced by Cr and Fe. The kinds of anions are widely variable by synthesis or ion exchange. Their structure consists of positively charged brucite layers, altering with negatively charged interlayers containing with anions and water molecules [33,34]. The basic sites in the alkali earth oxides can originate from O^{2-} (strong basicity), O^- species near hydroxyl groups (medium strength), and OH groups (weak). The addition of Al^{3+} alters the acid-base site distribution through the introduction of Al^{3+}-O^{2-} sites with moderate Lewis acidity and medium basicity. Hydrotalcite-like materials become active as solid base catalysts when heated at about 673 K to give dehydrated and dehydroxylated mixed oxides, especially in the case of Mg-Al combinations [33,35,36]. The base-catalyzed reactions studied so far include the aldol condensation of acetone [36], cross aldol condensation of acetone and formaldehyde to methyl vinyl ketone [37] and the isomerization of pent-1-ene [38]. Corma and coworkers studied the catalytic activity and selectivity of a calcined Mg-Al hydrotalcite for the Knoevenagel condensation of benzaldehyde with activated methylene compounds with different pK_a and concluded that the calcined hydrotalcite has basic sites with pK_a up to 16.5, most of them being in the range of $10{:}7 < pK_a < 13{:}3$ [39].

2.4.2 Lanthanum-Magnesium mixed oxide

Mixed metal oxides have been widely applied as a heterogeneous base catalyst due to their strong basic property as well as their large surface area compared to that of single metal oxides. Especially, Mg–Al hydrotalcite, Mg/Al/Zr mixed oxide, KF modified hydroxyapatite, and Co_3O_4/ZnO have been successfully applied to different chemical synthesis [40–43] . La_2O_3 is one of the strongest basic metal oxides but its low surface area decreases its activity as a heterogeneous base catalyst. To increase the surface area, and thereby to enhance the catalytic activity, La_2O_3 is frequently supported with MgO and CaO [44–47]. La-Mg mixed oxides are stable due to their preparation at high temperature and could be more easily regenerated after deactivation. La-Mg mixed oxides were active for base catalyzed reactions of epoxidation of activated olefins [48] and isomerization of isophorone [49] with activities comparable to rehydrated hydrotalcite. The La-Mg mixed oxide was reported in various chemical reactions like Wadsworth-Emmons reaction [50],

transesterification reaction[51], Wittig reaction[45], synthesis of glycerol carbonate[52], Michael addition reaction[53] and epoxidation of an olefin [54].

2.4.3 Potassium promoted La-Mg mixed oxide

Solid bases have been observed to be more active than metal compounds and require milder reaction conditions than acids [55,56]. More recently, there has been an increasing development of heterogeneous catalysts, such as NaOH and a series of potassium catalysts supported on alumina [57,58], alkali-doped metal oxide [59], and zeolite [60]. The activity of solid bases generally increased with base strength. Although the reaction is complete, there are some interests in the leaching of active species on the support. It was reported that the heterogeneous catalysts lose some activity after their use. The leaching of potassium on γ-Al_2O_3 to methanol during the reaction was reported [61]; however, no leaching tests of potassium on zeolite were investigated.

Solid superbases are materials that possess basic sites with strength (H_-) higher than 26 [62]. In the past decades, there was rapid development in the research of solid superbase catalysts due to their excellent catalytic performance and environment-benign characteristics. Many superbases (e.g., KNO_3/γ-Al_2O_3 [63,64], Eu_2O_3/γ-Al_2O_3 [65], KNO_3/ZrO_2 [66,67], KOH/ZrO_2 [68], K/MgO [69], Na/NaOH/MgO [70], KNO_3/KL [71] and $Ca(NO_3)_2$/SBA-15 [72]) were reported. In these cases, the common supports are γ-Al_2O_3, ZrO_2, MgO and mesoporous molecular sieves. Obviously, due to the limited use of support materials, a variety of solid superbases is restricted. It is envisaged that the use of new support materials is a way to enrich the diversity of solid superbase materials. Previously, a series of superbase materials were synthesized using composite oxides as supports and potassium salts as modifying agents [73–75]. However, most of them show unsatisfactory catalytic performance that can be related to the poor amount of super basic sites. Composite oxides have attracted much attention in recent years due to their unique physical and chemical properties [76]. The composites based on alkaline earth and rare earth metal oxides may afford a new type of supports for superbases preparation. Materials of this kind have been used as catalysts or supports in various chemical reactions, especially in the oxidative condensation of hydrocarbons [77,78]. Lanthanum–magnesium composite oxide with base strength (H_-) between 15.0 and 18.4 has basicity higher than that of the individual oxides [77,78]. However, there are no reports on superbases that are originated from lanthanum–magnesium composite oxide. Nonetheless, a study of Clacens et al.

demonstrated that the use of a basic support favored the generation of strong basic sites [79]. It is known that the use of a potassium compound such as KNO_3 [64,80,81], KOH [68], KF [82] and K_2CO_3 [83] can promote the formation of solid superbases. All these information prompted us to investigate the possibility of preparing a super base material using lanthanum–magnesium composite oxide as support and potassium salts as modifying agents.

2.5 Hydrogenation Reaction

Various metal catalysts were employed for the heterogeneous catalyzed hydrogenation reaction. It mainly contains Group VIII transition metals, i.e. Ru, Co, Rh, Ir, Ni, Pd, or Pt, or other base metals such as Cu and Fe. Sometimes the metals are used in combinations, optionally incorporating promoters, e.g. Cr, Ba, Mn. Precious metal catalysts are often preferred because they can operate under mild conditions and hence allow better control of selectivity [84–86].

Catalyst performance is optimized by careful control of the reaction parameters, e.g. temperature, pressure, catalyst concentration; by choice of reaction solvent; or in some cases by selective poisoning. After having proceeded through several stages of development catalytic hydrogenations is now carried out essentially in two ways: low-temperature low-pressure hydrogenations in glass apparatus at temperatures up to about 100 °C and pressures of 1-4 atm, and high pressure processes at temperatures of 20 –400 °C and pressures of a few to a few hundred atm (e.g. 350 atm) [87]. The great advantage of heterogeneous catalytic hydrogenation is a very easy isolation of the products. This aspect is especially important for large-scale industrial reductions for which, as a rule, complex hydride reductions are not suitable.

The most common hydrogenation catalysts are nickel, platinum, palladium, rhodium and ruthenium. Cobalt and copper chromite are also used and rhenium has catalytic properties which make it useful for the hydrogenation of some functional groups [88]. Here, only a limited literature about some metals are covered. Details about other metal can be easily found in earlier work [89].

2.5.1 Ruthenium

Ruthenium is the most active catalyst for hydrogenation of aliphatic carbonyl compounds, particularly in the presence of some water [90]. Hydrogenation of α, β unsaturated aldehydes to saturated aldehydes is readily achieved over most platinum

metals. The selective synthesis of unsaturated alcohols is, however, much more difficult to achieve. Platinum and ruthenium have been suggested for these reactions, in particular the latter because of its lower price and comparable catalytic properties [91].

Supported or unsupported ruthenium catalysts were seldom employed in the past to carry out hydrogenation reactions in petrochemistry and chemical synthesis. Instead, these reactions were usually achieved in the gas phase or in organic solvents over platinum, palladium, rhodium, and nickel catalysts tailored to obtain optimum activities and selectivities toward desired products. Triggered by the threat of dwindling fossil resources and by the hope to decrease CO_2 emissions, many attempts have been made during the past two decades to produce chemicals by catalytic conversion of platform molecules obtained from polysaccharides or lignocellulosic materials by depolymerization, fermentation, and pyrolysis processes [92–94]. These water-soluble, bio-sourced molecules were converted into chemicals currently produced from fossil resources, such as succinic acid and derivatives [95], or into new bioproducts that had no synthetic counterpart, such as isosorbide and lactic acid derivatives [96].

2.6 Conclusion

In this chapter, a brief introduction was provided to some of the key aspects of reactions and the terms used in the thesis. Heterogeneous catalyzed reaction leads to the goal of achievement of greener and economical route of synthesis. Different catalysts especially sulfated iron zirconia, potassium promoted La-Mg mixed oxide and ruthenium supported on octahedral molecular sieves proved to be a good catalyst to achieve the goal of green chemistry in several industrially relevant reactions.

CHAPTER 3

SELECTIVITY ENGINEERING IN HYDROXYALKOXYLATION OF PHENOL BY ETHYLENE CARBONATE USING CALCINED HYDROTALCITE

J. Molleti, G.D. Yadav, Selectivity engineering in hydroxyalkoxylation of phenol by ethylene carbonate using calcined hydrotalcite, Clean Technol. Environ. Policy. 19 (2017) 1413–1422.

3.1 Abstract

The high consumption of mono-ethylene glycol phenyl ether in various sectors requires clean and green synthesis. Herein we report an efficient, selective and green route of hydroxylation using calcined hydrotalcite for preparation of mono-ethylene glycol phenyl ether. Various types of solid base catalysts were prepared and well characterized by TGA-DSC, FT-IR, XRD, CO_2-TPD, NH_3-TPD, SEM, and BET surface area. The catalyst possesses very high activity for hydroxyalkoxylation of phenol and ethylene glycol with 96 % conversion at 180 °C in 2 h with catalyst loading of 0.03 g/cm^3. The insight of reaction reveals that it is kinetically controlled with second order reaction and follows power law model. The apparent activation energy for the reaction is 21.3 kcal/mol. The catalyst is highly reusable and shows green chemistry perspective and gives excellent results up to four runs.

3.2 Introduction

Phenoxy ethanol is a typical organic solvent and it is extensively used in solvents and has large applications in personal care items like fragrance, soaps, toiletries, detergents, preservatives, cosmetics, and antiseptic, pharmaceuticals. The commercial production of mono-ethylene glycol phenyl ether (MEGPE) in the world is 170000 Tons per annum and the biggest consumption is in the solvent sector which is nearly 80 % of the total. MEGPE prepared by hydroxyalkoxylation of ethylene oxide with phenol which deals with dangerous alkylene oxide and catalyst with high negative impact on the environment with high cost of production [97].

Butler and Renfrew [98] and Rindfusz [99] have reported mono chlorohydrins for hydroxyalkoxylation of phenol by trimethylamine as a homogeneous catalyst with extremely low yield. Morgan [100] and Carlson [101] have discussed the application of alkali carbonate as a catalyst for alkylation of phenol with ethylene carbonate as an alkylating agent. Use of alkali hydride, halogen based catalysts, solid alkaline metal oxides and tri organo phosphine catalysts were well cited in the literature for the synthesis of glycol phenyl ethers [102–104]. The homogenous method cited in the literature [105] faces obvious drawbacks like waste generation and poor recovery of desired product. The effectiveness of the process is also determined by nature product. Due to the application of halogen and phosphorous based homogeneous catalysts the physical appearance of product changes. Therefore, heterogeneous catalyst would be always welcome. Recently Kinage et al. [97] have reported zeolite catalyzed synthesis of MEGPE by reacting of phenol with

cyclic carbonates at 170 °C for 24 h and Ziosi et al. [106] have reported Na-mordenite catalyst at 210 ºC for 7 h.

A large number of papers are available in the literature for intensification of industrial processes using solid acid and super acid catalysts [107–109]. Production of valuable chemicals for pharmaceutical and biodiesel industry using KOH, $Ca(OH)_2$ and NaOH as homogeneous catalysts are well demonstrated previously [110,111]. The application of homogeneous catalysts gives raise various inevitable problems such as difficult product separation from reaction mass, recovery of catalyst, and reactor corrosion [112,113]. In the field of heterogeneous solid base catalyst hydrotalcite is a very important component to be focused due to its good reusability, stability and tunable acid base property.

Hydrotalcite ($Mg_9Al_2CO_3(OH)_{16}.\ 4H_2O$) is a layered double hydroxide (LDH) and it consisting of brucite type structure in which in Mg^{2+} and Al^{3+} are octahedrally separated by charge balancing anions and water which reside in the interlayer space [114]. In many samples of hydrotalcite, a few of the Mg^{2+} cations are replaced by trivalent Al^{3+} ions, which results in a net positive charge in the cation layers. The formation of anhydrous hydrotalcite was observed when calcination was conducted below 200 °C, due to loss of interstitial water molecule. At higher temperature, up to 450 °C, CO_3^{2-} and further water are removed. Up on further calcination up to 900 °C, they lead to the formation of well dispersed mixed metal oxides with characteristic properties [115–117]. The resulting so-called activated LDHs are known to be the effective solid base for a variety of base catalyzed organic reactions [118].

Here for the first time we a report detailed kinetic study of hydroxyalkoxylation of phenol by cyclic carbonates catalyzed by calcined hydrotalcite (CHT) as an effective and better catalyst from green chemistry point of view (Scheme 3.1). Several parameters affecting kinetics of the reaction are explored in detail and a kinetic model developed including its validation against experimental data.

3.3 Experimental

3.3.1 Chemicals

Magnesium nitrate hexahydrate ($Mg\ (NO_3)_2.\ 6H_2O$), aluminum nitrate nonahydrate ($Al\ (NO_3)_3.\ 9H_2O$), sodium carbonate (Na_2CO_3), ethylene carbonate ($C_3H_4O_3$) and sodium hydroxide (NaOH) were procured from Hi-Media Chem. Ltd., Mumbai, India. Phenol,

THF, magnesium oxide and aluminum oxide were procured from S. D. Fine chem. Ltd., Mumbai, India. Laboratory grade common chemicals were used.

3.3.2 Catalyst synthesis

CHT of Mg:Al ratio 3:1 was prepared by a combination of two solutions [119] : solution A containing 38.3 g (0.15 mol) of Mg $(NO_3)_2$. $6H_2O$ and 18.9 g (0.05 mol) of Al $(NO_3)_3$. $9H_2O$ in 30 mL distilled water was prepared. Solution B containing 18 g (0.45 mol) of NaOH and 14 g (0.1 mol) of Na_2CO_3 in 30 mL distilled water was prepared. Solution A and B were simultaneously added to round bottom flask (500 mL) using dropping funnel with speed of agitation with 400 rpm maintained by overhead stirrer in oil bath at 30 °C for 2 h. White precipitate of hydrotalcite (HT) was obtained and left at 60 °C for 12 h. HT was filtered, washed with distilled water to obtained pH 7 and then dried in oven at 100 °C for 24 h. The material was calcined at 450 °C for 6 h to get CHT (3:1). The composition of Mg: Al in the catalyst is varied as 1:1, 2:1and 5:1and they were identified as CHT (1:1), CHT (2:1) and CHT (5:1), respectively. Aluminium oxide (Al_2O_3) and Magnesium oxide (MgO) were used after calcination at 450 ^oC. CHT/HMS was prepared a by procedure reported in the literature [120].

3.3.3 Reaction procedure

In all experiments, a 100 ml Amar (Mumbai, India) autoclave equipped with 4 blade pitch turbine impeller was used. The autoclave was provided within built a proportional integral derivative controller for maintaining the desired temperature. The speed of agitation was maintained at ±5 rpm of the experimental value. The calculated amount of reactants were taken in the autoclave. The autoclave was tightened and the desired temperature was set, and after attaining the temperature zero-minute sample was removed. A typical experiment consisted of 0.025 mol of phenol, 0.05 mol of ethylene carbonate, 0.2 m L of n-decane as an internal standard with a catalyst loading of 0.03 g/ cm^3 of total volume of the liquid. The speed of agitation and temperature were maintained at 180 °C and 1000 rpm respectively. The total reaction mixture of volume was 30 cm^3. Being a heterogeneous catalytic reaction recovery of catalyst was done by simple filtration, and all the experiments were performed in triplicate to determine the experimental variability (within a standard deviation of ±5%).

3.3.4 Method of analysis

Samples were withdrawn periodically from the reaction mixture and analyzed by GC equipped with a capillary column BPX-50 (0.25 mm diameter and 30 m length) and FID detector. The product was confirmed by GC-MS (Perkin Elmer, Clarus 500 with Elite-1 capillary column) and by matching the retention time of pure samples.

3.4 Results and Discussion

3.4.1 FT-IR analysis

FT-IR spectra of hydrotalcite (HT) show absorption band at 3506 cm^{-1} attributed to the stretching of hydrogen bonding located between the brucite layers (Figure 3.1). The band at 1641 cm^{-1} is ascribed to H_2O bending vibration, whereas peak at 1372 cm^{-1} is assigned to interlayer carbonates. The low frequency shows a band at about 858 cm^{-1}, corresponding to the Al-O and the band at 658 cm^{-1} could be assigned to the Mg-O [121]. In case of CHT (3:1) catalyst, the peak at 3506 cm^{-1} has significantly decreased due to de-hydroxylation. The decrease in intensity of vibration corresponds to interlayer carbonates at around 1372 cm^{-1} in CHT (3:1). It supports the fact that layered structure of hydrotalcite is remained intact after calcination.

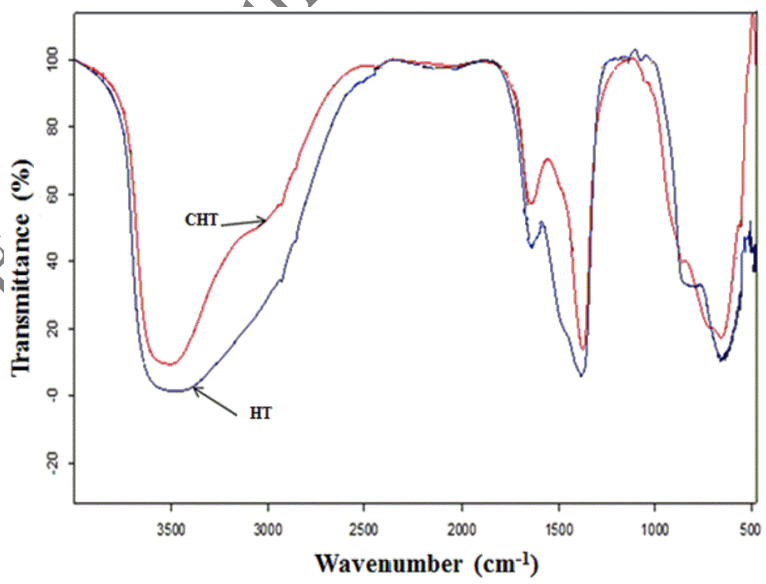

Figure 3.1 FT-IR spectra of HT and CHT (3:1)

3.4.2 XRD

XRD patterns of hydrotalcite show reflections (003), (006) (012) for 2-theta values of 11.6°, 22.9° and 34.8° respectively (JCPDS card number 35-0965), indicating layered crystalline structure (Figure 3.2). The crystalline nature of material results in a basal spacing decrease (d_{003}) and shifts towards higher 2-theta values. The calcination of material at 450 °C results in the creation of holes in the crystal surface due to loss of its water and carbon dioxide molecules [121]. The formation of fine pores in 20-40 A° range results in increased surface area and the crystalline morphology supports above observation.

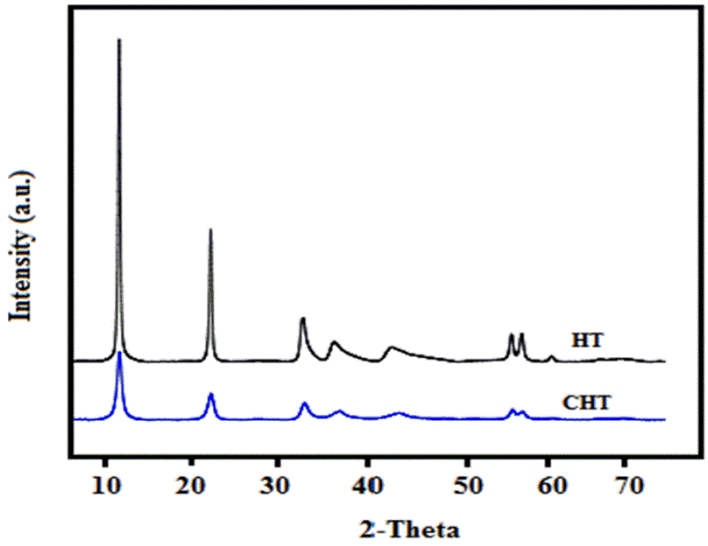

Figure 3.2 XRD of HT and CHT (3:1)

3.4.3 TGA-DSC

TGA-DSC was obtained in STA 449 F3 Jupiter from NETZSCH simultaneous Thermal Analyser. The analysis of CHT (3:1) catalyst was carried out at 25-600 ^{o}C with a heating rate of 10 ^{o}C/ min in N_2 atmosphere. Three endothermic peaks were observed as shown in Figure 3.3. First peak was observed at 25-100 ^{o}C due to loss of water content of catalyst. Second peak was observed at 100-260 ^{o}C due to loss of crystallinity. Third peak was observed at 260-450 ^{o}C due to the formation of oxide from hydroxide. Above 450 ^{o}C temperature, significant weight loss is not obtained which indicates catalyst is thermally stable.

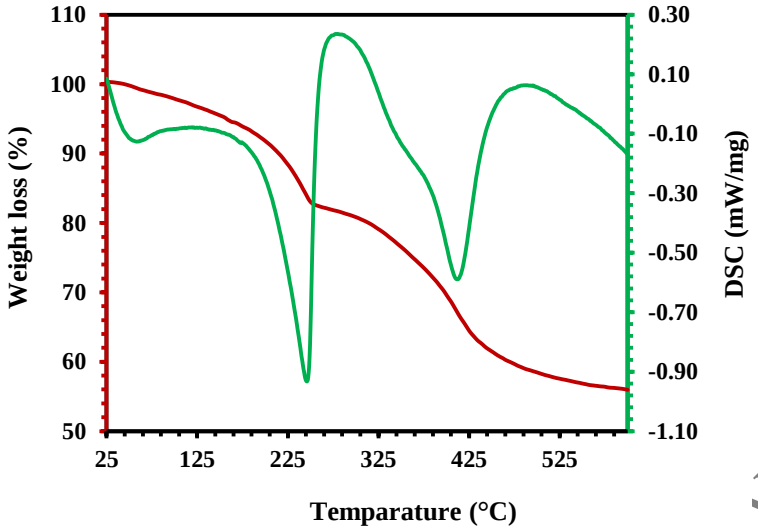

Figure 3.3 TGA-DSC analysis of CHT (3:1)

3.4.4 NH_3 and CO_2-TPD

TPD of CHT (3:1) was carried out in Micromeritics AutoChem II 2920 in which 10 % CO_2-He was used as probe molecule to find out basicity and 10 % NH_3-He was used as probe molecule to find out the acidity of catalyst. NH_3 desorption peak was observed at 243 ^oC corresponds to weak acidic sites of concentration 0.74 mmol g^{-1} as shown in Figure 3.4 (Table 3.1). CO_2 desorption peaks were observed at 270 ^oC corresponds to weak basic sites of concentration 0.84 mmol g^{-1} as shown in Figure 3.5. Regenerated CHT (3:1) is also showing about the same quantity of acidity and basicity as shown in Table 3.1.

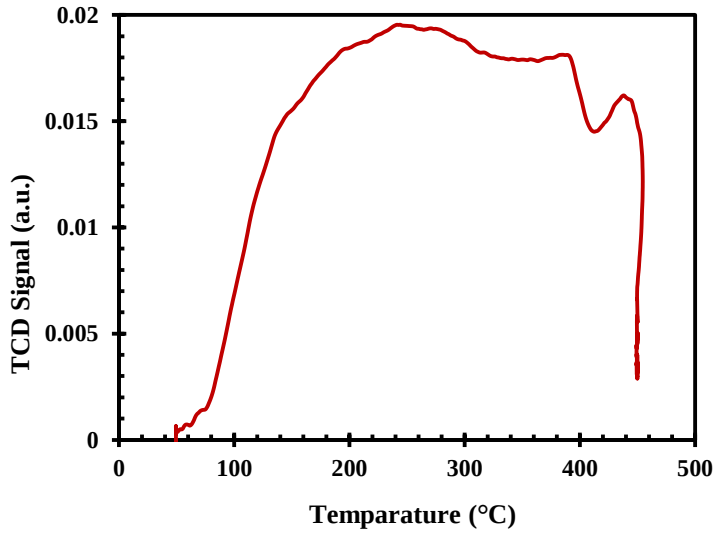

Figure 3.4 NH_3-TPD pattern of CHT (3:1)

Table 3.1 CO_2-TPD and NH_3-TPD analysis of CHT (3:1) and Reused CHT (3:1)

Catalyst	Acidity in mmol g^{-1}	Basicity in $mmol^{-1}$
CHT (3:1)	0.74	0.84
Reused CHT (3:1)	0.72	0.81

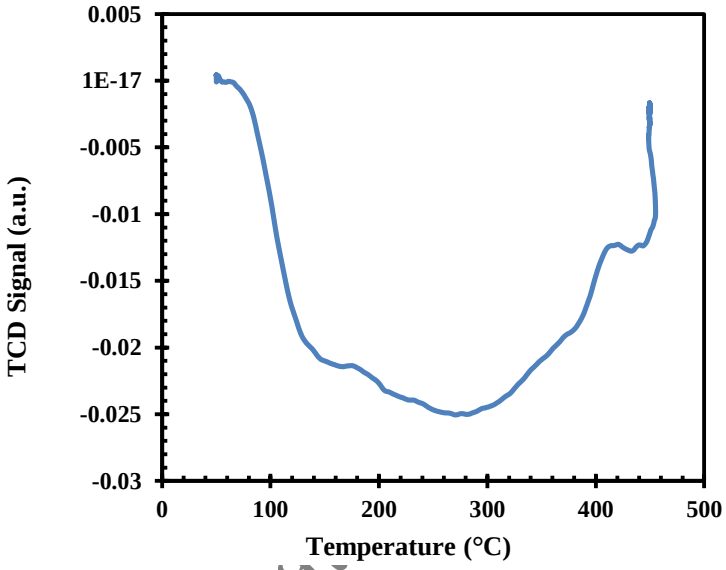

Figure 3.5 CO_2-TPD pattern of CHT (3:1)

3.4.5 Surface area and pore size analysis

The surface area of HT and CHT (3:1) were determined by Micromeritics ASAP 2020 (USA) at 77 K. Both catalysts showed type IV adsorption isotherms with well-defined steps in nitrogen adsorption and desorption isotherm (Figure 3.6) which indicates the presence of mesoporous material. HT and CHT (3:1) showed H1 type of hysteresis which indicates the presence of pores of capillary type open at both ends. Table 3.2 shows surface area, average pore and pore volume of HT and CHT (3:1) catalysts.

Table 3.2 Surface area, pore volume and pore diameter analysis of HT, CHT (3:1)

Catalyst	BET surface area (m^2 g^{-1})	BJH pore volume (cm^3 g^{-1})	BJH average pore size (nm)

HT	107	0.49	18
CHT (3:1)	209	0.66	12

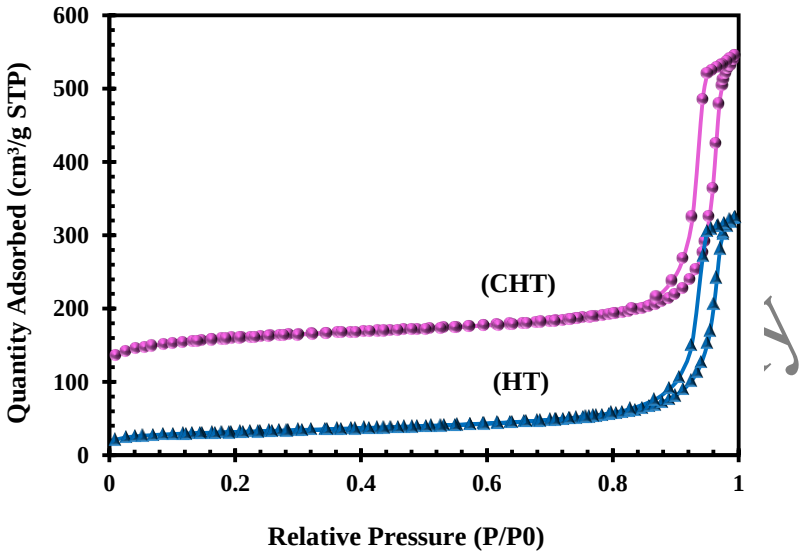

Figure 3.6 N_2 adsorption-desorption isotherms of HT and CHT (3:1)

3.4.6 SEM analysis

The particle morphology of prepared HT, CHT (3:1) and reused CHT are shown in Figure3.7. The size distribution is very broad, the particles size in all three samples are in the range of 10-100 µm. There is no difference in the topography of sample after reuse.

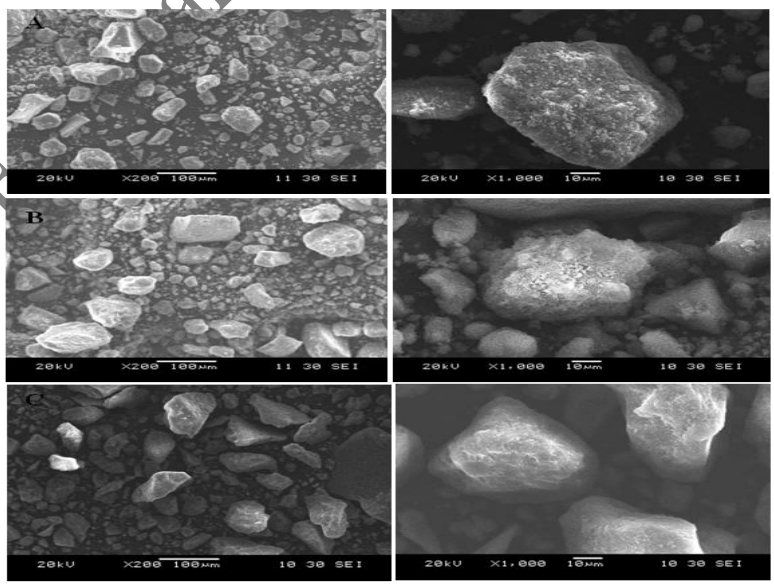

Figure 3.7 SEM Images of (A) HT, (B) CHT (3:1) and (C) Reused CHT (3:1)

3.4.7 Hydroxyalkoxylation of phenol by ethylene carbonate

The reaction of hydroxyalkoxylation of phenol by ethylene carbonate using CHT (3:1) given in Scheme 3.1.

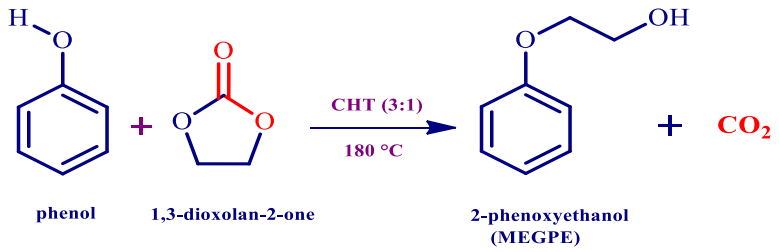

Scheme 3.1 Hydroxyalkoxylation of phenol by ethylene carbonate

3.4.8 Efficacy of solid base catalyst

The activity of various base catalysts towards the synthesis of MEGPE was demonstrated using phenol and ethylene carbonate. Calcined hydrotalcite with varying Mg: Al mole ratio like CHT (1:1), CHT (2:1), CHT (3:1), CHT (5:1), HT (3:1), CHT supported on hexagonal mesoporous silica and commercially available Al_2O_3, MgO, were studied for hydroxyalkoxylation reaction (Figure 3.8). The reaction was conducted in an autoclave using phenol to ethylene carbonate mole ratio 1:2 at 1000 rpm with a catalyst loading of 0.03 g/cm^3 on the basis of total volume. The reactivity of hydrotalcite was greatly affected by various parameters like magnesium to aluminum ratio, calcination temperature and method of preparation. It was observed that highest conversion of MEGPE was obtained when the ratio of Mg: Al was 3:1 in CHT. The obvious reason for excellent conversion is the maximum basicity of catalyst observed at 3:1 mole ratio of Mg: Al. The further increase in the molar ratio of Mg: Al leads to decreased in the conversion possibly due to a disturbance in the structure of calcined hydrotalcite. The activity of pure Al_2O_3 was found very less due to lack of basic sites. Supporting 20 % w/w CHT on HMS leads to increase in surface area but, the number of active sites available for the reaction decreased thus conversion is less when compared to CHT (3:1). 40 % conversion obtained in the case of pure MgO with poor reusability. The combination of proper Mg and Al is very necessary for the good conversion and reusability of the catalyst; hence the synergistic effect of both leads to catalyst of choice. Hence CHT (3:1) was selected as a superior catalyst for detailed kinetic investigation.

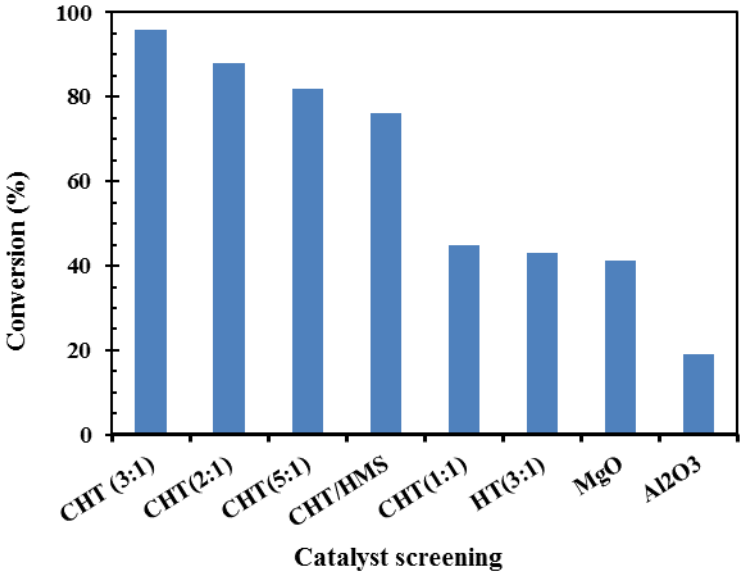

Figure 3.8 Catalyst screening for phenol conversion: Phenol-0.025 mol, Ethylene carbonate-0.050 mol, Catalyst loading-0.03 g/cm^3, Temparature-180 °C, total volume 30 cm^3, reaction time 120 min.

3.4.9 Effect of Speed of Agitation

The agitation speed was varied from 600 rpm to 1200 rpm at 180 °C. The catalyst loading was 0.03 g/cm^3 on the basis of total volume of the reaction. Figure 3.9 shows there is no effect of mass transfer resistance on percentage conversion when speed of agitation was changed from 1000-1200 rpm. Hence all reactions were conducted at 1000 rpm.

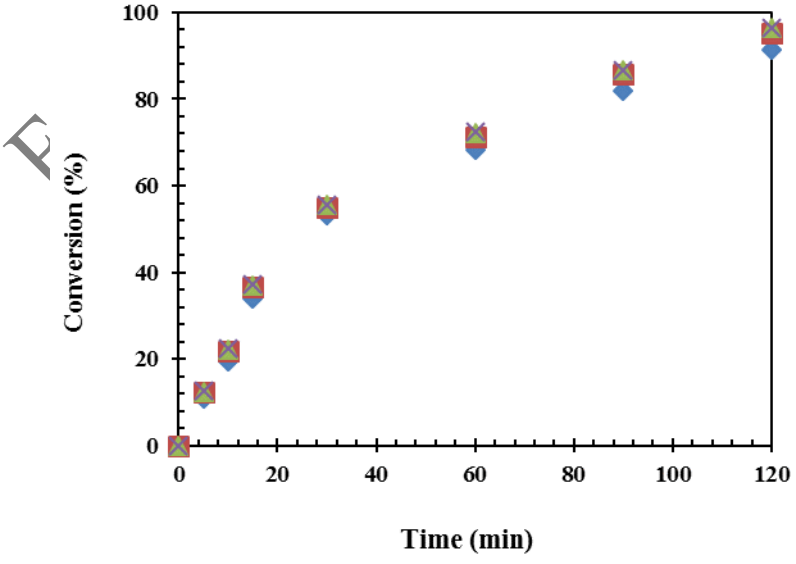

Figure 3.9 Agitation effects on phenol conversion: Phenol-0.025 mol, Ethylene carbonate-0.050 mol, Catalyst loading-0.03 g/cm^3, Temparature-180 °C, Solvent-Tetrahydrofuran. (♦) 600 rpm, (■) 800 rpm, (▲) 1000 rpm, (x) 1200 rpm.

3.4.10 Effect of catalyst loading

Effect of speed of agitation reveals that reaction is free from mass transfer resistance. Hence in order to evaluate the influence of catalyst loading on rate of reaction it was changed from 0.01 g/cm^3 to 0.035 g/cm^3. In Figure 3.10 shows that up to 0.03 g/cm^3 there is an increase in rate of reaction due to the availability of active sites where as from 0.03-0.035 g/cm^3 there is no appreciable changes in the reaction. The conversion remains almost same i.e. 96 % of conversion of reactant into a product for 0.03-0.035 g/cm^3 of catalyst loading. It is due to surpassing the number of active sites available for reaction than the number of molecules actually present for the reaction.

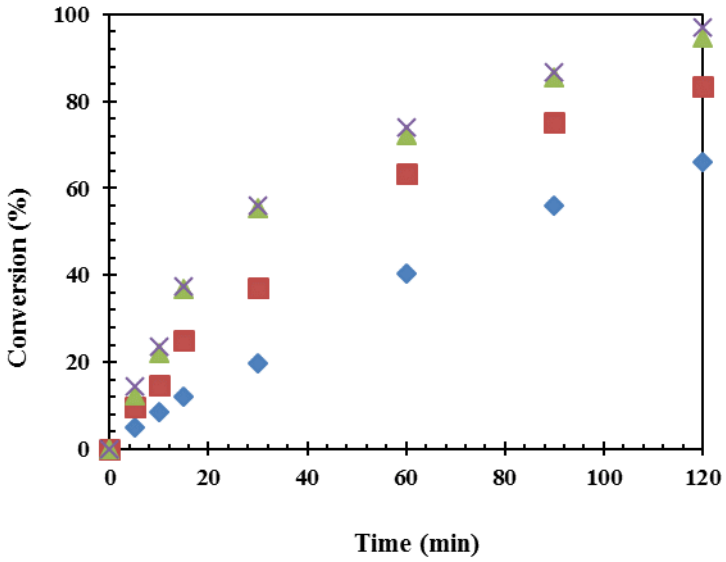

Figure 3.10 Effect of catalyst loading on conversion on phenol: Phenol-0.025 mol, Ethylene carbonate-0.050 mol, Speed of agition-1000 rpm, Temparature-180 °C, Solvent-Tetrahydrofuran. (♦) 0.015 g/ cm^3, (■) 0.020 g/ cm^3, (▲) 0.03 g/ cm^3, (x) 0.035 g/ cm^3

3.4.11 Effect of mole ratio

Herein we have varied the mole ratio phenol to ethylene carbonate from 1:1 to 1:3. The catalyst loading and the reaction temperature were 0.03 g/cm^3 and 180 °C, respectively (Figure 3.11). There is no effect on conversion at mole ratios of 1:2 to 1:3 phenol to ethylene carbonate ratio was taken as optimized value.

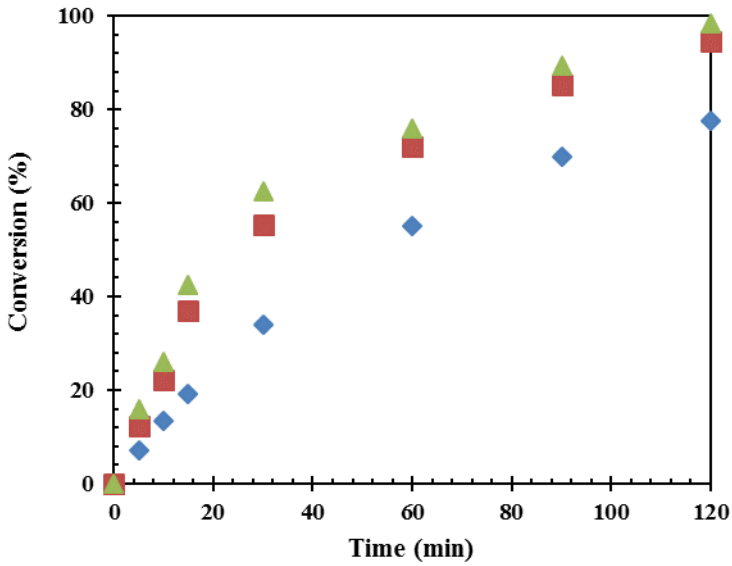

Figure 3.11 Effect of mole ratio on conversion of phenol: Speed of agition-1000 rpm, Catalyst loading-0.03 g/cm^3, Temparature-180 °C, Solvent-Tetra hydro furan. (♦) 1:01, (■) 1:02, (▲) 1:03

3.4.12 Effect of temperature

Figure 3.12 shows the effect of temperature on the conversion of hydroxyalkoxylation reaction. It is very much clear that rate of reaction and conversion dramatically increases with increase in temperature. This confirms that reaction is kinetically controlled. The Arrhenius plot (Figure 3.14) of lnk vs 1/T was used to calculate the energy of activation of hydroxyalkoxylation between phenol and ethylene carbonate. The apparent activation energy was found to be 21.3 kcal/mol.

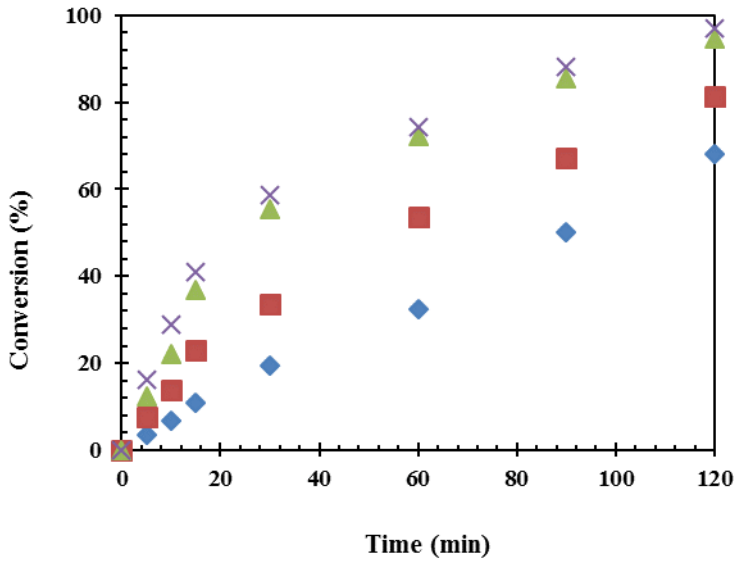

Figure 3.12 Effect of temperature on conversion of phenol: Speed of agitation- 1000 rpm, Phenol-0.025 mol, Ethylene carbonate-0.050 mol, Catalyst loading-0.03 g/cm^3, Solvent-Tetra hydro furan. (♦) 160 °C, (■) 170 °C, (▲) 180 °C, (x) 190 °C

3.4.13 Reusability of catalyst

The strength and applicability of heterogeneous catalyst depend on its reusability. Hence after completion of reaction, the reaction mass was filtered. The obtained spent catalyst was every time washed with reaction solvent in order to desorb any material adsorbed on the surface of catalyst and it was dried for 12 h at 120 °C. The volume of the reaction mass was adjusted so that added spent catalyst matches with desired optimized catalyst loading or the makeup amount of fresh catalyst was added to match desired loading of catalyst. Figure13 shows that catalyst is reusable four cycles without any loss of its activity.

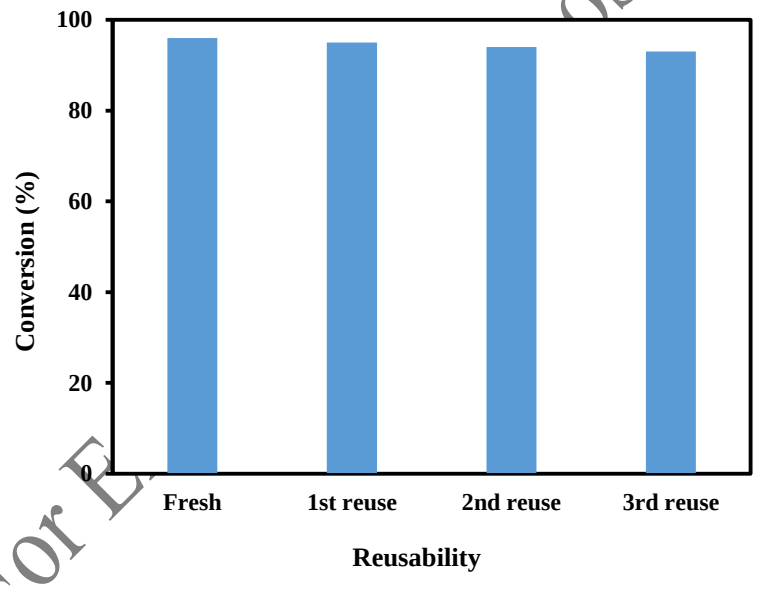

Figure 3.13 Reusability of catalyst: Phenol-0.025 mol, Ethylene carbonate-0.050 mol, Speed of agitation- 1000 rpm, Catalyst loading-0.03 g/cm^3, Temparature-180 °C**.**

3.4.14 Reaction mechanism and mathematical model

The detail reaction mechanism is given in Scheme 3.2**.** CHT catalyst consists of both basic sites (S_1) and acidic sites (S_2). Phenol gets adsorbed on basic site and ethylene carbonate gets adsorbed on acidic site. Hydroxyl group of phenol get converted to phenoxy ion which attacks carbocation of ethylene carbonate to give intermediate. This intermediate undergoes decarboxylation on catalyst sites to give MEGPE. This product gets desorbed from the catalytic site into the solution and makes it available for the next cycle. We have

also done the theoretical calculations to see the effect of intra particle diffusion resistance on the rate. The detail can be easily found in our earlier work [122,123]. The value of Cwp was found to be 0.0005 which is far less than unity hence confirms that there is no effect of intra particle diffusion resistance. Using power law model because of weak adsorption of all species on the sites, the following is developed.

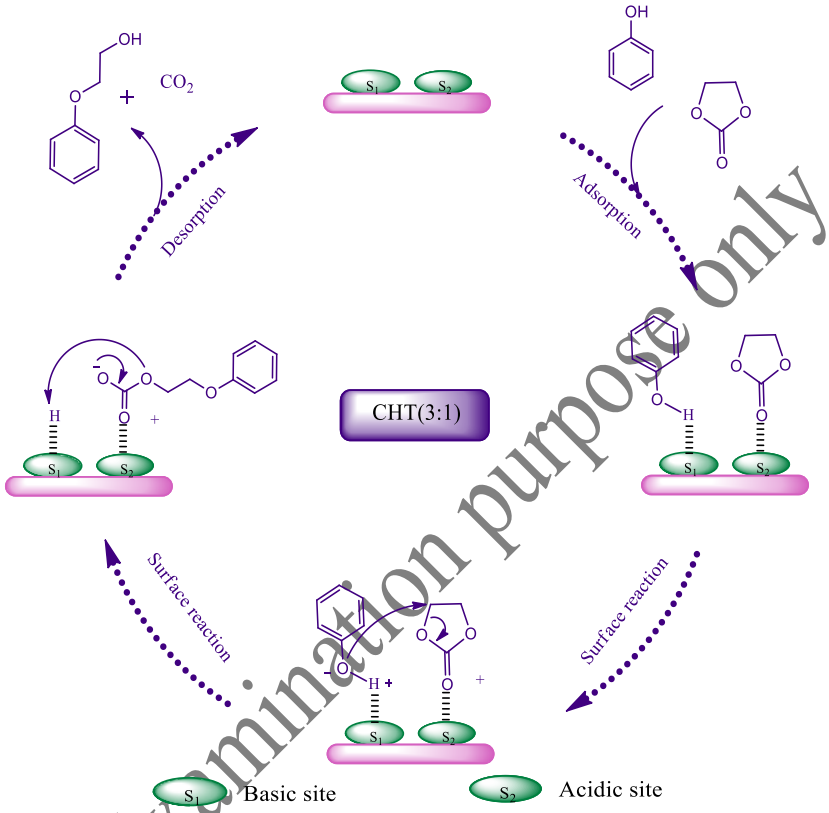

Scheme 3.2 Reaction mechanism of hydroxyalkoxylation of phenol by ethylene carbonate

The rate of reaction of A can be given as

$$r_A = k_1 C_A C_B w \qquad (1)$$

$$r_A = -\frac{dC_A}{dt} = k_1 w C_A C_B \qquad (2)$$

Let $C_{B_o} / C_{A_o} = M$ at t=0. Then the above equation

$$\frac{dX_A}{dt} = k_1 w C_{Ao} (1 - X_A)(M - X_A) \qquad (3)$$

Integrating above equation

$$\ln\left\{\left(\frac{M - X_A}{M\left(1 - X_A\right)}\right)\right\} = k_2 C_{A_0}\left(M - 1\right)t \qquad (4)$$

The plot of $\ln\left\{\frac{\left(M - X_A\right)}{M\left(1 - X_A\right)}\right\}$ vs t (Figure 3.15) was made for different temperatures which give an excellent fit and hence validates the proposed model. Using above plot rate constants were calculated to make Arrhenius plot (Figure 3.14) to get apparent activation energy. The activation energy was found to be 21.3 kcal/mol which confirms the kinetically controlled reaction.

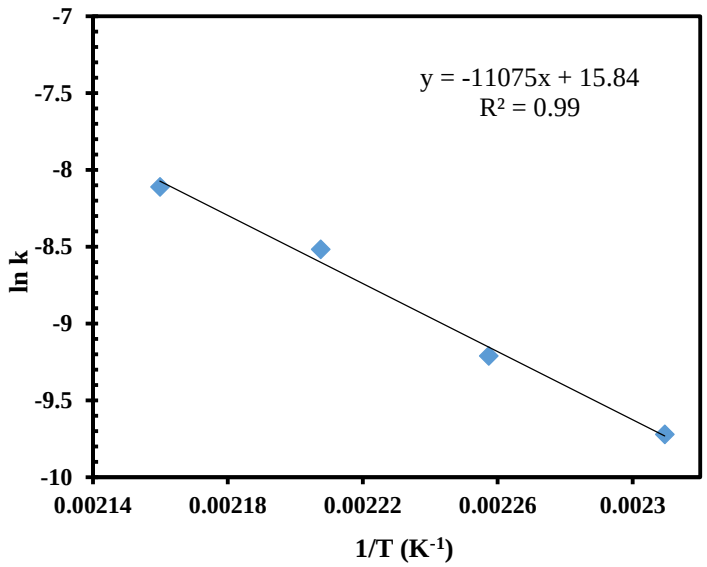

Figure 3.14 Arrhenius plot

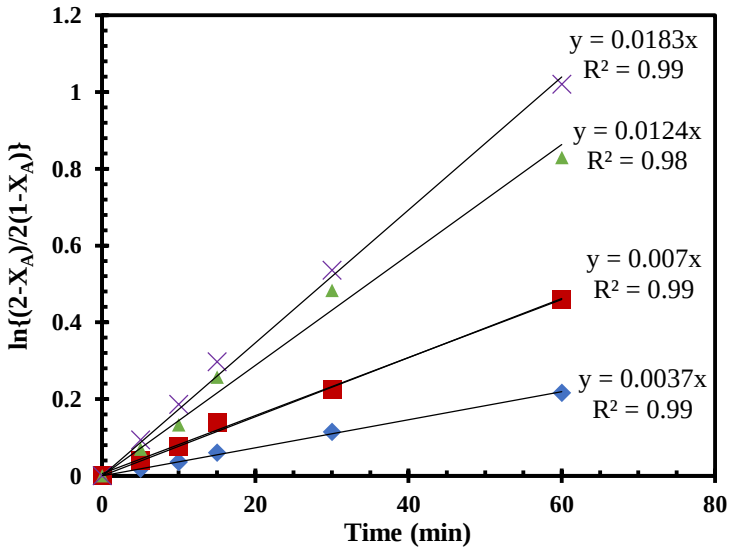

Figure 3.15 Kinetic plots for various temperatures: Speed of agitation- 1000 rpm, Phenol-0.025 mol, Ethylene carbonate-0.050 mol, Catalyst loading-0.03 g/cm^3, Solvent-Tetra hydro furan. (♦) 160 °C, (■) 170 °C, (▲) 180 °C, (x) 190 °C

3.5 Conclusion

The hydroxyalkoxylation of phenol and ethylene carbonate was successfully carried out in presence of different mole ratios of Mg/Al to study the nature of basicity. CHT (3:1) was found to be an excellent catalyst. The factors affecting the rate of reaction and efficiency of catalyst towards this reaction have been thoroughly studied. A detailed kinetic study was carried out, which indicates that reaction follows the power law model. The activation energy was found to be 21.3 kcal/m

CHAPTER 4

NOVEL SYNTHESIS OF RU SUPPORTED ON OMS BY SOLVENT-FREE METHOD AS A CATALYST FOR SELECTIVE HYDROGENATION OF LEVULINIC ACID TO γ-VALEROLACTONE IN AQUEOUS MEDIUM AND KINETIC MODELLING

J. Molleti, M. S. Tiwari, G. D. Yadav; Novel synthesis of Ru supported on OMS by solvent-free method as a catalyst for selective hydrogenation of levulinic acid to γ-valerolactone in aqueous medium and kinetic modelling ,Chem. Eng. J. (Communicated)

4.1 Abstract

γ-Valerolactone (GVL) is an important biomass –derived molecule for the sustainable production of value-added chemicals and fuels mainly synthesized by levulinic acid hydrogenation using supported ruthenium catalyst. Here we are reporting the synthesis of ruthenium supported on manganese oxide octahedral molecular sieve (OMS-2) catalyst prepared by different methods. Three different methods i.e. reflux, hydrothermal and solventless was used for the preparation of OMS-2. The prepared catalysts were used for the selective hydrogenation of biomass-derived levulinic acid (LA) to GVL using molecular hydrogen in water. Solventless synthesized OMS (OMS-2_S) is energy efficient, rapid and economical way of synthesis. Among three different catalysts, Ru supported on solventless OMS-2 i.e.1 wt % Ru/OMS-2_S catalyst showed LA conversion of 99.9 % and selectivity of 100 % towards GVL in 1h with the overall turnover frequency of 0.95 s^{-1} at mild conditions (100° C, 30 atm H_2). Different OMS-2 supported Ru catalyst shows a very high turnover frequency in comparison with literature for the synthesis of GVL. The specific textural and chemical properties of catalysts were characterized by various techniques. Moreover, 1 wt % Ru/OMS-2_S catalyst is reusable up to four times without significant loss of activity and is very stable. By studying the effects of different process parameter kinetic model was developed based on LHHW type of mechanism. The apparent activation energy for LA hydrogenation to GVL is 11.75 kcal/mol.

4.2 Introduction

The depletion of fossil fuels and increasing global climate change concerns have led to research activities for alternate resources, for the value–added chemicals and production fuel [124–126]. Biomass is a promising alternative for fossil resources because it is renewable, abundant, and low cost [127]. Cellulose is a leading component of biomass. Extensive work has been done to converting biomass into platform chemicals such as levulinic acid (LA) [128], 5-hydroxymethylfurfural [129], and γ-valerolactone (GVL) [130]. In biorefinery concepts, the production of GVL from LA is a key transformation because of its versatile functions and benign properties [131].

GVL is extensively used as liquid fuel, food additive and solvent [132–134]. It can be synthesized through hydrogenation of LA followed by cyclization using either homogeneous or heterogeneous catalyst [135–140]. Published literature specified that

homogeneous Ru-based catalysts show higher activity for the selective conversion of LA to GVL [141–143]. However, there are many problems in using homogeneous catalysts such as separation, recovery and recycle of the catalyst. Several heterogeneous catalysts such as Pt, Ru, Ir, Au and Rh anchored on different supports like metal oxides or carbon supports have been tried [144]. Also for the same reaction non–noble catalysts such as Cu/SiO_2 [145], Cu/ZrO_2 [146,147], Cu-Fe [148], Cu-Cr[149] also have been reported to achieve a high conversion of LA. However, these catalysts have seviour drawbacks such as long reaction time and poor reusability. Different types of Ni-based catalysts were investigated to overcome those problems. However, because of harsh conditions (6.5-8.0 MPa and/or 250 ºC), it still was not preferred [150,151]. Activated carbon-supported ruthenium catalyst displayed remarkable activity among all the catalysts towards LA hydrogenation reaction. Al-Shall et al. reported 97.5 % selectivity of GVL and 100 % conversion of LA over Ru/C catalyst at room temperature [152]. Recently Huang et al. reported that 100% GVL selectivity and 99.7 % LA conversion using Ru/FLG catalysts under 40 atm H_2 in 8 h reaction time at room temperature demonstrating the best results obtained to date [153]. Further, the long reaction time, high metal content, use of typically high-cost support and reusability problems still exist which need to be overcome. Also, several authors reported formic acid as a hydrogen source to get maximum yields of the hydrogenation of LA [134,154,155]. However, there are several drawbacks using a formic acid like leaching of metals into solutions, due to the corrosive medium of reaction and undesirable side reactions. Hence, the use of molecular hydrogen is considered more favorable as a source of hydrogen for hydrogenation of LA.

Manganese octahedral molecular sieves (OMS) have open tunnel structure based on linked MnO_6 octahedral moieties. Cryptomelane (OMS-2, also known as K-OMS-2) possesses excellent redox properties due to the presence of Mn ions and has a variety of applications including batteries [156] and adsorption, catalysis [157]. OMS-2 supported metal catalysts reported mostly on oxidation reactions [158,159], have also been used in hydrogenation reactions with cinnamaldehyde and ketoisophorone [160], acetophenone [161], and nitrobenzene [162,163]. It also has acidic sites which help for hydrogenolysis as earlier reported [160,161]. Hence it could be very useful in the synthesis of GVL from LA. OMS-2 synthesis usually requires a long reaction time and controlled reaction condition which gives very low surface area. Ding et al. have reported rapid, high surface area and solventless synthesis of OMS-2 (designated OMS-2_S) which gives better results than

conventionally synthesized counterparts. Based on their results and advantages offered by the current method we have synthesized OMS-2_S and used for the Ru metal loading and used for the synthesis of GVL. We have also compared the activity of different prepared OMS-2.

Here, we report the synthesis of novel ruthenium impregnated on OMS-2 prepared by different methods. The catalysts were characterized by different techniques and reveal that high dispersion of Ru particle. Prepared catalysts were used for the synthesis of GVL from LA and based on the literature and our experimental results, Ru supported on OMS-2_S gives very promising results. Different reaction parameters were studied to evaluate their effects on the rate and suitable mathematical model was developed.

4.3 Experimental

4.3.1 Chemicals

All chemicals were procured from reputed firms and used as such without further purification. Potassium permanganate, manganese acetate, ruthenium chloride (S. D. Fine Chem. Ltd., Mumbai, India.), hydrogen (99.9% purity) cylinder (INOX, Mumbai, India). Levulinic acid was procured from Thermo Fisher Scientific Pvt. Ltd., Mumbai, India.

4.3.2 Preparation of catalyst

Three types of OMS-2 supports were prepared using three different methods such as solvent-free (S), reflux (R), and hydrothermal (H) named as OMS-2_S, OMS-2_R and OMS-2_H depending on the method of preparation all procedures can be found in the literature [164–166].

1 wt % Ru/OMS-2_S was prepared by wet impregnation method. 1 g OMS-2_S was dispersed in water (100 mL) for 1 h with ultrasonication and 3 mL aqueous solution of $RuCl_2$ (0.04 g) was added dropwise to the above suspension and stirred for 2 h. Then an aqueous solution of hydrazine hydride was added (2 mL) dropwise and kept for 2 h under vigorous agitation. The precipitate was filtered and washed with water and then dried at 100 °C for 8 h. We followed a similar procedure for the preparation of 1 wt % Ru/OMS-2_R and 1 wt % Ru/OMS-2_H catalysts.

4.3.3 General procedure for hydrogenation of LA

All experiments were carried out in a 100 cm^3 autoclave made of stainless steel (Amar equipment's, Mumbai, India) equipped with 4 blade pitched turbine impeller. The temperature was maintained at ±2 °C of the desired value. A typical experiment consisted of 7.5×10^{-4} mol/cm^3 of LA, 30 atm hydrogen pressure, water (total volume 40 ml) as a solvent and 100 mg of catalyst, at 100 °C with an agitation speed of 800 rpm.

4.3.4 Characterization Methodology

XRD Patterns were recorded on Bruker AXS, D8 Discover instrument using Cu Kα radiation (1.5406 A°) at 40kV and 100mA. The measurements were step scanned in the 2θ range of 5-80° with stepping time of 0.5 s. FTIR spectra of catalysts were collected on a Perkin Elmer instrument and a blank KBr pellet was taken as a reference to each sample. KBr and samples were mixed in 100:1 ratios (approximately) and pressed to make pellets. The FTIR spectra of prepared catalyst pellets were obtained in the wave number range of 4000-600 cm^{-1} at 2 cm^{-1} resolution at room temperature. Temperature programmed adsorption of ammonia (NH_3-TPD) of different catalyst were recorded on AutoChem II 2920 TPD/TPR, Micromeritics, USA using 10%NH_3 in helium gas. Approximately 50 mg of catalyst was pre-treated at 350°C under Helium flow of 50 ml/min for 1hr. After pre-treatment, the temperature was cooled to 100 °C and the 10% NH_3 in helium was passed for the adsorption of ammonia on the surface for 1 h. The physisorbed ammonia was removed by helium flushing at the same temperature for 30 min. Finally, the catalyst was heated to 650°C at 30°C/min heating rate. The temperature programmed desorption of ammonia was measured by using TCD of a gas chromatograph. The morphology of the prepared sample was studied by using Field Emission gun-scanning electron microscopy (FEG-SEM) images collected on Tescan MIRA 3 microscope. The dried samples were mounted on specimen studs and sputter coated with a thin film of platinum to prevent charging. The platinum-coated surface was then scanned at various magnifications using FEG-SEM. The surface area, pore volume and pore diameter of samples were measured by BET method on ASAP 2010 instrument, Micromeritics, USA using nitrogen adsorption - desorption process at 77K temperature. The samples were degassed under high vacuum at 300°C for 6 h prior to measurement. Thermo gravimetric analysis was conducted by taking 20 mg of the sample on TGA instrument (NETZSCH). The temperature was varied from 30 °C to 700°C with a scan rate of 30°C/min under nitrogen atmosphere. TEM micrographs of samples were obtained using a PHILIPS CM200 transmission electron microscope

having 2.4 A° resolution and operating voltage range between 20 – 200kV. The catalyst samples were dispersed in ethanol by means of sonication and then deposited on Cu grid coated with carbon film. H_2-pulse chemisorption was conducted on a Micromeritics AutoChem 2920 instrument to calculate the active surface area of palladium. The sample was reduced at 300 °C for 1 h under 10% H_2 /Ar flow and then cooled to 50 °C. The chemisorption was carried out by a pulse of a mixture of 10% H_2 /Ar.

4.4 Results and Discussion

4.4.1 XRD

XRD patterns of OMS-2_S, Ru loaded different OMS-2 and used 1 wt % Ru/OMS-2_S catalyst are shown in Figure 4.1. XRD pattern of OMS-2_S shows diffraction peaks at 2θ =28.45°, 37.24°, 41.62°, 49.59° and 59.90° corresponding to reflections of (301), (211), (310), (114), and (600) respectively of standard crystalline cryptomelane structure as confirmed with JCPDS (29-1020) [164]. The crystalline phases of metallic ruthenium were recognized with JCPDS (06-0663). Peaks related to Ru metal were observed for a reflection at 2θ =38.5°, 44.1°, 54.3° and 58.4°, which corresponds to the diffractions of the (100), (101), (211) and (102) planes of the Ru respectively [167]. Diffraction corresponding to Ru at 2θ = 38.4°, 44.0° and 58.2° cannot be distinguished , which is due to low loading and high dispersion of Ru on OMS-2 support as same reported in earlier cases [168,169]. Crystallinity and crystalline size of the 1 wt % Ru/OMS-2_S and OMS-2_S were calculated using Scherrer's formula. The average crystallinity of the OMS-2s decreases after loading of Ru from 77 % to 64 % and average crystallite size of 1 wt % Ru/OMS-2_S and OMS-2_S was 12.3 nm and 6.2 nm respectively. The particle size of different materials are listed in Table 1. The particle size of 1 wt % Ru/OMS-2_S, 1 wt % Ru/OMS-2_H and 1 wt % Ru/OMS-2_R were found to be 12.3 nm, 14.9 nm and 18.2 nm respectively. The XRD patterns of 1 wt % Ru/OMS-2_S and reused 1 wt % Ru/OMS-2_S were compared and XRD patterns are almost same which further confirms that prepared catalyst is stable.

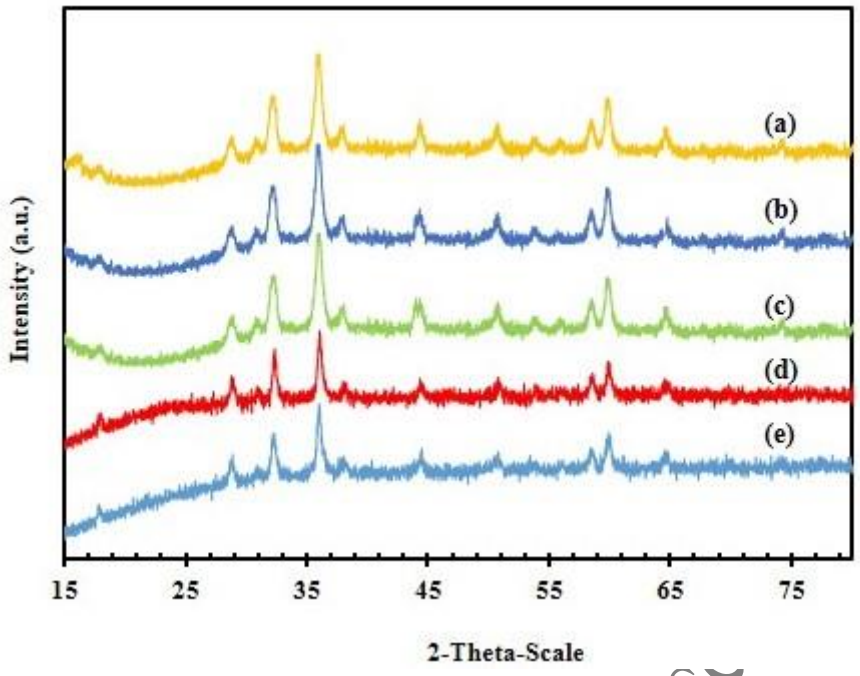

Figure 4.1 XRD of (a) OMS-2$_S$, (b) 1 wt % Ru/OMS-2$_S$, (c) used 1 wt % Ru/OMS-2$_S$, (d) 1 wt % Ru/OMS-2$_H$, (e) 1 wt % Ru/OMS-2$_R$

4.4.2 FT-IR

The FT-IR spectra of OMS-2$_S$, 1 wt % Ru/OMS-2$_S$ and reused 1 wt % Ru/OMS-2$_S$ catalysts are shown in Figure 4.2. The OMS-2$_S$ spectra show bands of stretching and bending vibration of hydroxyl groups at 3420 and 1628 cm^{-1}, respectively, which are also seen in spectra of 1 wt % Ru/OMS-2$_S$. It provides a strong evidence that ruthenium metal incorporated succesfully on manganese dioxide molecular sieve with its structure being intact. FT-IR spectra of virgin and reused catalysts also indicated there are no structural changes. It indicates that there is no externally adsorbed species on the surface of the reused catalyst.

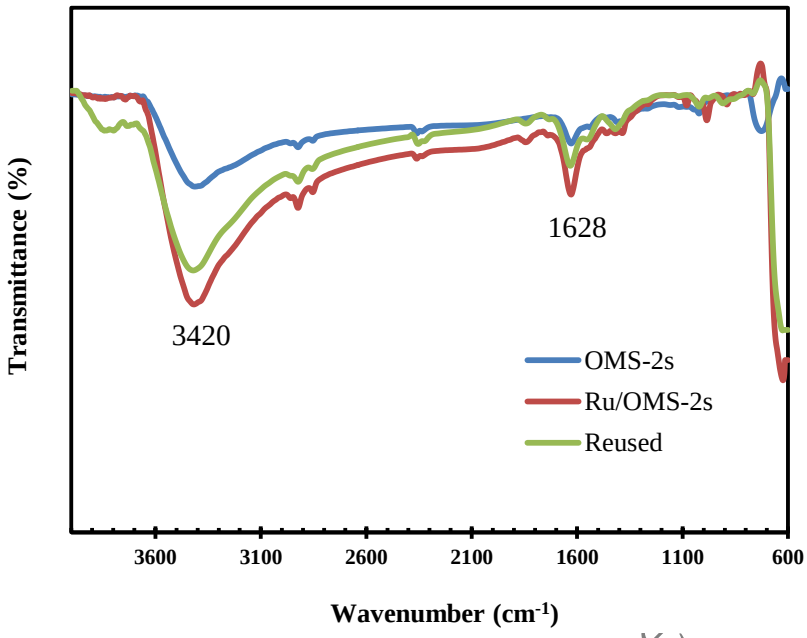

Figure 4.2 FTIR of OMS-2S, 1 wt % Ru/OMS-2S and reused 1 wt % Ru/OMS-2S

4.4.3 Surface area and pore size analysis

Table 1 lists the BET surface area, average pore diameter, and pore volume for OMS-2_S, OMS-2_R, OMS-2_H, 1 wt % Ru/OMS-2_S, 1wt % Ru/OMS-2_R, 1wt % Ru/OMS-2_H and reused Ru/OMS-2_S catalysts. All catalysts showed a type IV isotherm, indicative of the formation of mesoporous material (Figure 4.3) [170]. The adsorption curve has the hysteresis loop type H3 at relative pressures between 0.8 and 1 corresponding to rod-like fibres given rise to narrow slit porous shape [171]. The BET surface area, average pore diameter and pore volume of OMS-2_S was 164 m^2 g^{-1}, 12.7 nm and 0.54 cm^3g^{-1} respectively. The surface area of Ru/OMS-2_S catalyst decreased to 65 m^2 g^{-1} after the addition of ruthenium metal. This indicates the Ru is successfully supported on OMS-2_S. The average pore diameter and pore volumes of 1 wt % Ru/OMS-2_S and reused 1 wt % Ru/OMS-2_S catalysts were almost same.

Table 4.1 BET surface area of the Ru/OMS materials

Catalysts	BET surface area(m^2/g)	Average pore diameter(nm)	BJH pore volume (cm^3/g)
OMS-2_S	164	12.7	0.54
OMS-2_H	101	14.6	0.45

OMS-2_R	98	17.8	0.48
1 wt % Ru/OMS-2_S	65	22.2	0.36
1 wt % Ru/OMS-2_H	61	22.3	0.34
1 wt % Ru/OMS-2_R	58	20.6	0.30
Reused 1wt % Ru/OMS-2_S	63	21.5	0.35

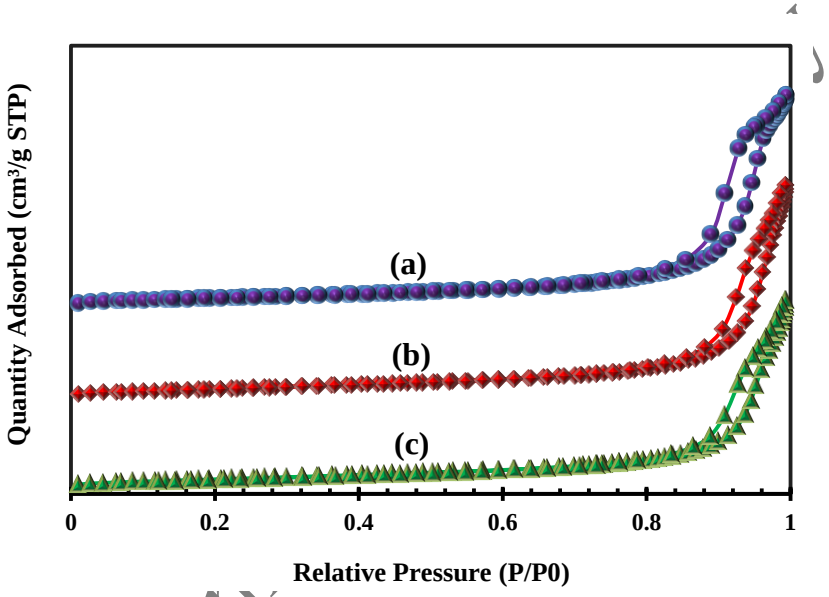

Figure 4.3 N_2 adsorption-desorption plot for the catalyst: (a) 1 wt % Ru/OMS-2_S, (b) 1 wt % Ru/OMS-2_R, (c) 1 wt % Ru/OMS-2_H

4.4.4 Ammonia TPD

Acidity of different catalysts were determined by TPD analysis with ammonia as probe molecules and are depicted in Table 4.2. NH_3–TPD values of different samples i.e. OMS-2_S, OMS-2_H, OMS-2_R, 1 wt % Ru/OMS-2_H, 1 wt % Ru/OMS-2_R, and reused 1 wt % Ru/OMS-2_S are given in Table 4.2. 1 wt% Ru/OMS-2_S catalyst shows as NH_3 desorption peaks at 131º C and 532 º C corresponds to weak and strong acidic sites (Figure 4.4), and the quantity of NH_3 was 0.10 and 0.15 mmolg^{-1}. All samples show two distinct peaks around 200 and 520 corresponding to the presence of weak and strong acidic sites. The acidic sites of 1 wt% Ru/OMS-2_S were not affected too much by the loading of the

ruthenium metal on OMS-2_S. The acidity of regenerated catalyst have no significant changes.

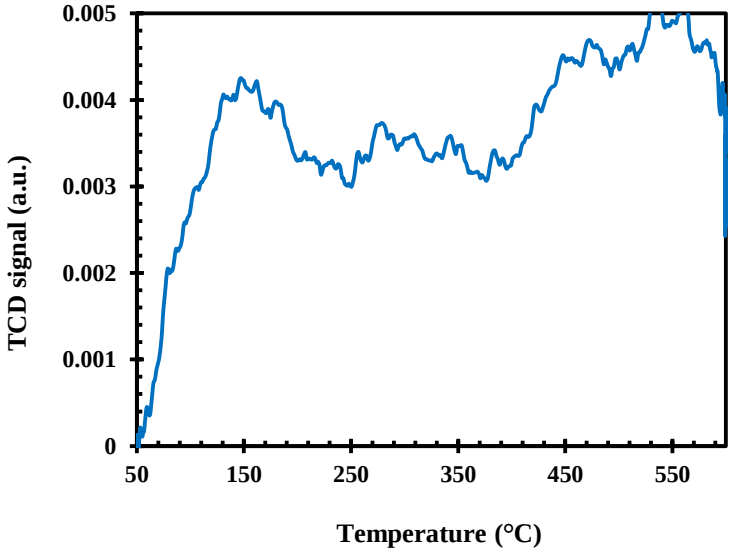

Figure 4.4 NH_3-TPD pattern of 1 wt% Ru/OMS-2_S

Table 4.2 Ammonia -TPD of different samples

Catalysts	NH_3 TPD analysis Acidity (mmol g^{-1})		
	Weak	Moderate/strong	Total
OMS-2_S	0.22	0.23	0.45
OMS-2_H	0.06	0.16	0.22
OMS-2_R	0.15	0.22	0.37
1 wt % Ru/OMS-2_S	0.10	0.15	0.25
1 wt % Ru/OMS-2_H	0.06	0.10	0.16
1 wt % Ru/OMS-2_R	0.08	0.02	0.10
Used 1 wt % Ru/OMS-2_S	0.09	0.12	0.21

4.4.5 TGA

Figure 4.5 shows the TGA of 1 wt % Ru/OMS-2_S. The initial weight loss below 120 ºC due to the removal of water presents on the surface or physisorbed water molecules on the manganese oxide lattice structure. There is no significant weight loss observed in TGA results. It verifies the catalyst is stable up to 600 ºC and can be used for high temperature reaction.

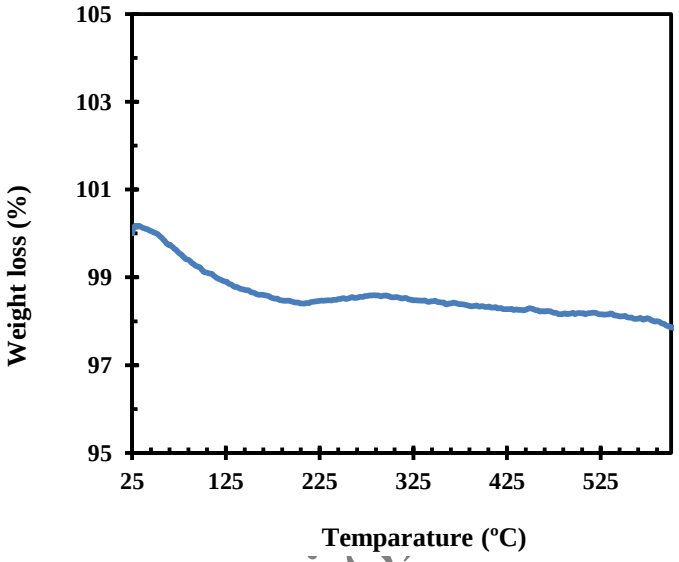

Figure 4.5 TGA of 1 wt % Ru/OMS-2_S catalyst.

4.4.6 TEM

Figure 4.6 shows TEM micrographs of 1wt % Ru/OMS-2_S catalyst. The impregnation of ruthenium particles on the OMS-2_S support can lead to deposition on the external surface or cramped to channels. As shown in Figure 4.6a the ruthenium particles (black spots) were well dispersed on the OMS-2_S support and the catalyst reveals a particle aggregate morphology and the average particle size is 18.4 nm

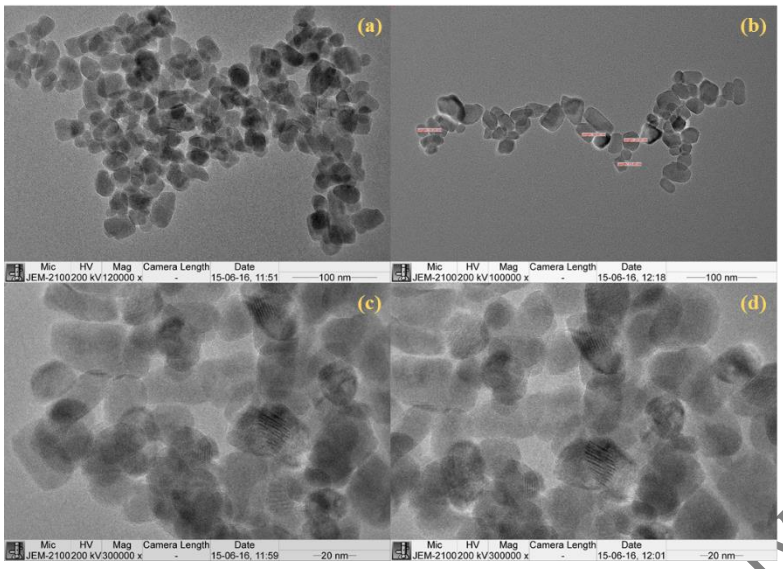

Figure 4.6 TEM images of 1 wt% Ru/OMS-2S (a and b)

4.4.7 FESEM and EDXS

Figure 4.7 shows field emission SEM images of OMS-2S (Figure 4.7a and b) and 1 wt% Ru/OMS-2S (Figure 4.7c and d). The morphology of OMS-2S catalyst changed from nanofibrous structure to clusters of nanocrystallites after the loading of ruthenium metal. Table 4.3. Shows EDXS analysis of 1 wt % Ru/OMS-2S catalyst, which confirms the incorporation of ruthenium metal on the surface of OMS-2S support.

Table 4.3 EDXS analysis.

Element	Mass%	
	OMS-2S	1 wt% Ru/OMS-2S
O	22.50	22.55
K	0.79	0.41
Mn	76.71	76.64
Ru	0	0.80

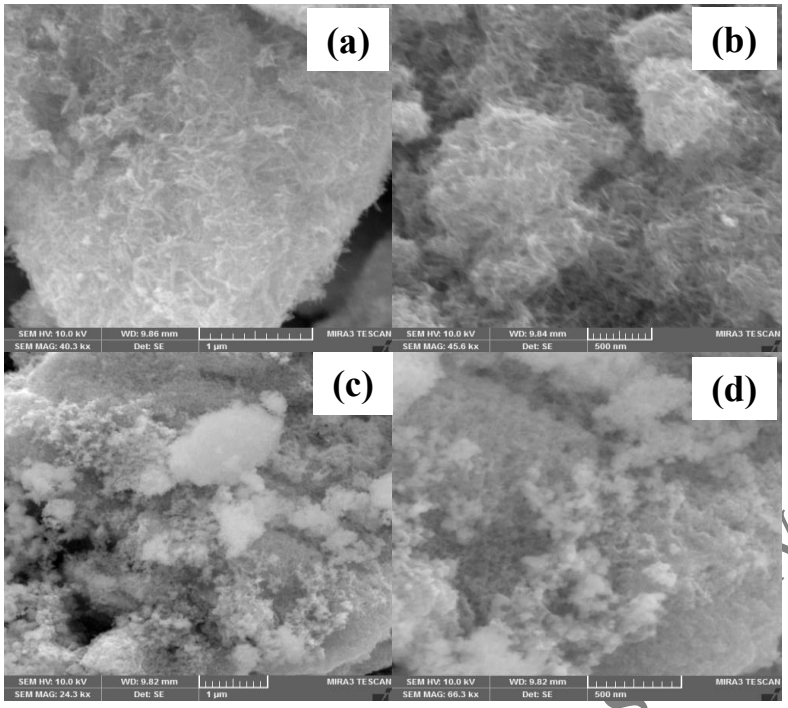

Figure 4.7 FESEM images of OMS-2S (a and b) and 1 wt% Ru/OMS-2S (c and d)

4.4.8 H_2-pulse chemisorption

H_2 pulse chemisorption studies conducted for 1 wt % Ru/OMS-2_S, 1wt % Ru/OMS-2_H and1 wt % Ru/OMS-2_R catalysts (Table 4.4). Ruthenium metal dispersion, surface area and average particle size were calculated using the stoichiometric factor (Ru_s/H) as 1. The results suggest that 1 wt % Ru/OMS-2_S catalyst has high metal dispersion and Ru metal surface area in comparison with other catalysts and the order follows as 1 wt % Ru/OMS-2_S >1 wt % Ru/OMS-2_H>1 wt % Ru/OMS-2_R.

Table 4.4 H_2-pulse chemisorption analysis.

Catalysts	H_2 uptake (µmol/g)	(%) Dispersion	Ru surface area (m^2/g)	Particle size (nm)
1 wt % Ru/OMS-2_S	155.7	78.7	423.3	1.7
1 wt % Ru/OMS-2_H	115.8	58.5	314.8	1.6

1 wt % Ru/OMS-2_R	104.6	52.9	284.5	1.5

4.4.9 Catalytic reaction

The reaction of hydrogenation of LA to GVL using 1 wt % Ru/OMS-2_S catalyst given in Scheme 4.1

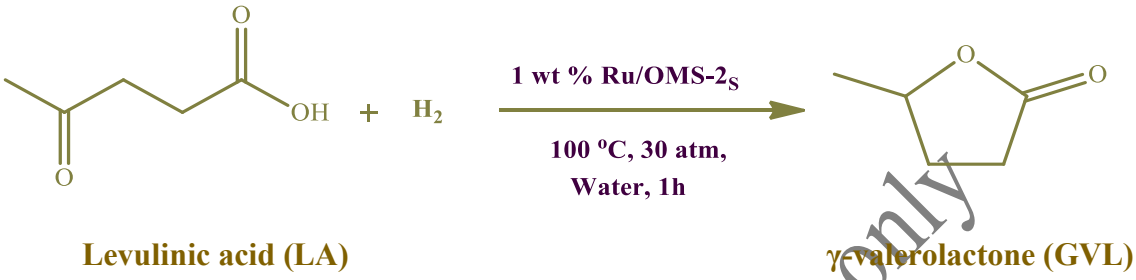

Levulinic acid (LA) **γ-valerolactone (GVL)**

Scheme 4.1 Hydrogenation of LA to GVL

4.4.10 Efficacy of various catalysts

Different Ru supported catalysts such as 1 wt % Ru/OMS-2_S, 1 wt % Ru/OMS-2_R and 1 wt % Ru/OMS-2_H were tested for LA hydrogenation to GVL using water as a solvent at the same conditions (100 ºC, and 30 atm H_2) (Figure 4.8). The order of activity was found as follows: 1 wt % Ru/OMS-2_S >1 wt % Ru/OMS-2_H >1 wt % Ru/OMS-2_R. Hydrogenation of LA to GVL is a two-step reaction in which firstly LA is hydrogenated to form hydroxypentanoic acid which further undergoes dehydration to form GVL. In the presence of acid sites, dehydration is very fast and hence, acidity of OMS-2 can play an important role. Differently synthesized OMS-2 have acidity in the following order 1 wt % Ru/OMS-2_S (highest)>1 wt % Ru/OMS-2_H >1 wt % Ru/OMS-2_R (least). Our results are also in the same order. Apart from acidity, surface area and active metal dispersion on the 1 wt % Ru/OMS-2_S is also high and hence, it shows the maximum activity for the reaction. OMS-2 prepared by the solvent-free method is superior to other methods. The performance of 1wt %Ru/OMS-2_S catalyst for production of GVL in water was compared with the activity of previously reported literature [152,153,172–176,90,177] (Table 4.6). In the present work, the main aspect of 1 wt %Ru/OMS-2_S catalyst is a high S/M ratio (substrate to metal mole ratio). The 99.9 % yield of GVL with 100 % selectivity over 1wt %Ru/OMS-2_S catalyst at 100 ºC, 30 atm H_2 in 1h, corresponding to S/M of 3831.Yulei et al. reported LA conversion of 100 % with GVL yield of 99.9 % at 70 ºC with high S/M value (4789), but

the pressure was 40 atm and the reaction time was long (4h). Hence, 1wt %Ru/OMS-2S catalyst showed competitive activity towards the production of GVL from LA in an aqueous medium.

Table 4.5 Catalytic Performance of Ru Catalysts in the synthesis of GVL from LA in an aqueous medium.

No.	Catalyst	T (°C)	H_2 source	t(h)	Conversion (%)	Y_{GVL} (%)	S/M	Ref
1	(5%Ru/SBA-15)	150	Formic acid	5	31	21	204	172
2	5%Ru/Al_2O_3	150	Formic acid	5	16	22	204	172
3	5%Ru/TiO_2	150	Formic acid	5	10	3	204	172
4	5%Ru/C	150	Formic acid	5	100	90	204	172
5	5%Ru/Hydroxyapatite	70	5 atm H_2	4	99	99	351	173
6	Ru-NPs	130	25 atm H_2	24	100	99	307	174
7	Ru/C	190	Formic acid	2	87	75	581	175
8	Ru/TiO_2	30	50 atm H_2	1	64	62	296	176
9	Ru/TiO_2	70	50 atm H_2	1	99	95	296	176
10	(1 wt%)Ru/TiO_2	70	40 atm H_2	4	100	99.9	4789	177
11	(0.6 wt%)Ru/TiO_2	150	35 atm H_2	5	100	93	---	178

12	5 wt%Ru/C	130	12 atm H_2	3	99.5	86.2	359	152
13	2%Ru/FLG	20	40 atm H_2	8	99.3	99.3	1460	153
14	1wt %Ru/OMS-2_S	100	30 atm H_2	1	99.9	99.9	3831	This work
15	1wt %Ru/OMS-2_H	100	30 atm H_2	1	70	69.93	3831	This work
16	1wt %Ru/OMS-2_R	100	30 atm H_2	1	58	57.94	3831	This work

Note Y: yield of GVL, S/M: molar ratio of substrate (LA) to active metal (Ru).

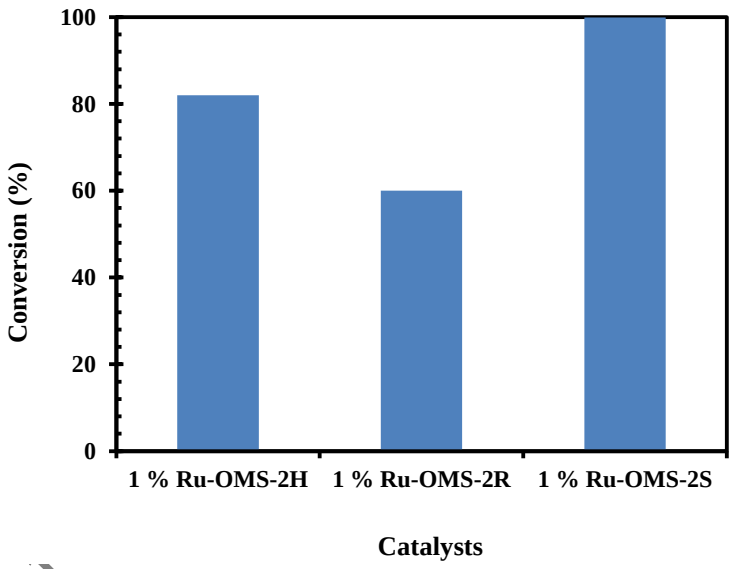

Figure 4.8 Effect of various catalysts on conversion of LA: LA 7.5×10^{-4} mol/cm^3, speed of agitation 800 rpm, temperature 100 ºC, total volume 40 cm^3 (water solvent), H_2 pressure 30 atm, reaction time 1 h, catalyst loading 2.5×10^{-3} g/cm^3

4.4.11 Effect of speed of agitation

The effect of agitation speed was studied from 600 to 1000 rpm in order to understand the effect of external mass transfer resistance on the rate of reaction. Figure 4.9 shows beyond 800 rpm there is no effect on the conversion of LA signifying that the mass transfer resistance was absent. Thus, 800 rpm taken for further experiments.

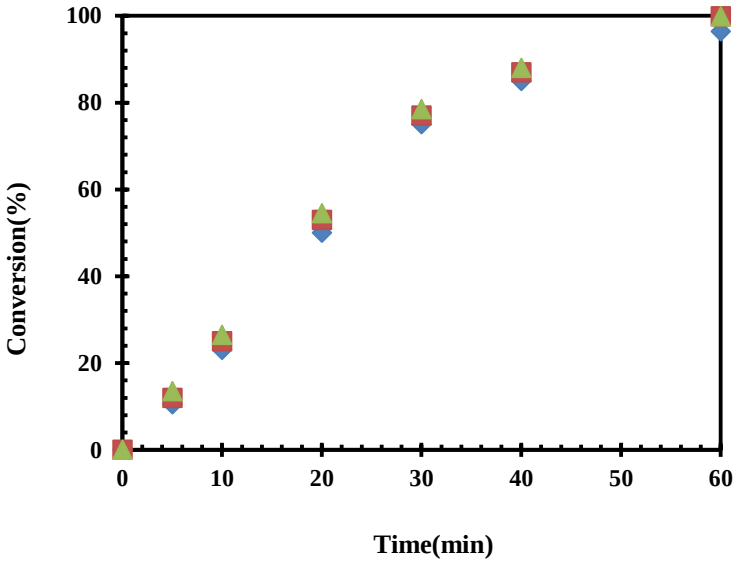

Figure 4.9 Effect of speed of agitation on conversion of LA: LA 7.5×10^{-4} mol/cm^3, catalyst 1 wt% Ru/OMS-2$_S$, temperature 100 ºC, total volume 40 cm^3 (water solvent), H_2 pressure-30 atm, reaction time 1 h, catalyst loading 2.5×10^{-3} g/cm^3 (♦) 600 rpm, (■) 800 rpm, (▲) 1000 rpm.

4.4.12 Effect of catalyst loading

Figure 4.10 depicts the effect of catalyst loading on conversion of LA from 0.6×10^{-3} to 3.7×10^{-3} g/cm^3. The conversion increases with increase in catalyst amount up to 2.5×10^{-3}g/cm^3, which is due to the linear increase in the number of active sites. However, beyond the 2.5×10^{-3}g/cm^3 catalyst loading, no significant change in conversion was observed within the experimental error. Thus, further reactions were carried out at 2.5×10^{-3}g/cm^3. Figure 4.11 shows the initial rate of reaction increases linearly with the catalyst loading which confirms that mass transfer resistance is not acting.

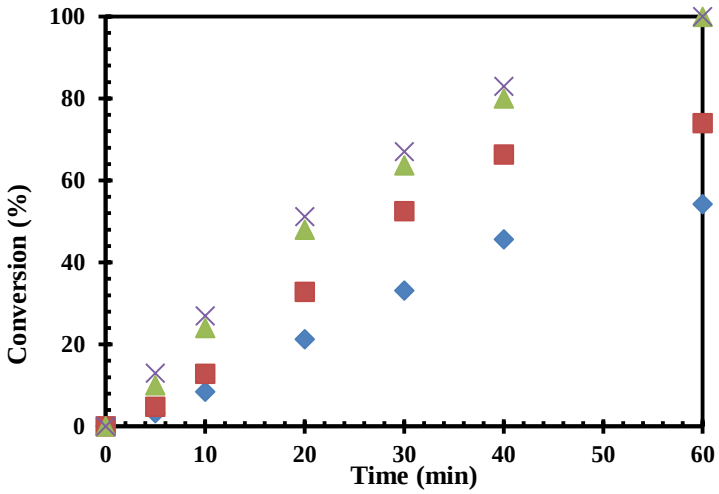

Figure 4.10 Effect of catalyst loading on conversion of LA: LA 7.5×10^{-4} mol/cm^3, catalyst 1 wt% Ru/OMS-2$_S$, temparature-100 ºC, total volume 40 cm^3 (water solvent), H_2 pressure 30 atm, reaction time 1h, speed of agitation 800 rpm. (♦)0.6×10^{-3} g/cm^3, (■) 1.2×10^{-3} g/cm^3, (▲)2.5×10^{-3} g/cm^3, (x) 3.7×10^{-3} g/cm^3.

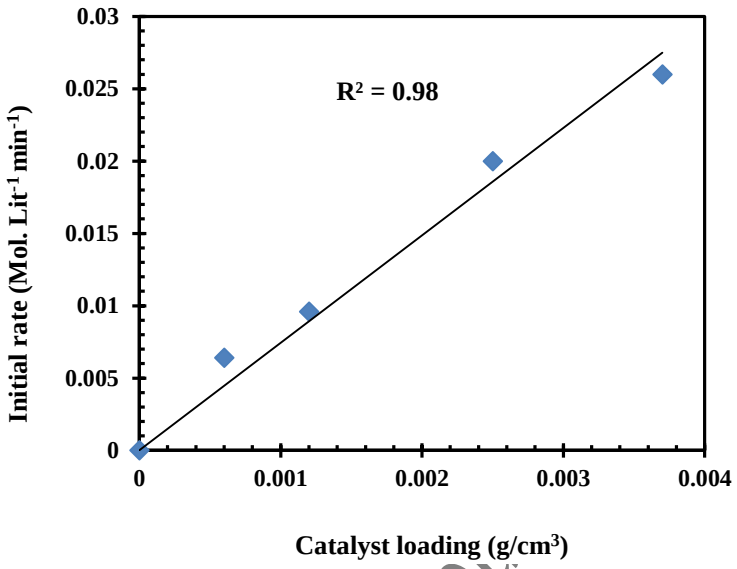

Figure 4.11 Plot of initial rate versus catalyst loading: LA 7.5×10^{-4} mol/cm^3, catalyst 1 wt% Ru/OMS-2$_S$, temparature-100 ºC, total volume 40 cm^3 (water solvent), H_2 pressure 30 atm, reaction time 1h, speed of agitation 800 rpm.

4.4.13 Effect of hydrogen pressure

The influence of hydrogen pressure on the conversion of LA was studied from 10 to 40 atm (Figure 4.12). With the increase in hydrogen pressure, the solubility of hydrogen increases and therefore, the rate of hydrogenation of LA also increases up to 30 atm. There was no significant difference in the conversion of LA at 40 atm due to the constant concentration of hydrogen on active sites. Therefore, further experiments were carried out at a hydrogen pressure of 30 atm.

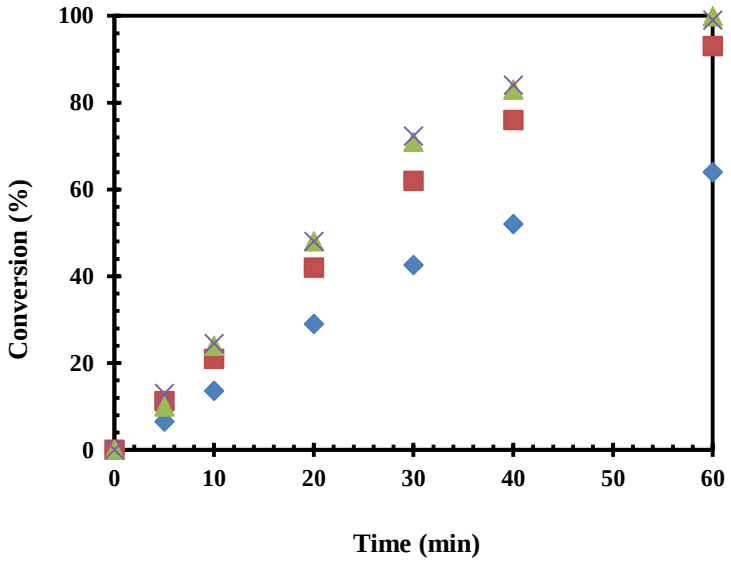

Figure 4.12 Effect of hydrogen pressure on conversion of LA: LA 7.5×10^{-4} mol/cm^3, catalyst 1 wt% Ru/OMS-2$_S$, temperature 100 ºC, total volume 40 cm^3 (water Solvent), reaction time 1 h, speed of agitation 800 rpm, catalyst loading 2.5×10^{-3} g/cm^3 (♦) 10 atm, (■) 20 atm, (▲) 30 atm, (x) 40 atm.

4.4.14 Effect of LA concentration

Figure 4.13 shows the effect of LA concentration from 4.2×10^{-4} to 12.5×10^{-4} mol/cm^3. With increase in concentration reaction rate increases but the conversion of LA decreases which is due to the very high concentration of LA and decrease in vacant site to substrate ratio. At 7.5×10^{-4} mol/cm^3 high rate and conversion was observed. Hence, the further studies were carried out at 7.5×10^{-4} mol/cm^3.

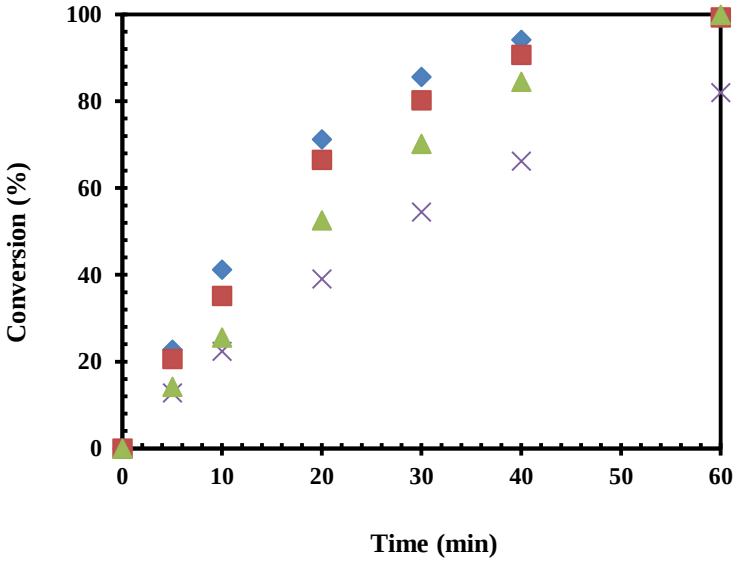

Figure 4.13 Effect of LA concentration on conversion of LA: Speed of agitation 800 rpm, catalyst 1 wt% Ru/OMS-2_S, temperature 100 ºC, total volume 40 cm^3 (water solvent), H_2 pressure 30 atm, reaction time 1 h, catalyst loading 2.5×10^{-3} g/cm^3 (♦) 4.2×10^{-4} mol/cm^3, (■) 5.0×10^{-4} mol/cm^3, (▲) 7.5×10^{-4} mol/cm^3, (x) 12.5×10^{-4} mol/cm^3

4.4.15 Effect of temperature

Figure 4.14 shows the effect of temperature on the conversion of LA in the hydrogenation reaction. Temperature was varied from 80 to 110 ºC to study its significance on the rate of hydrogenation. The increase in conversion of LA with an increase in temperature confirmed that the reaction is kinetically controlled.

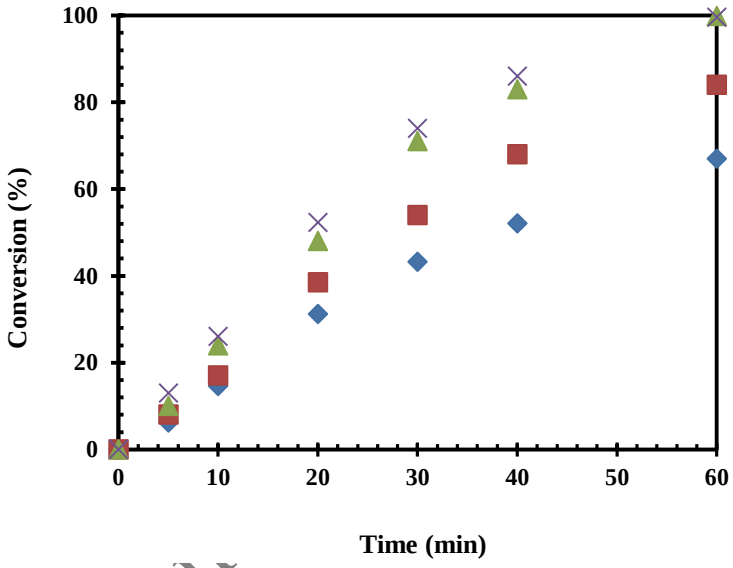

Figure 4.14 Effect of temperature on conversion of LA: LA 7.5×10^{-4} mol/cm^3, catalyst 1 wt % Ru/OMS-2_S, speed of agitation 800 rpm, total volume 40 cm^3 (water solvent), H_2 pressure 30 atm, reaction time 1 h, catalyst loading 2.5×10^{-3} g/cm^3 (♦) 80 ºC, (■) 90 ºC, (▲) 100 ºC, (x) 110ºC

4.4.16 Reaction mechanism and mathematical model

Reaction mechanism for the formation of GVL from LA on 1 wt % Ru/OMS-2_S catalyst is shown in scheme 4.2. Hydrogen is dissociatively adsorbed on the metal surface and LA gets adsorbed subsequently on acid sites. The reaction between adsorbed species gives HPA which undergoes hydrolysis and forms GVL.

Based on above and using LHHWS mechanism a mathematical model is developed same as reported earlier[125,126,178]and detail derivation is given below .

The detail kinetic model is developed assuming dissociative adsorption of hydrogen on ruthenium metal site.

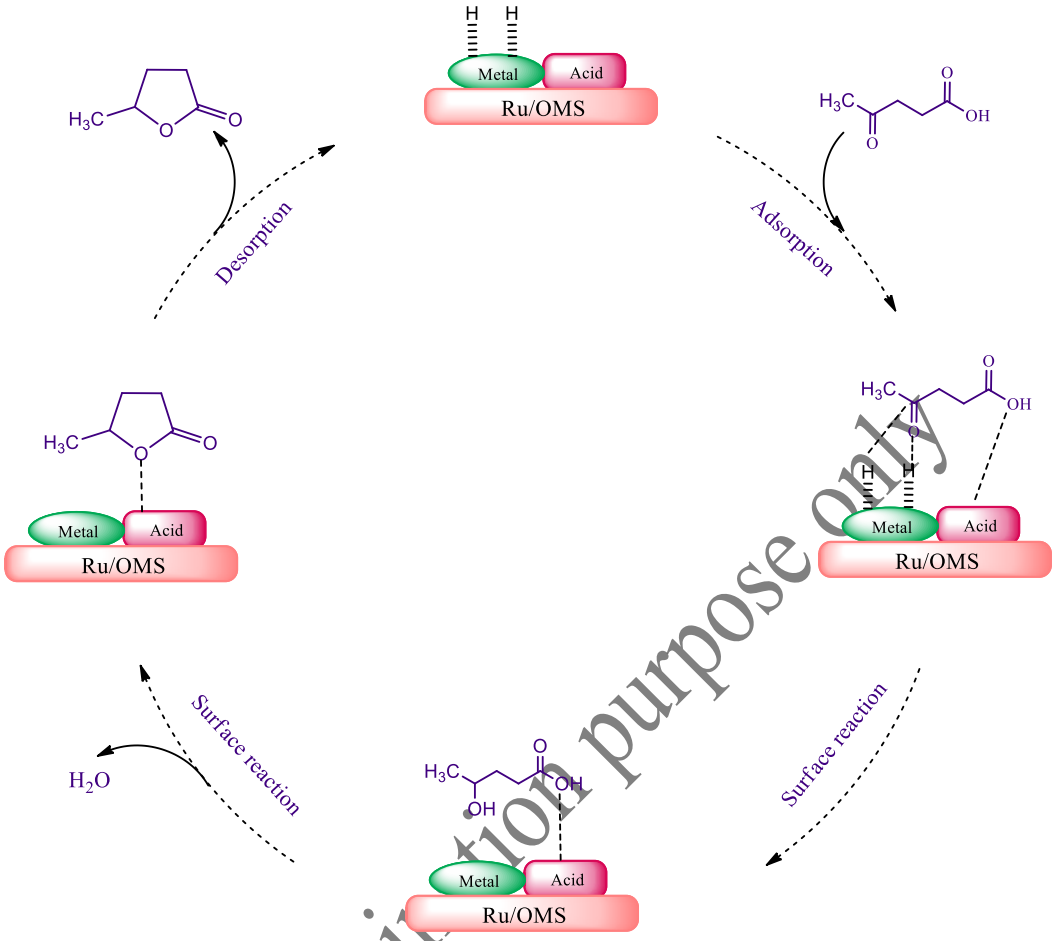

Scheme 4.2 Reaction mechanism of hydrogenation of LA to GVL

Different steps are given as:

Adsorption of LA on metal site S_m

$$A + S_a \xleftrightarrow{K_A} A.S_a \quad (1)$$

Dissociative adsorption of hydrogen on metal site

$$H_2 + 2S_m \xrightarrow{K_B} 2H.S_m \quad (2)$$

Surface reaction of adsorbed LA and hydrogen on adjacent metal sites

$$A.S_a + H.S_m \xrightarrow{k_1} C.S_a + S_m \quad (3)$$

Dehydration reaction on acid site to form GVL

$$C.S_a \xrightarrow{k_2} D.S_a + W \quad (4)$$

Desorption of LA on acid site

$$D.S_a \xleftrightarrow{1/K_{Da}} D + S_a \quad (5)$$

The hydrogenation reaction of LA on metal site was assumed to be rate controlling step.

$$-r_A = k_1 C_{A.S_a} C_{H.S_m} - k_1^{'} C_{C.S_a} C_{S_m} \quad (6)$$

$$-r_A = k_1 K_A C_A \sqrt{K_H P_{H_2}} C_{S_a} C_{S_m} - k_1^{'} K_C C_C C_{S_a} C_{S_m} \quad (7)$$

$$C_{t_m} = C_{S_m} + \sqrt{K_H P_{H_2}} C_{S_m} \quad (8)$$

$$C_{S_m} = \frac{C_{t_m}}{\left[1+\sqrt{K_H P_{H_2}}\right]}$$

$$C_{t_a} = C_{S_a} + K_A C_A C_{S_a} + K_C C_C C_{S_a} + K_D C_D C_{S_a}$$

$$C_{S_a} = \frac{C_{t_a}}{[1+K_A C_A + K_C C_C + K_D C_D]} \quad (9)$$

From equations 6-9 we have

$$-r_A = \frac{\left[k_1 K_A C_A \sqrt{K_H P_{H_2}} - k_1^{'} K_C C_C\right] C_{t_a} C_{t_m}}{\left[1+K_A C_A + K_C C_C + K_D C_D\right]\left[1+\sqrt{K_H P_{H_2}}\right]} \quad (10)$$

For initial rate of reaction,

$$-r_A = \frac{k_1 K_A C_A \sqrt{K_H P_{H_2}} C_{t_a} C_{t_m}}{\left[1+K_A C_A\right]\left[1+\sqrt{K_H P_{H_2}}\right]} \quad (11)$$

$$-r_A = \frac{k_1 w K_A C_A \sqrt{K_H P_{H_2}}}{\left[1+K_A C_A\right]\left[1+\sqrt{K_H P_{H_2}}\right]} \quad (12)$$

From equation 12, we have calculated different adsorption constant and rate constant at different temperature and listed in Table 6. Arrhenius plot (Figure 4.15) was made by using calculated rate constant and the activation energy was found to be 11.75 kcal/mol. This further confirms that reaction is kinetically controlled.

Table 4.6 Values of Reaction Rate Constant and Adsorption Constants for Hydrogenation of LA.

Temp (°C)	k_1 (L^2 mol^{-1} g^{-1} min^{-1})	K_A ($L.mol^{-1}$)	K_H ($L.mol^{-1}$)

80	0.06	0.90	5.20
90	0.08	0.75	4.16
100	0.14	0.65	3.13
110	0.22	0.45	2.32

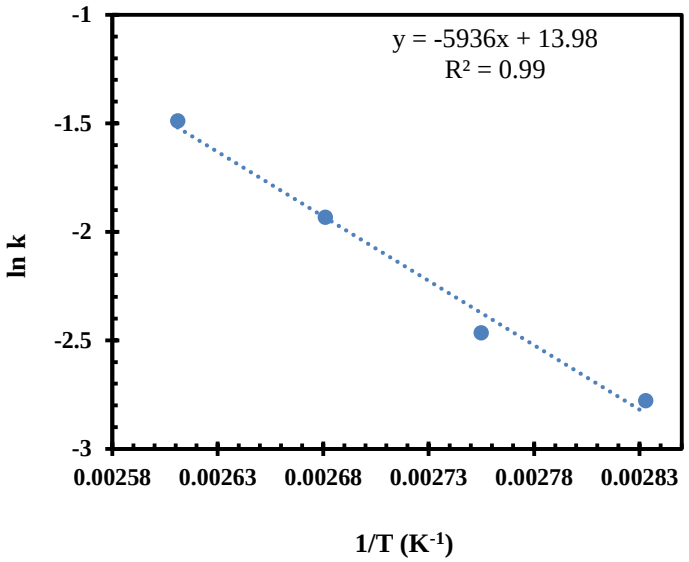

Figure 4.15 Arrhenius plot

4.4.17 Reusability of catalyst

The reusability of 1 wt% Ru/OMS-2_S catalyst for hydrogenation of LA was studied under the optimized conditions: temperature 100 °C, catalyst loading 2.5×10^{-3} g/cm^3, agitation speed 800 rpm and reaction time of 1 h. The catalyst was filtered and washed with methanol five times in order to eliminate absorbed substance from the catalyst. It was dried at 100°C. The losses of catalyst were made up with fresh catalyst in the next experiment. Figure 4.16 shows that 1 wt % Ru/OMS-2_S catalyst is reusable and very stable up to four times without significant loss of activity.

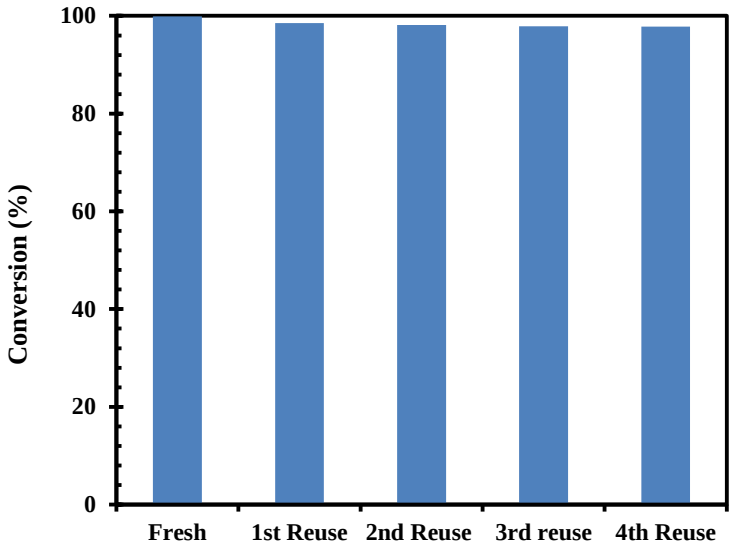

Figure 4.16 Catalyst reusability: LA 7.5×10^{-4} mol/cm^3, catalyst 1 wt % Ru/OMS-2$_S$, speed of agitation 800 rpm, temperature 100 ºC, total volume 40 cm^3 (water solvent), H_2 pressure 30 atm, reaction time 1 h, catalyst loading 2.5×10^{-3} g/cm^3

4.4.18 Stability of catalyst

The catalyst stability was verified by hot filtration method. The reaction was stopped after 15 min, the catalyst filtered and reactor washed with water in order to collect the traces of catalyst particle from the reactor, if any. The reaction mass was then again fed to reactor and reaction was continued for 1h. The sample after 1 h was analyzed to see the progress of the reaction. The conversion of LA was almost constant which confirms that there was no leaching in reaction. Also, we did the ICP-AES of reaction mass and found less than 0.0001 ppm of Ru which is negligible. It further confirms that catalyst is highly stable.

4.5 Conclusion

A novel 1wt% Ru/OMS-2$_S$ catalyst prepared by wet impregnation was used for hydrogenation of LA to GVL in an aqueous medium, with high conversion of LA and high yield of GVL with the low loading of Ru (1 wt %). Three different methods (Hydrothermal, Solventless, and Reflux) of OMS supports were prepared in which OMS-2$_S$ was the best support for Ru. The synthesized 1 wt% Ru/OMS-2$_S$ catalyst exhibited excellent stability and activity in water due to higher Ru dispersion and acidity than other catalysts. It was found that the LA conversion rate was mainly related to the acidity and Ru dispersion of the catalyst. The highest GVL yield of 99.9 % and LA conversion of 99.9 % were achieved

at 100º C and 30 atm after 1 h. The catalyst was used four times and shows excellent reusability. Various parameters were studied systematically to establish LHHW kinetics and the apparent activation energy for hydrogenation of LA was found to be 11.75 kcal/mol.

CHAPTER 5

POTASSIUM MODIFIED LA-MG MIXED OXIDE AS ACTIVE AND SELECTIVE CATALYST FOR MONO-METHYLATION OF PHENYLACETONITRILE WITH DIMETHYL CARBONATE

J. Molleti, G.D. Yadav, Potassium modified La-Mg mixed oxide as active and selective catalyst for mono-methylation of phenylacetonitrile with dimethyl carbonate, Mol. Catal. 438 (2017) 66–75.

5.1 Abstract

Herein, we report incipient wet impregnation of potassium promoted lanthanum-magnesium oxide. It is used first time for the selective mono-methylation of phenylacetonitrile to 2-phenyl propionitrile with dimethyl carbonate as a methylating agent. The catalyst with different loadings of potassium (1-4 wt %) on La_2O_3-MgO was prepared and the activity of catalyst verify for the mono-methylation of phenylacetonitrile with dimethyl carbonate. Two wt % K/ La_2O_3-MgO catalyst showed 100 % of conversion of phenylacetonitrile and 100 % selectivity of 2-phenyl propionitrile at 150 ºC after 2 h. The characterization of 2 wt % K/ La_2O_3-MgO was done using different techniques such as FTIR, SEM, TGA-DSC, CO_2-TPD, XRD, and BET surface area analysis. Two wt % K/ La_2O_3-MgO catalyst was used to study the reaction mechanism, and a kinetic model was developed using LHHW type of mechanism. The apparent activation for mono-methylation of phenylacetonitrile to 2-phenyl propionitrile is found to be 13.77 kcal/mol.

5.2 Introduction

Developing strategies for the synthesis of fine chemicals using economical and environmentally clean process is a current trend. Most of these technologies employ homogeneous catalysts, which are difficult to recover and recycle. Hence, substitution of homogeneous catalysts by heterogeneous catalysts is essential to make the process green [179]. Over the years, various solid bases have been used for the production of fine chemicals [31,180,181]. During past few recent years, monomethylated products of phenyl acetonitrile (PAN) derivatives have been used for the preparation of non-steroidal anti-inflammatory drugs (NSAID) such as Ketoprofen, Ibuprofen, and Naproxen. These are commercially well known and used to treat pain, swelling, fever, and inflammation [182,183]. In industry, base catalyzed monomethylation of methylene-active compounds using usual methylating agents (methyl halides or dimethyl sulfate) is not easy because the reaction mainly proceeds towards the formation of dimethyl derivatives [184,185]. These methylating agents are toxic, corrosive and those methods require a stoichiometric amount of strong base to neutralize acidic by-products. Hence, there was a need to develop in the synthesis of heterogeneous catalytic materials and green alkylating agents. Dimethyl carbonate (DMC), which is a green, safe, and cheap reagent has been reported as a potential

methylating agent [182]. Therefore, DMC is considered as an environmentally friendly substitute for those hazardous methylating reagents [186].

The synthesis of 2-phenylpropionitrile (2-PPN) by monomethylation of PAN with DMC had been extensively investigated using phase transfer catalysts (PTC). Tundo et al. [187–189] reported 99.5 % 2-PPN selectivity for the reaction of PAN with DMC using gas liquid PTC and homogeneous catalysts (organic bases and alkali metal carbonates). However, there was still big problems to use homogeneous systems with the drawbacks such as separation, recovery and recycle. Fu and Ono [190] reported vapour phase monomethylation of PAN with methanol as an alkylating agent using alkali- exchanged zeolites. Normally, zeolite catalysts required higher reaction temperature and they produced various side products. Singh et al. [191] reported with 98.4 % conversion of PAN and 92 % selectivity to 2-PPN with DMC using NH_2-Na-Al-MCM-41catalyst for 10 h at 180 ºC. Kaneda et al. [192] reported monomethylation of PAN over Ru/HT catalyst at 180 ºC with 98 % yield of 2-phenylbutyronitrile using ethanol as a methylating agent at higher reaction time (20 h). However, these reported catalysts are not favorable due to harsh condition and long reaction time. Thus, development of highly active, stable and recyclable catalyst for the efficient synthesis of 2-PPN is highly desired.

In the past decades, mixed oxides have been widely used as solid base catalysts due to their unique chemical and physical properties [76]. Lanthanum oxide (La_2O_3) is one of the strongest basic oxides but it has low activity due to its low surface area. The activity of La_2O_3 is increased when it mixed with magnesium oxide (MgO) due to increasing basicity [77,78]. The Mg-La mixed oxide was reported in various chemical reactions like Wadsworth-Emmons reaction [50], transesterification reaction [51], Wittig reaction [45], synthesis of glycerol carbonate [52], Michael addition reaction [53] and epoxidation of olefins [54]. Stronger basic sites generate with the loading of alkali or alkaline earth metal on the support materials [79]. Several researchers reported that the use of potassium precursors like KOH [68], K_2CO_3 [193], KNO_3 [63,64] and KF [194] can help the formation of solid super base. Recently, Yin et al. [73] reported solvent-free Knoevenagel condensation over 10 wt % KOH/La_2O_3-MgO as a solid super base. Based on their results we synthesized solid base catalyst using La-Mg mixed oxide as support and potassium as a modifier.

In the present work, we report a selective monomethylation of PAN using DMC over 2 wt % K/ La_2O_3-MgO catalyst. The fresh and spent 2 wt % K/ La_2O_3-MgO catalysts

were characterized by various techniques. The catalyst activity was compared by using various solid base catalysts such as MgO, La_2O_3, and different loadings of potassium on La-Mg mixed oxide support. The effect of different parameters was studied systematically to establish the reaction mechanism and kinetics.

5.3 Experimental

5.3.1 Materials

Phenyl acetonitrile and dimethyl carbonate were procured from SD Fine chemicals limited, Mumbai. Magnesium nitrate, Lanthanum nitrate, urea and potassium carbonate were procured from Thomas Baker Chemicals, Mumbai.

5.3.2 Catalyst synthesis

Lanthanum- magnesium mixed oxide (La_2O_3-MgO) with a different mole ratio of La and Mg were prepared by a hydrothermal method using urea as a precipitating agent [195].

The role of urea as a precipitating agent is well described by Ogawa et al. [196]. The typical process for the synthesis of La: Mg with 1:3 molar ratio is as follows, 2.1 g of La $(NO_3)_3$. $9H_2O$, 3.86 g of Mg $(NO_3)_3.H_2O$ and 6 g of urea were dissolved in 150 mL distilled water and stirred for 1 h until the solution became homogeneous. Then it was transferred into Teflon lined bomb reactor and heated at 160 ºC for 12 h in a muffle furnace. The solid material was washed with distilled water. After filtration, the solid material was dried at 120 ºC. MgO and La_2O_3 catalyst were prepared by the same procedure as described earlier and calcined at 650 ºC for 4 h. Similarly, we use the same method for the preparation of La_2O_3 and MgO catalysts.

Potassium modified La_2O_3-MgO was prepared by incipient wetness impregnation method. The required quantity of potassium carbonate dissolved in 2 mL water. The resultant solution was added to 1 g of La_2O_3-MgO via wet impregnation technique, under vigorous agitation at 80 ºC. On completion of adsorption of Potassium solution onto the surface of mixed oxide, the resultant solid dried at 100 °C for 10 h and calcined at 650 ºC for 4 h. Here we prepared 1 to 4 wt % K on La_2O_3-MgO by taking the appropriate amount of precursor and catalyst were named as 1wt % K/ La_2O_3-MgO, 2 wt % K/ La_2O_3-MgO, 3 wt % K/ La_2O_3-MgO and 4 wt % K/ La_2O_3-MgO, respectively.

5.3.3 Characterization methodology

Catalysts were characterized by different techniques. The detailed description of characterization methodology is given in chapter 4 (Section 4.2.4)

5.3.4 General procedure for methylation of PAN

All experiments were carried out in a 100 ml Amar (Mumbai, India) autoclave equipped with pitched turbine impeller and controllers for pressure and temperature. In a standard experiment, 0.034 mole of PAN, 1.025 mole of DMC and 0.2 mL of n-decane as an internal standard with a catalyst loading of 0.03 g/ cm^3 against total volume (30 cm^3) of the liquid. The reaction mass was heated at 150 °C and 1000 rpm for 2 h. At regular intervals of time sample was taken out for the analysis.

5.3.5 Method of analysis

Samples were withdrawn occasionally from the reaction mass and analyzed by GC equipped with a capillary column BPX-50 (length 30 m and inner diameter 0.25 mm) and FID detector. Product confirmation was carried out by GC-MS from Perkin Elmer, Clarius model 500 on Elite-1 capillary column of length 30 m and inner diameter 0.25 mm. The conversions were based on the decrease in conversion of the limiting reagent, PAN.

5.4 Results and Discussion

5.4.1 XRD

The XRD patterns of La_2O_3-MgO and K/ La_2O_3-MgO with different wt % loadings of potassium are depicted in Figure 5.1. La_2O_3-MgO (Figure 5.1 (a)) catalyst showed the presence of $La_2(CO_3)_2(OH)_2$ signal at 2θ=30.36°, in addition to La_2MgO_X (JCPDS:42-339), La_2O_3 (JCPDS:40-1281) and MgO (JCPDS: 27-759). The existence of La_2MgO_X confirms the interaction between the La_2O_3 and MgO constituents during the synthesis of La_2O_3-MgO [46,78]. All potassium loaded catalysts showed similar XRD patterns of La_2O_3-MgO because potassium can be well dispersed on the La_2O_3-MgO support. Figure 5.1 (b), (c), (d), (e) and (f) shows no typical diffraction peaks corresponding to the K_2CO_3 (2θ =12°,25°, 32°,38° and 41°), which suggests that potassium carbonate has completely decomposed. With the loading of potassium, there was disappearance of La_2O_3 peak at 2θ=30.36° and the detection of new peak attribute to K_2O (JCPDS: 27-431) [197,198]. This K_2O phase may be the cause of basicity of catalyst and high catalytic activity. The

crystalline size of the La_2O_3-MgO and 2 wt % K/ La_2O_3-MgO was calculated using Scherrer's formula. The average crystallite size of La_2O_3-MgO and 2 wt % K/ La_2O_3-MgO was 15.16 nm and 30.89 nm, respectively. The XRD pattern of 2 wt % K/ La_2O_3-MgO and reused catalysts were compared to find that they are almost same which confirms that prepared catalyst is stable.

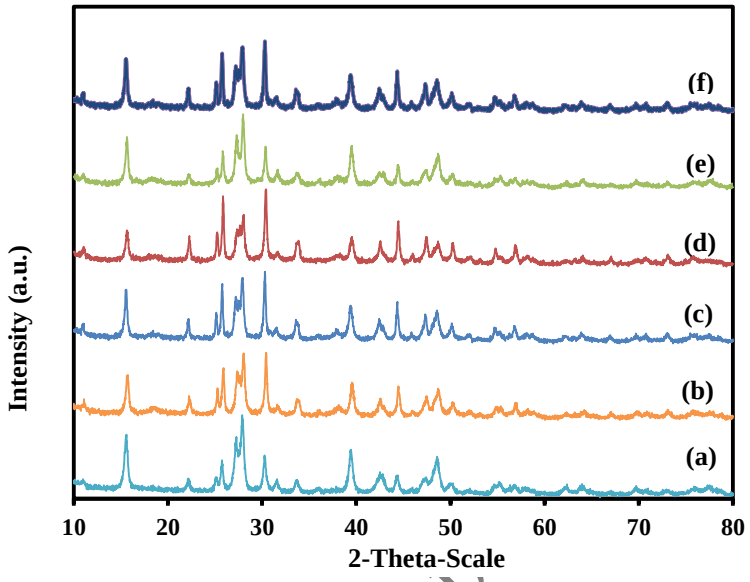

Figure 5.1 XRD pattern of (a) La_2O_3-MgO, (b) 1 wt % K/ La_2O_3-MgO, (c) 2 wt % K/ La_2O_3-MgO, (d) 3 wt % K/ La_2O_3-MgO, (e) 4 wt % K/ La_2O_3-MgO and (f) reused 2 wt % K/ La_2O_3-MgO catalyst.

5.4.2 FT-IR

Figure 5.2 shows FT-IR spectra of La_2O_3-MgO, 1 wt % K/ La_2O_3-MgO, 2 wt % K/ La_2O_3-MgO, 3 wt % K/ La_2O_3-MgO, 4 wt % K/ La_2O_3-MgO and reused 2 wt % K/ La_2O_3-MgO catalyst. 2 wt % K/ La_2O_3-MgO catalyst showed strong band at 650 cm^{-1}, which is attributed to the lattice vibration of lanthanum oxide bond. The band at 3560 cm^{-1}indicates the presence of hydroxide species of adsorbed water molecule and two bands at 1460 and 1380 cm^{-1} are due to the carbonate species. The weak band at 1080 cm^{-1} indicates the presence of symmetric $(CO_3)^{2-}$. The band at 1460 cm^{-1} reveals that the inclusion of potassium promotes the formation of basic sites and the adsorption of carbon dioxide on the surface of La_2O_3-MgO. FT-IR spectra of virgin and used catalyst signifies that there were no structural changes. It also indicates that there were no externally adsorbed species on the surface of the 2 wt % K/ La_2O_3-MgO catalyst.

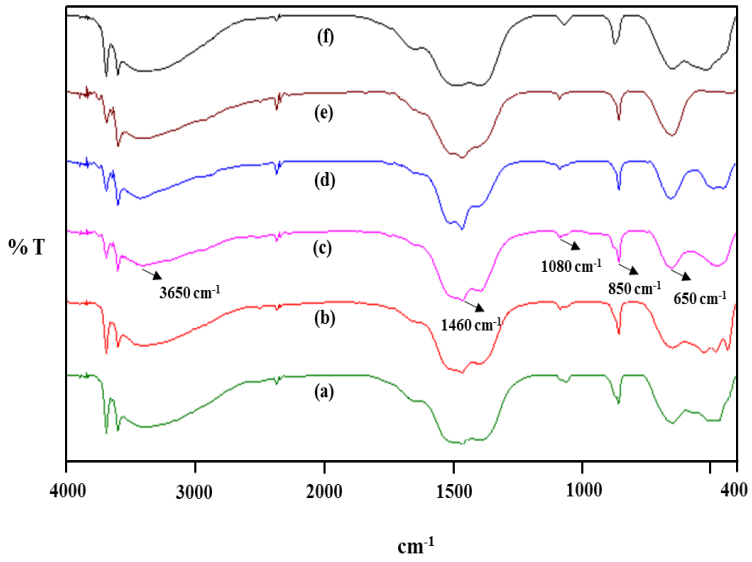

Figure 5.2 FT-IR of (a) La_2O_3-MgO, (b) 1 wt % K/ La_2O_3-MgO, (c) 2 wt % K/ La_2O_3-MgO, (d) 3 wt % K/ La_2O_3-MgO, (e) 4 wt % K/ La_2O_3-MgO and (f) reused 2 wt % K/ La_2O_3-MgO catalyst.

5.4.3 Surface area and pore size analysis

N_2 adsorption/desorption isotherms of samples are depicted in Figure 5.3. All the catalysts showed that they have the form of type-IV isotherm, and type H3 hysteresis loop, indicates that materials are mesoporous. The surface area, pore volume and average pore diameter of La_2O_3-MgO catalyst are 48 $m^2\ g^{-1}$, 0.13 $cm^3\ g^{-1}$ and 11 nm, respectively (Table 5.1). With increase in the loading of potassium, surface area as well as pore volume decreases. Cosimo et al. [199,200] reported that the introduction of alkali metals on MgO would result in a decrease in surface area and pore volume. The decline in pore volume and surface area upon potassium loading observed over La_2O_3-MgO and K/ La_2O_3-MgO catalysts are in good agreement with the results of SEM and CO_2-TPD analysis. The structural parameters of 2 wt % K/ La_2O_3-MgO and used 2 wt % K/ La_2O_3-MgO catalysts were observed almost same.

Table 5.1 Surface properties of various synthesized catalysts for mono-methylation of PAN

Catalysts	BET surface area (m^2/g)	Average pore diameter (nm)	BJH pore volume (cm^3/g)

La_2O_3-MgO	48	11	0.13
1 wt % K/ La_2O_3-MgO	22	25	0.12
2 wt % K/ La_2O_3-MgO	20	28	0.11
3 wt % K/ La_2O_3-MgO	18	21	0.09
4 wt % K/ La_2O_3-MgO	13	23	0.07
Reused 2 wt % K/ La_2O_3-MgO	19	26	0.10

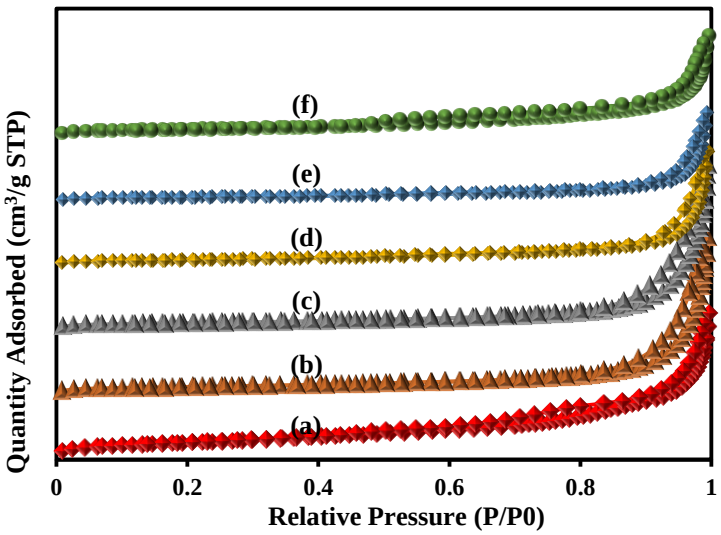

Figure 5.3 N_2 adsorption-desorption plot for the (a) La_2O_3-MgO, (b) 1wt % K/ La_2O_3-MgO, (c) 2 wt % K/ La_2O_3-MgO, (d) 3 wt % K/ La_2O_3-MgO, (e) 4 wt % K/ La_2O_3-MgO and reused (f) 2 wt % K/ La_2O_3-MgO catalyst

5.4.4 DSC-TGA

TGA-DSC analysis of 2 wt % K/ La_2O_3-MgO catalyst was carried out from 50 to 700 ºC (FigureS2). Two endothermic peaks were observed in DSC curve; first peak at 80 to 130 ºC due to the removal of water (humidity) and resulted in 8 % weight loss. Second endothermic peak between 320 ºC and 400 ºC was due to evolution of CO_2 and decomposition of oxycarbonate corresponding to 12 % weight loss to get stable oxide

forms. The overall analysis shows around 20 % weight loss and the catalyst was stable after 450 ºC up to 700 ºC.

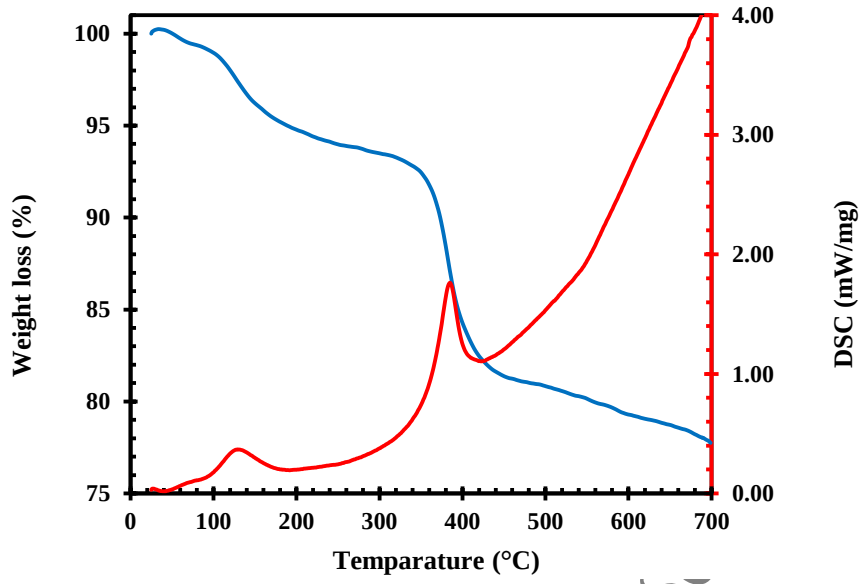

Figure 5.4 TGA-DSC analysis of 2 wt % K/ La_2O_3-MgO

5.4.5 CO_2-TPD

The basicity of all the samples was analyzed by using CO_2-TPD. As showed in Figure 5.5 La_2O_3-MgO catalyst CO_2 desorption peaks were observed at 285 ºC and 470 ºC corresponding to moderate /strong basic sites, and the quantity of CO_2 desorbed were 0.36 and 0.38 $mmolg^{-1}$. The introduction of potassium results in an increase in the desorption temperature and enhancement in the amount of CO_2 desorption. Two wt % K/ La_2O_3-MgO catalyst showed desorption peaks at 106 ºC, 324 ºC, 498 ºC and 745 ºC corresponding to weak, moderate, strong, and super basic sites and the quantity of CO_2 desorbed were 0.15, 0.21, 0.05 and 1.09 $mmolg^{-1}$, respectively. The desorption peak at 745 ºC is a clear indication of super basic sites [201]. Further increasing the concentration of potassium, there is a decline in the basicity of 3 and 4 wt % K/ La_2O_3-MgO catalysts (Table. 5.2). This is due to the coverage of excess potassium on the surface of basic sites. The basicity of fresh and used catalyst showed almost similar results.

Table 5.2 CO_2-TPD analysis for various synthesized catalysts

Catalysts	CO_2-TPD analysis Basicity (mmol g^{-1})		
	Weak	**Moderate/strong**	**Total**
La_2O_3	0.02	0.25	0.27
MgO	0.05	0.31	0.36
La_2O_3-MgO	0.04	0.70	0.74
1 wt % K/ La_2O_3-MgO	0.10	0.88	0.98
2 wt % K/ La_2O_3-MgO	0.15	1.35	1.50
3 wt % K/ La_2O_3-MgO	0.09	1.17	1.26
4 wt % K/ La_2O_3-MgO	0.08	1.05	1.13
Reused 2 wt % K/ La_2O_3-MgO	0.13	1.33	1.46

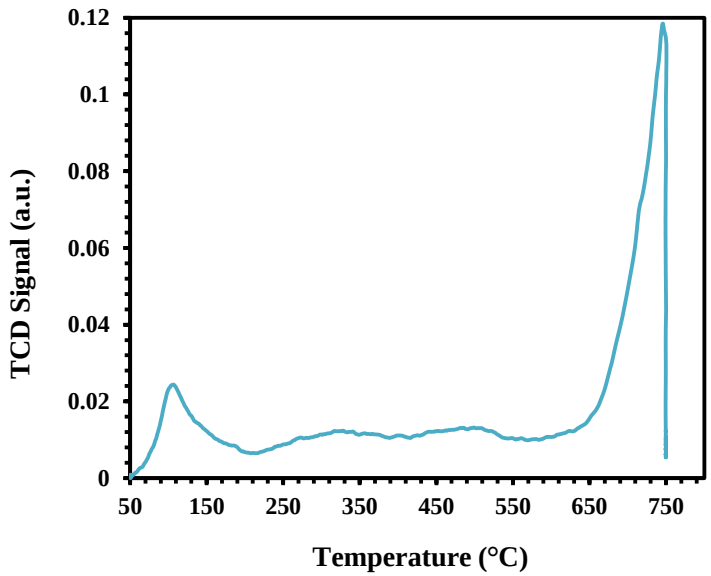

Figure 5.5 CO_2-TPD pattern of 2 wt % K/ La_2O_3-MgO

5.4.6 SEM

The SEM images of La_2O_3-MgO, 2 wt % K/ La_2O_3-MgO catalysts are shown in Figure 5.6. La_2O_3-MgO catalyst forms a spherical and dendritic structure. There is no agglomeration takes place after the introduction of 2 wt % potassium on La_2O_3-MgO. Hence, it is assumed that with low loading of potassium, a high dispersion was obtained and the La_2O_3-MgO support intact its original structure.

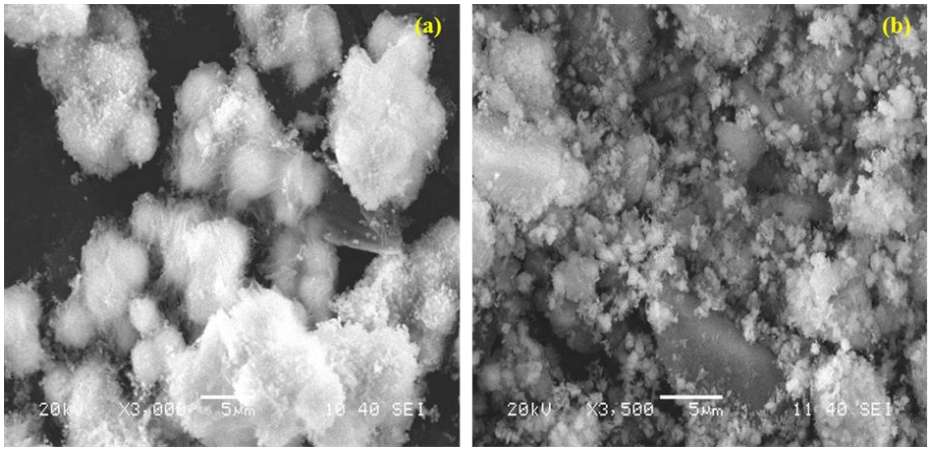

Figure 5.6 SEM images of (a) La_2O_3-MgO and (b) 2 wt % K/ La_2O_3-MgO

5.4.7 Catalytic reaction

The reaction of mono-methylation of PAN by DMC using 2 wt % K/ La_2O_3-MgO catalyst given in Scheme 5.1.

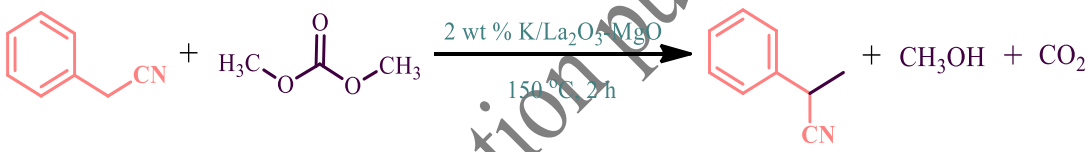

Scheme 5.1 Mono-methylation of PAN by DMC

5.4.8 Efficacy of various catalysts

Mixed oxides have been studied in a number of systems. Hence, a series of potassium loaded on La-Mg oxide catalysts were used to measure their efficacy in the mono-methylation of PAN (Figure 5.7). A catalyst loading of 0.03 g/cm^3 based on the total volume of reaction mixture was employed at a mole ratio of 1: 30 PAN to DMC at 150 ºC and speed of 1000 rpm. A series of catalysts such as MgO, La_2O_3, La_2O_3-MgO, 1wt % K/ La_2O_3-MgO, 2 wt % K/ La_2O_3-MgO, 3 wt % K/ La_2O_3-MgO, and 4 wt % K/ La_2O_3-MgO were developed and characterized. The conversion of PAN was greatly affected by loading of potassium on La_2O_3-MgO. The activity of MgO, La_2O_3, and La_2O_3-MgO were found to be very less due to less basicity. The activity of catalyst increases with increase in loading of potassium, and maximum conversion was obtained at 2 wt %. It is due to increase of moderate and strong basic sites in promoted La_2O_3-MgO catalysts. Further increase of potassium loading on the La_2O_3-MgO leads to decrease in activity. The decline in conversion of PAN could be attributed to the blocking of active sites due to excess amount

of potassium and/or agglomeration of catalyst particles. For the mono-methylation reaction, the optimum potassium loading is 2 wt %, in agreement with the results of BET surface area and CO_2-TPD.

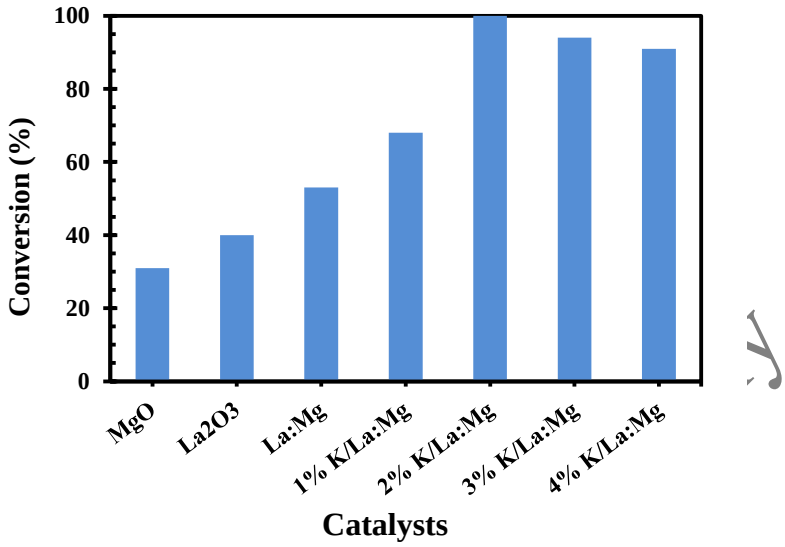

Figure 5.7 Effect of various catalysts on conversion of PAN: PAN 0.034 mol, DMC 1.025 mol, speed of agitation 1000 rpm, temperature 150 ºC, total volume 30 cm^3, reaction time 2 h, catalyst loading 0.03 g/cm^3

5.4.9 Effect of speed of agitation

The effect of agitation speed was varied from 600 rpm to 1200 rpm at 150 ºC (Figure 5.8). There is no change in conversion of PAN at agitation from 1000 rpm to 1200 rpm. Thus, it indicated that there is no effect of mass transfer resistance beyond 1000 rpm. Thus, all reactions were conducted at 1000 rpm.

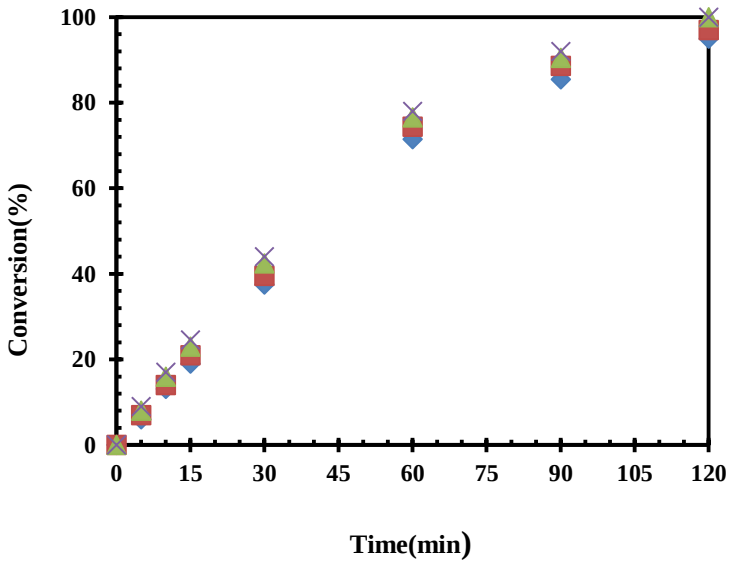

Figure 5.8 Effect of speed of agitation on conversion of PAN: PAN 0.034 mol, DMC 1.025 mol, temperature 150 ºC, total volume 30 cm^3, reaction time 2 h, catalyst loading 0.03 g/cm^3 (♦) 600 rpm, (■) 800 rpm, (▲) 1000 rpm, (x) 1200 rpm

5.4.10 Effect of catalyst loading

In order to evaluate the influence of catalyst loading on conversion of PAN, loadings were studied from 0.01 g/cm^3 to 0.04 g/cm^3. Figure 5.9 shows that up to 0.03 g/cm^3 there is an increase in PAN conversion due to the availability of active sites where as from 0.03 g/cm^3-0.04 g/cm^3 there is no appreciable changes in the conversion of PAN. This happens due to surpassing the number of active sites available for reaction than the number of reactant molecules actually present for the reaction. Figure 5.10 depicts initial rate of reaction increases linearly with the catalyst loading which confirms that mass transfer resistance is not acting.

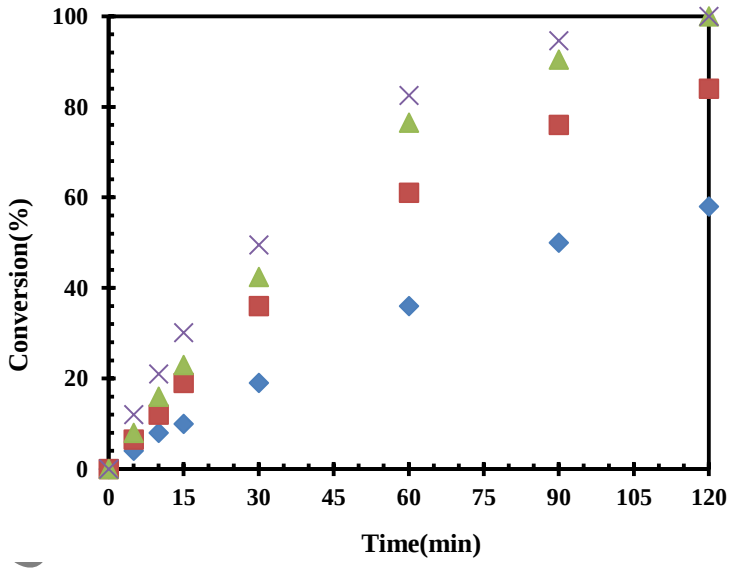

Figure 5.9 Effect of catalyst loading on conversion of PAN: PAN 0.034 mol, DMC 1.025 mol, catalyst 2 % K/ La_2O_3-MgO, temparature-150 ºC, total volume 30 cm^3, reaction time 2 h, speed of agitation 1000 rpm. (♦) 0.01 g/cm^3, (■) 0.02 g/cm^3, (▲) 0.03 g/cm^3, (x) 0.04 g/cm^3

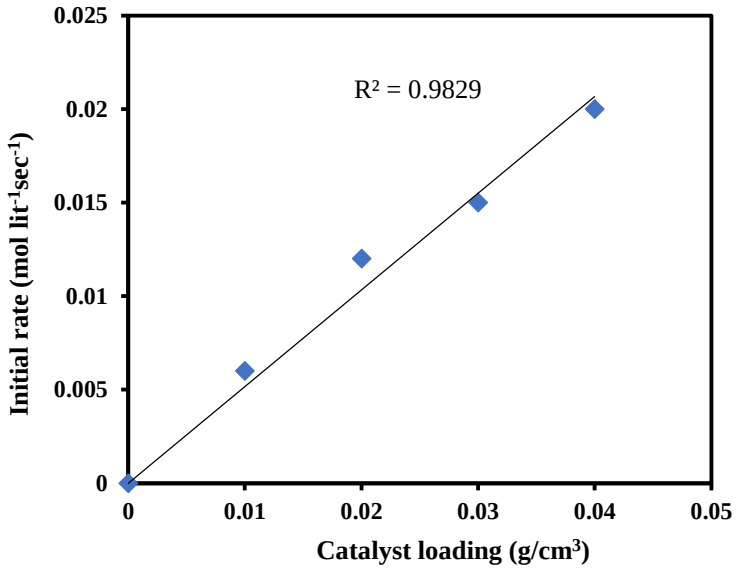

Figure 5.10 Plot of initial rate on conversion of PAN: PAN 0.034 mol, DMC 1.025 mol, catalyst 2 % K/La_2O_3-MgO, temparature-150 ºC, total volume 30 cm^3, reaction time 2 h, speed of agitation 1000 rpm.

5.4.11 Effect of mole ratio of PAN to DMC

Figure 5.11 showed the effect of mole ratio of PAN to DMC were studied from1:10 to 1:40 over 2 wt % K/ La_2O_3-MgO catalyst. PAN conversion was increased with increasing molar ratio. At 1:10 mole ratio, the conversion was 51 % which increased to 100 % at 1:30 mole ratio. Hence mole ratio of 1:30 was selected to be optimum and used for further studies.

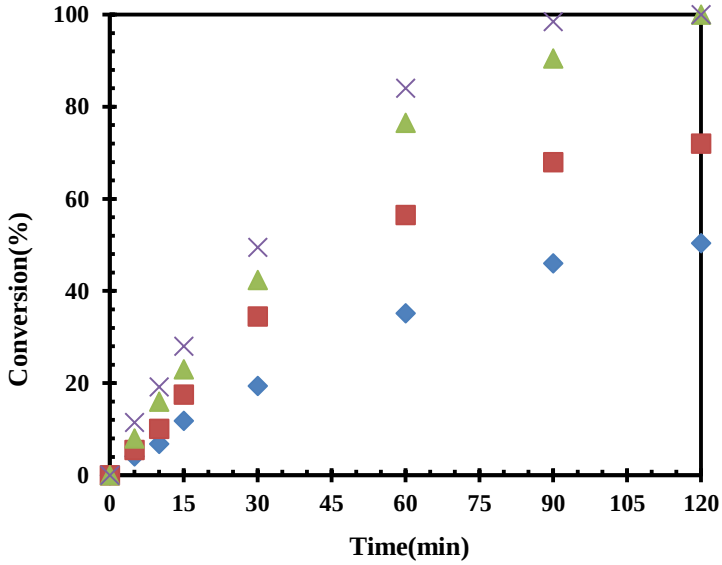

Figure 5.11 Effect of mole ratio on conversion of PAN: PAN 0.034 mol, catalyst 2 % K/ La_2O_3-MgO, temparature-150 ºC, total volume 30 cm^3, reaction time 2 h, speed of agitation 1000 rpm. (♦) 1:10, (■) 1:20, (▲) 1:30, (x) 1:40.

5.4.12 Effect of temperature

The conversion of PAN was studied from 130 to 160 ºC keeping other parameters at optimum conditions (Figure 5.12). The increase in temperature leads to increases the rate of reaction and conversion of PAN increases dramatically, which suggests that reaction is kinetically controlled.

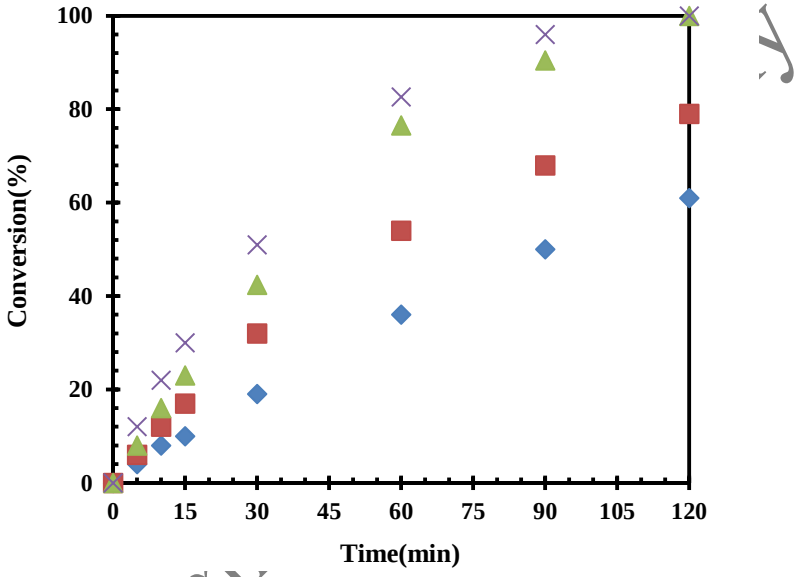

Figure 5.12 Effect of temperature on conversion of PAN: PAN 0.034 mol, DMC 1.025 mol, catalyst 2 % K/ La_2O_3-MgO, speed of agitation 1000 rpm, total volume 30 cm^3, reaction time 2 h, catalyst loading 0.03 g/cm^3. (♦) 130 ºC, (■) 140 ºC, (▲) 150 ºC, (x) 160 ºC

5.4.13 Reaction mechanism and mathematical model

The possible mono-methylation mechanism of PAN with DMC on basic sites of 2 wt % K/ La_2O_3-MgO catalyst is shown in Scheme 5.2. Mono-methylation of PAN (A) with DMC (B) occurs by strong adsorption of PAN on basic sites leading to the formation of 2-PPN.

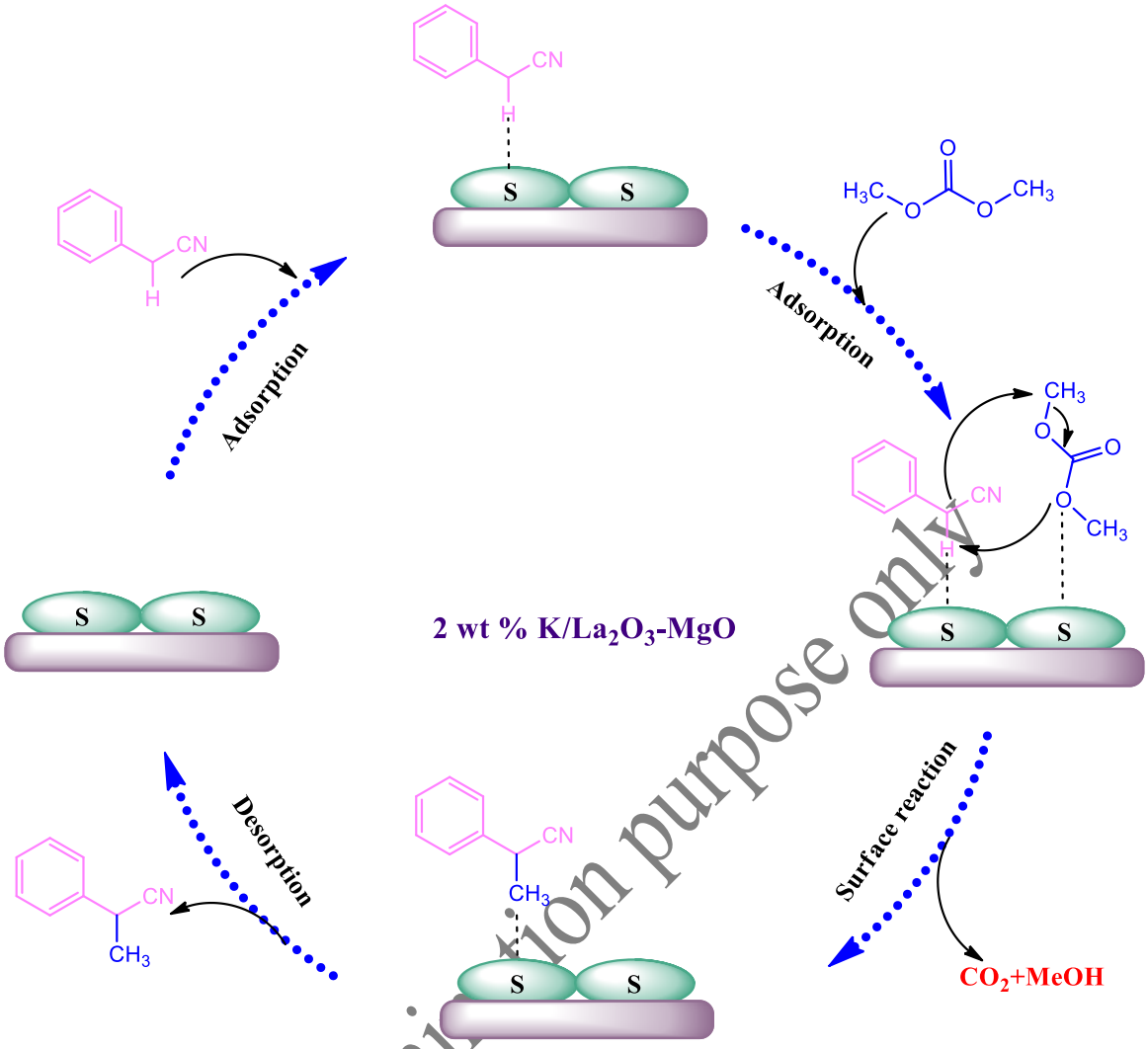

Scheme 5.2 Reaction mechanism of mono-methylation of PAN by DMC

The detail mathematical model was developed using LHHW mechanism as same reported in the recent literature [126,202].

The rate of reaction of PAN can be given as:

Let A = PAN, B = DMC, ES = 2-PPN, W= Methanol, S=vacant sites.

Chemisorption of A and B on vacant site S

Adsorption

Adsorption of PAN (A) on a vacant site S is given by:

$$A + S \xleftrightarrow{K_A} AS \qquad (1)$$

Adsorption of DMC (B) on a vacant site S is given by:

$$B + S \xleftrightarrow{K_B} BS \qquad (2)$$

Surface reaction

Surface reaction of AS and BS in the vicinity of an active site, leading to the formation of ES and WS on the active

$$AS + BS \xleftrightarrow{K_2} ES + WS + CO_2 \quad (3)$$

Desorption of 2-PPN (ES) and methanol (WS) is given by:

$$ES \xleftrightarrow{1/K_E} E + S \quad (4)$$

$$WS \xleftrightarrow{1/K_W} W + S \quad (5)$$

The total concentration of the sites, C_t expressed as,

$$C_t = C_S + C_{AS} + C_{BS} + C_{ES} + C_{WS} \quad (6)$$

Or

$$C_t = C_S + K_A C_A C_S + K_B C_B C_S + K_S C_E C_S + K_W C_W C_S \quad (7)$$

When the adsorption and desorption steps are assumed to be equilibrium,

The concentration of vacant sites can be written as,

$$C_S = \frac{C_t}{\left(1 + K_A C_A + K_B C_B + K_S C_E + K_W C_W\right)} \quad (8)$$

If the surface reaction controls the rate of reaction, then the rate of reaction of A is given by

$$-r_A = -\frac{dC_A}{dt} = k_2 C_{AS} C_{BS} - k_2 C_{ES} C_{WS} p_{CO_2}$$

$$-\frac{dC_A}{dt} = \frac{k_2 \left\{ K_A K_B C_A C_B - \frac{K_E K_W C_E C_W p_{CO_2}}{K_2} \right\} C_t^2}{\left(1 + K_A C_A + K_B C_B + K_S C_E + K_W C_W\right)^2} \quad (9)$$

When the reaction is far away from equilibrium

$$-\frac{dC_A}{dt} = \frac{k_2 C_t^2 K_A K_B C_A C_B}{\left(1 + \sum K_i C_i\right)^2} \quad (10)$$

$$-\frac{dC_A}{dt} = \frac{k_{R_2} w C_A C_B}{\left(1 + \sum K_i C_i\right)^2} \quad (11)$$

Since $k_{R_2} w = k_2 C_t^2 K_A K_B$ where, w is catalyst loading. If the adsorption constants are small, then the above equation reduces to:

$$-\frac{dC_A}{dt} = C_{A_0} \frac{dX_A}{dt} = k_{R_2} w C_{A_0} \left(1 - X_A\right) C_{B_0} \quad (12)$$

DMC was taken in molar excess over PAN ($C_{B_0} > C_{A_0}$), it becomes a pseudo-first order equation which can be integrated as follows:

$$-\ln\left(1-X_A\right) = k_1 wt \qquad (13)$$

Where k_1 is the pseudo-first order constant.

A plot of -ln (1-X_A) versus t at various temperatures gives an excellent fit and shows the reaction is pseudo-first order (Figure 5.13). The rate constant values were calculated and activation energy of the reaction estimated from Arrhenius plot (Figure 5.14). The apparent energy of activation was found to be 13.77 kcal/mol.

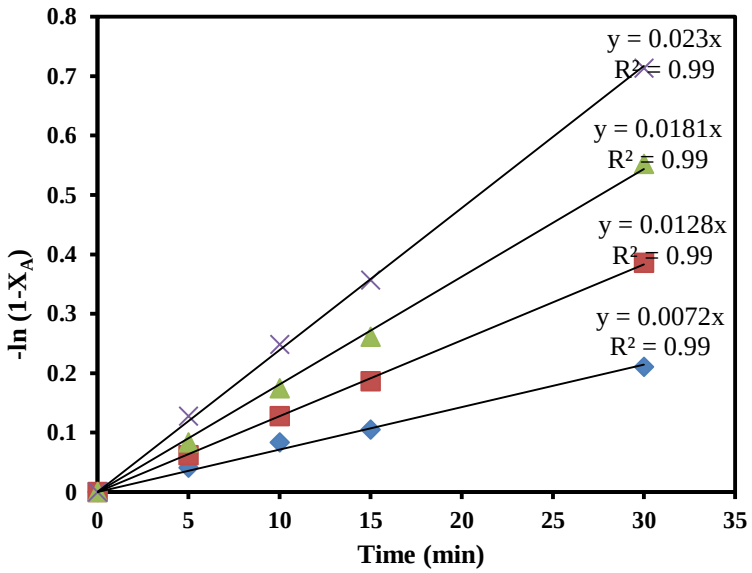

Figure 5.13 Kinetics plots for various temperatures: PAN 0.034 mol, DMC 1.025 mol, catalyst 2 % K/ La_2O_3-MgO, speed of agitation 1000 rpm, total volume 30 cm^3, reaction time 2 h, catalyst loading 0.03 g/cm^3. (♦) 130 ºC, (■) 140 ºC, (▲) 150 ºC, (x) 160 ºC

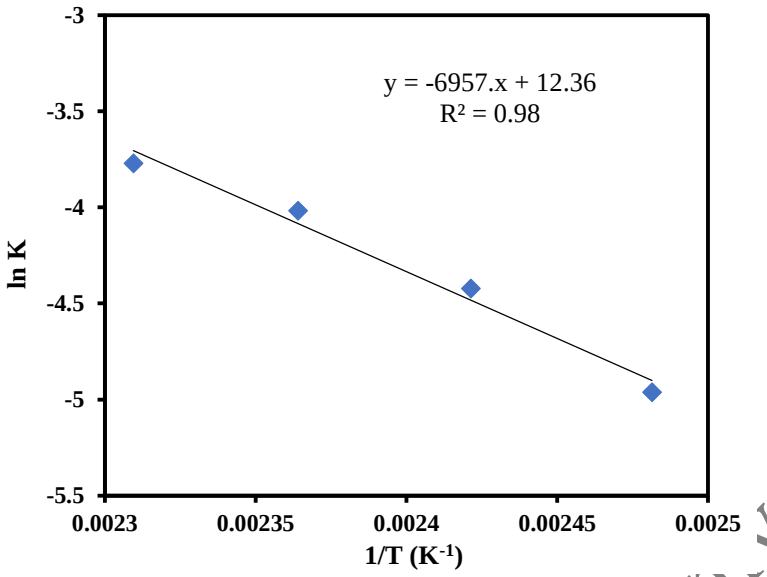

Figure 5.14 Arrhenius plot

5.4.14 Reusability of catalyst

The reusability of 2 wt % K/ La_2O_3-MgO catalyst was tested for methylation of PAN under the optimized conditions: temperature 150 ºC, catalyst loading 0.03 g/cm^3, speed of agitation 1000 rpm, the reaction time 2 h. The catalyst was filtered, washed with methanol and dried at 120 °C after every reaction. The volume of the reaction mass was adjusted so that spent catalyst matches desired optimized catalyst loading or makeup amount of fresh catalyst was added to match the desired loading of catalyst. Figure 5.15 depicts that 2 wt % K/ La_2O_3-MgO catalyst is reusable for four cycles without any loss of its activity.

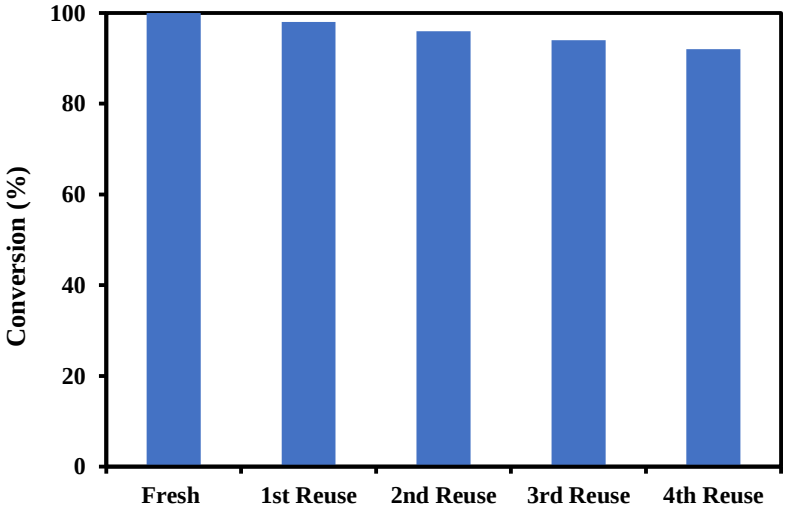

Figure 5.15 Catalyst reusability: PAN 0.034 mol, DMC 1.025 mol, catalyst 2 % K/La_2O_3-MgO, speed of agitation 1000 rpm, temperature 150 ºC, total volume 30 cm^3, reaction time 2 h, catalyst loading 0.03 g/cm^3

5.5 Conclusion

Different loadings of potassium (1 to 4 % wt) promoted on La_2O_3-MgO catalysts were synthesized, characterized with various techniques and screened. Potassium promoted mixed oxides showed much higher catalytic activity than the corresponding pure La_2O_3-MgO mixed oxide in the mono-methylation of PAN with DMC, due to increase in moderate, strong, super basic sites. Moreover, loading of potassium on La_2O_3-MgO changes the structural properties like pore volume and surface area, and it gives higher conversion towards the desired product. In which 2 wt % K/ La_2O_3-MgO catalyst was found to be the best for the methylation of PAN. By using this catalyst, we studied various parameters systematically to establish kinetics. The maximum conversion of PAN was achieved at 150 ºC, PAN to DMC mole ratio 1:30 and catalyst loading 0.03 g/cm^3. The catalyst is reusable up to four cycles. The activation energy for methylation of PAN was calculated as 13.77 kcal/mol.

CHAPTER 6

GREEN SYNTHESIS OF VERATRALDEHYDE USING NOVEL POTASSIUM PROMOTED LANTHANUM-MAGNESIUM MIXED OXIDE CATALYST

J. Molleti, G.D. Yadav, Green Synthesis of Veratraldehyde Using Potassium Promoted Lanthanum–Magnesium Mixed Oxide Catalyst, Org. Process Res. Dev. 21 (2017) 1012–1020.

6.1 Abstract

Veratraldehyde is an important chemical used in perfumery, agrochemical and pharmaceutical industries. Current processes of manufacture of veratraldehyde use homogeneous catalysts which make them highly polluting creating problems of disposal effluents and product purity. In the current work, veratraldehyde was synthesized from O-alkylation of vanillin with an environmentally benign reagent, dimethyl carbonate. A series of potassium loaded La_2O_3-MgO were prepared by incipient wetness impregnation method and their performance was evaluated vis-à-vis MgO, La_2O_3, La_2O_3-MgO and a series of 1-4 wt % K/ La_2O_3-MgO. All catalysts were characterized by different techniques such as N_2 adsorption/desorption, XRD, TGA-DSC, FT-IR, CO_2-TPD and SEM techniques. Effect of different loadings (1-4 wt %) of potassium on La_2O_3-MgO was studied among which 2 wt % K/La_2O_3-MgO showed the best activity and selectivity due to high dispersion of potassium and high basicity in comparison with the rest. The activity of 2 wt % k/ La_2O_3-MgO in O-methylation of vanillin with dimethyl carbonate (DMC) was closely associated with basicity. Various parameters were studied to achieve maximum yield of the desired product. The maximum conversion was found with catalyst loading of 0.03 g/cm^3 and mole ratio of vanillin and DMC of 1:15 at 160 °C in 2 h. The reaction follows pseudo first order kinetics for the O-methylation of vanillin. The energy of activation was found to be 13.5 kcal/mol. Scale-up was done using the kinetic model to observe that the process could be scaled up using the process parameters. The overall process is clean and green.

6.2 Introduction

Lignocellulosic biomass, abundantly available everywhere, is a source of renewable chemicals and fuels [203]. Biomass is converted to obtain phenolic compounds, sugars, and fine chemicals via gasification, anaerobic digestion, fermentation, pyrolysis, and transesterification [204]. Lignocellulosic biomass mainly contains cellulose, hemicellulose and lignin. Lignin is a main renewable source for chemicals such as guaiacol, vanillic acid, phenol, benzene, acetic acid and methanol [205]. Vanillin is also one of the important chemicals obtained from lignin by condensation of guaiacol with glyoxylic acid [206]. Heterogeneous catalysis has tremendous scope for conversion of biomass into value added-chemicals [207] .

Veratraldehyde is present in *Cymbopogon jevenensis* essential oil. It is extensively used in perfume compounds, food aromatizers, odorants and pharmaceutical intermediates [208]. Veratraldehyde can be obtained from O-methylation of vanillin with alkylating agents. The traditional synthesis of O-methylation reactions involved harmful alkylating agents like dimethyl sulfate [209], methyl halides [210], and diazomethane [211], or nontoxic alkylating agents under harsh condition, using a solvent like dimethylformamide [212]. These reagents are hazardous which produce a large amount of waste. These reactions are also reported with methanol as an alkylating agent which require a strong acid [213] or zeolite as catalyst. Usually, they require higher temperature and produce various side products [190]. Hence, development of a green process for the synthesis of veratraldehyde is essential.

Dimethyl carbonate (DMC) is a sustainable, non-toxic, and biodegradable reagent [182]. It can be used either as a methoxycarbonylating agent (<120 °C) or as a methylating agent (>120 °C). In recent years, various applications of DMC were reported [214]. DMC was used in methylation of phenols [215], indoles [216], and anilines [217] as well as methylation of active methylene groups [218]. It is an alternative for hazardous alkylating agents.

Generally, methylation reaction by DMC requires high temperatures (>160 °C) and long reaction times. In order to attain reasonable conversion, strong organic[215,219] or inorganic bases [220,221] have been used in excess quantities. The synthesis of veratraldehyde by O-methylation of vanillin with DMC as a methylating agent has been reported recently. Thomas [222] demonstrated this reaction with 77 % yield to veratraldehyde using 1,3-dimethylimadazolium-2-carboxylate (DMI-CO_2) catalyst in ~3h at 160 °C. The homogenous catalysts showed high catalytic performance but there are several problems to use homogeneous catalysts. Hence, there was an essential need to overcome those problems with the heterogeneous catalysts.

Over the last decades, mixed oxides have been extensively used due to their distinctive physical and chemical properties [76]. Lanthanum oxide (La_2O_3) is a strongest basic oxide, but the activity of is low due to its low surface area. Its activity increased when it mixed with magnesium oxide (MgO) due to increasing basicity [77,78]. La_2O_3-MgO mixed oxide has been widely used in several chemical reactions such as Wittig reaction [45], Michael addition reaction [53], Wadsworth-Emmons reaction [50], synthesis of glycerol carbonate [52], epoxidation of an olefin [54] and transesterification reaction [51].

Several researchers demonstrated that the use of potassium precursors such as KF [194], K_2CO_3 [193], KNO_3 [63,64], and KOH [37] can help the formation of super base. Very recently, Yin et al.[73] demonstrated Knoevenagel condensation reaction over 10 wt % KOH/La_2O_3 as a solid super base.

Here in this report, an efficient and environmentally friendly process for solventless O- methylation of vanillin with DMC over 2 % K/La_2O_3-MgO catalyst. The fresh and spent 2 % K/ La_2O_3-MgO has been fully characterized by different techniques. The catalyst activity was compared with the different solid base catalysts such as calcined hydrotalcite (CHT), MgO, Lithium promoted hydrotalcite (Li-HT), La_2O_3, and different loadings of potassium on La_2O_3-MgO support. The effect of different kinetic parameters was studied to explore the activity of the catalyst in the reaction of vanillin with DMC. Plausible reaction kinetics, reaction mechanism and catalyst reusability were studied.

6.3 Experimental

6.3.1 Chemicals

Magnesium nitrate, Lanthanum nitrate, urea and potassium carbonate were procured from Thomas Baker Chemicals, Mumbai. Vanillin, dimethyl carbonate and n-decane were obtained from SD Fine chemicals limited, Mumbai.

6.3.2 Preparation of catalyst

The catalyst was synthesized by incipient wetness impregnation method and details are given in Chapter 5 (Section 5.2.2).

6.3.3 Characterization of catalysts

Different characterization techniques were employed to characterize the fresh and used catalyst. The detailed methodology is given in Chapter 4 (Section 4.2.4).

6.3.4 General procedure for O-methylation of vanillin

A stainless-steel Amar autoclave (Mumbai, India) of 100 mL equipped with a 4-blade pitch turbine impeller was used for the reaction. The agitation speed was maintained at ±5 rpm of the experimental value. The calculated amount of reactants were taken in the autoclave. The autoclave was tightened and the desired temperature was set, after attaining the temperature zero-minute sample was removed. A typical standard experiment, 0.02 mole of vanillin, 0.3 mole of DMC and 0.2 mL of n-decane as an internal standard with a

catalyst loading of 0.03 g/ cm^3 against total volume (30 cm^3) of the liquid. The reaction mass was heated at 160 °C with speed of agitation 800 rpm for 2 h.

6.3.5 Method of analysis

Samples were withdrawn periodically and analyzed by GC (Chemito Model 1000 with FID detector) using a capillary column BP-1 (length 30 m and inner diameter 0.32 mm). The injector and detector temperature were programmed from 60 to 300 °C with a ramp rate of 10 °C/min. The results were based on the decrease in conversion of the limiting reagent, vanillin. The product was confirmed by GC-MS (Perkin Elmer, Clarius model 500) on the Elite-1 capillary column (length 30 m and inner diameter 0.25 mm).

6.4 Results and Discussion

6.4.1 Characterization

The catalyst was well characterized and details are explained in Chapter 5 (Section 5.3.1). In this work, the 2 wt % K/ La_2O_3-MgO catalyst was characterized after reuse with reference to fresh catalysts. XRD pattern of fresh and reused catalyst shows no change in crystallinity (Figure 6.1). Fresh and reused 2 wt % K/ La_2O_3-MgO catalyst show characteristic type-IV isotherm of mesoporous material (Figure 6.2). The surface area, pore volume and average pore diameter of La_2O_3-MgO catalyst are shown in Table 6.1. CO_2-TPD analysis has been done to study basicity of fresh as well as used catalyst (Table 6.2). CO_2-TPD results show 2 wt % K/ La_2O_3-MgO catalyst possess a reasonable amount of basicity. The scanning electron micrographs reveal that both fresh and reused catalyst samples show almost similar external morphology (Figure 6.3).

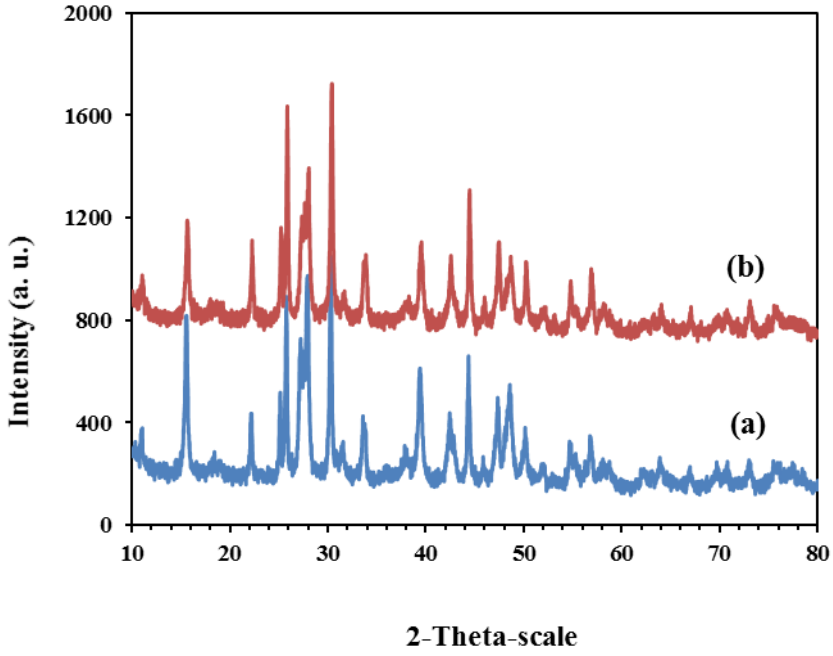

Figure 6.1 XRD pattern of (a) 2 wt % K/ La_2O_3-MgO, (b) reused 2 wt % K/ La_2O_3-MgO

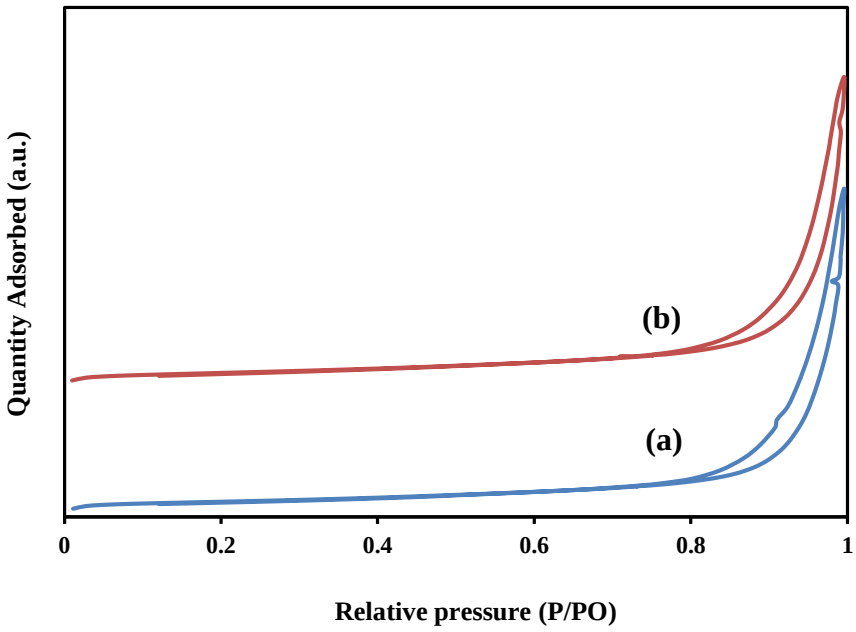

Figure 6.2 N_2 isotherms of catalysts: (a) 2 wt % K/ La_2O_3-MgO, (b) reused 2 wt % K/ La_2O_3-MgO

Table 6.1 Textural characteristics of catalysts.

Catalysts	BET surface area (m^2/g)	Average pore diameter (nm)	BJH pore volume (cm^3/g)
2 wt % K/ La_2O_3-MgO	20	28	0.11

reused 2 wt % K/ La_2O_3-MgO	18	25	0.9

Table 6.2 Basicity of catalysts.

Catalysts	CO_2-TPD analysis		
	Basicity (mmol g^{-1})		
	Weak	Moderate/strong	Total
2 wt % K/ La_2O_3-MgO	0.15	1.35	1.50
reused 2 wt % K/ La_2O_3-MgO	0.12	1.34	1.47

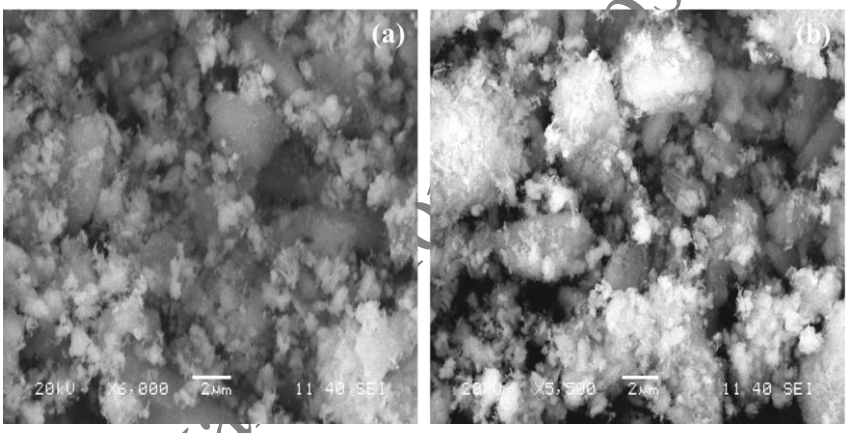

Figure 6.3 SEM images of (a) 2 wt % K/ La_2O_3-MgO, (b) Reused 2 wt % K/ La_2O_3-MgO

6.4.2 Catalytic reaction

The reaction of O-methylation of vanillin with DMC using 2 wt % K/ La_2O_3-MgO catalyst given in Scheme 6.1.

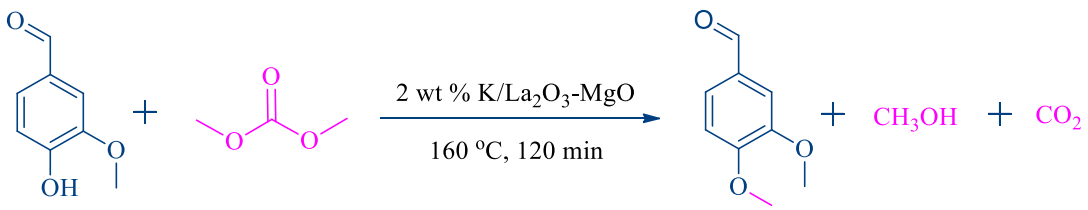

Scheme 6.1: O-methylation of vanillin with DMC

6.4.3 Efficacy of various catalyst

Activity of different solid base catalysts towards the synthesis of veratraldehyde was demonstrated using vanillin and DMC. The reaction was carried out using vanillin to DMC mole ratio 1:15 at 800 rpm with a catalyst loading of 0.03 g/cm^3 on the basis of total volume (30 mL). A variety of catalysts such as CHT, Li-HT, MgO, La_2O_3, La_2O_3-MgO with different loadings (1-4 wt %) of potassium on La_2O_3-MgO like 1 wt % K/ La_2O_3-MgO, 2 wt % K/ La_2O_3-MgO, 3 wt % K/ La_2O_3-MgO and 4 wt % K/ La_2O_3-MgO catalysts were studied for O-methylation reaction (Figure 6.4). The obvious reason for excellent conversion of vanillin is the maximum basicity of catalyst observed at a loading of 2 wt % potassium on La_2O_3-MgO. It is due to increase of moderate and strong basic sites. The further increase in the loading of potassium leads to decreased in the conversion possibly due to blocking of active sites by an excess amount of potassium and/or agglomeration of catalyst particles. The activity of CHT, Li-HT, MgO, La_2O_3 catalysts was found to be less due to lack of strong basic sites. The optimum loading of potassium is 2 wt %, in good agreement with the results of CO_2-TPD and BET surface area. Hence, 2 wt % K/ La_2O_3-MgO was selected as a superior catalyst for detailed kinetics.

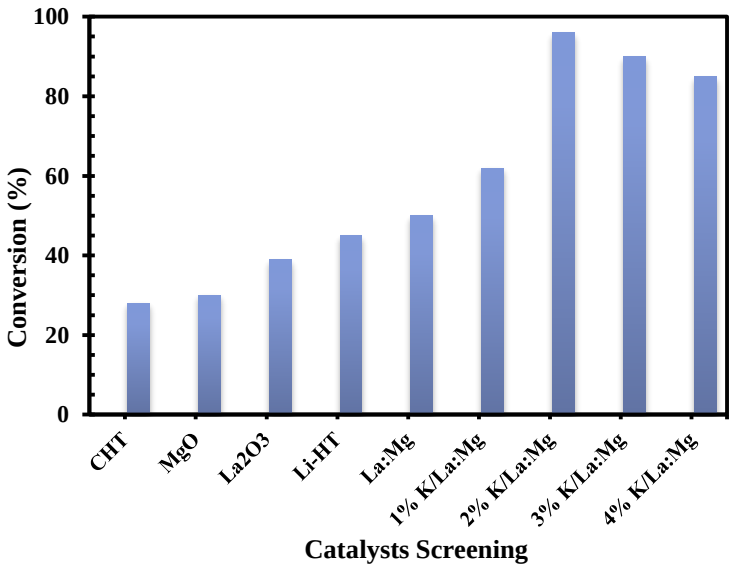

Figure 6.4 Effect of various catalysts on conversion of vanillin: vanillin 0.02 mol, DMC 0.3 mol, speed of agitation 800 rpm, temperature 160 ºC, total volume 30 cm^3, reaction time 2 h, catalyst loading 0.03 g/cm^3

6.4.4 Effect of speed of agitation

The agitation speed was studied at 400, 600, 800 and 1000 rpm at 160 °C in order to understand the effect of external mass transfer resistance on the rate of reaction (Figure

6.5). It is clear that beyond 800 rpm there is no effect on the conversion of vanillin signifying that the mass transfer resistance was absent. Thus, further experiments were carried out 800 rpm.

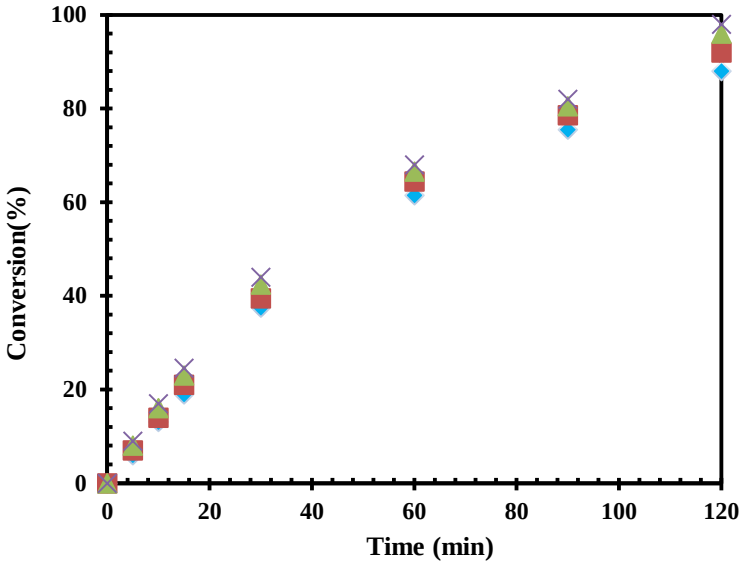

Figure 6.5 Effect of speed of agitation on conversion of vanillin: vanillin 0.02 mol, DMC 0.3 mol, catalyst 2 % K/ La_2O_3-MgO, temperature 160 °C, total volume 30 cm^3, reaction time 2 h, catalyst loading 0.03 g/cm^3. (♦) 400 rpm, (■) 600 rpm, (▲) 800 rpm, (x) 1000 rpm

6.4.5 Effect of catalyst loading

The influence of catalyst loading on conversion of vanillin was studied from 0.01 to 0.04 g/cm^3 (Figure 6.6). Vanillin conversion increases with the increase in catalyst loading which is due to a proportional increase in a number of active sites. Catalyst loading from 0.03-0.04 g/cm^3 there is no appreciable changes in the conversion of vanillin. It is due to surpassing the number of active sites available for reaction than the number of vanillin molecules actually present for the reaction. Figure 6.7 shows an initial rate of reaction increases linearly with the catalyst loading which confirms that mass transfer resistance is not acting.

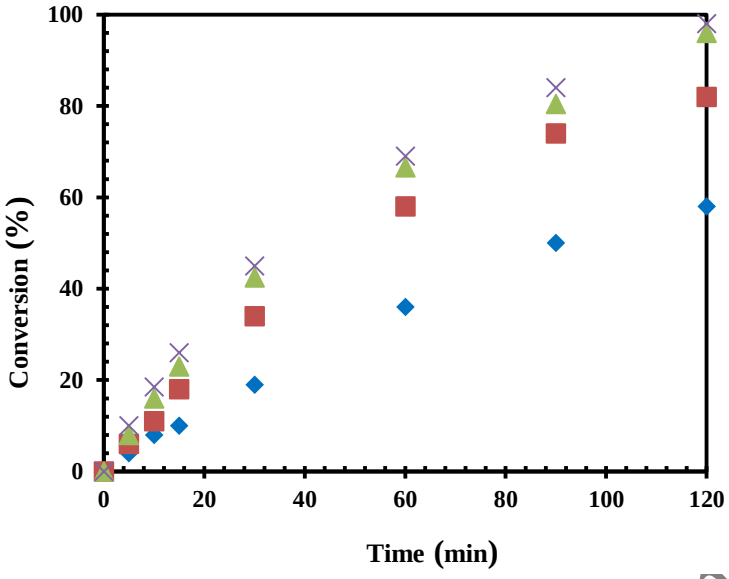

Figure 6.6 Effect of catalyst loading on conversion of vanillin: vanillin 0.02 mol, DMC 0.3 mol, catalyst 2 % K/La_2O_3-MgO, temperature 160 ºC, total volume 30 cm^3, reaction time 2 h, speed of agitation 800 rpm. (♦) 0.01 g/cm^3, (■) 0.02 g/cm^3, (▲) 0.03 g/cm^3, (x) 0.04 g/cm^3.

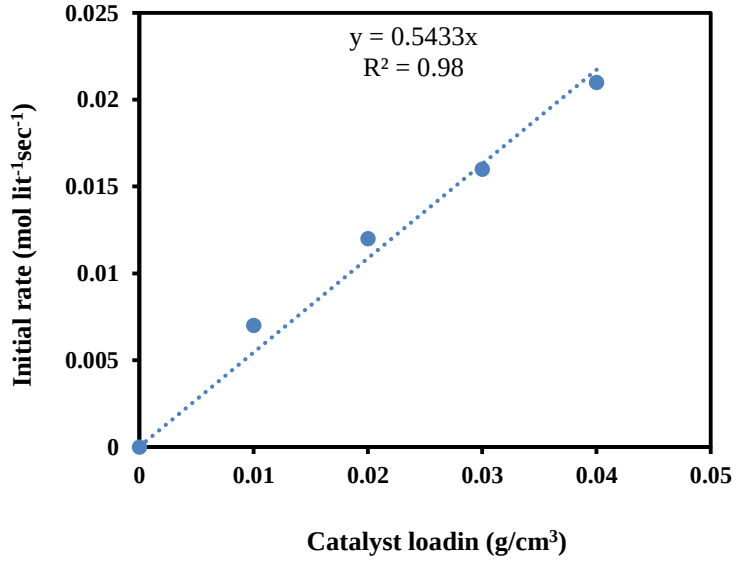

Figure 6.7 Plot of initial rate on conversion of vanillin: vanillin 0.02 mol, DMC 0.3 mol, catalyst 2 % K/ La_2O_3-MgO, temparature-160 ºC, total volume 30 cm^3, reaction time 2 h, speed of agitation 800 rpm.

6.4.6 Effect of mole ratio

Mole ratio of vanillin to DMC was studied at 1:5, 1:10, 1:15 and 1:20 by keeping the total reaction volume constant (Figure 6.8). The conversion of vanillin increases with increase in mole ratio. The conversion of vanillin at 1:5 mole ratio is 50 % which increased

to 96 % at 1:15 mole ratio. There was no significant change in conversion in between 1:15 to 1:20 mole ratio. So, we conclude that 1:15 mole ratio is an ideal parameter for this reaction and used for further reactions.

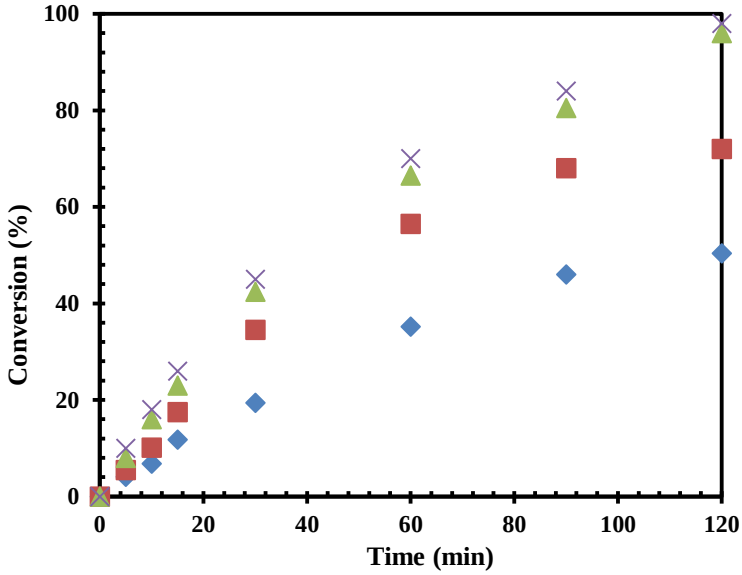

Figure 6.8 Effect of mole ratio on conversion of vanillin: vanillin 0.02 mol, catalyst 2 % K/ La_2O_3-MgO, temparature-160 ºC, total volume 30 cm^3, reaction time 2 h, speed of agitation 800 rpm. (♦) 1:05, (■) 1:10, (▲) 1:15, (x) 1:20.

6.4.7 Effect of temperature

The effect of temperature was studied at 140, 150, 160 and170 °C in order to consider its effect on the rate of reaction at optimum conditions (Figure 6.9). The increase in temperature leads to increases the rate of reaction and conversion of vanillin increases dramatically, which suggest that reaction is kinetically controlled.

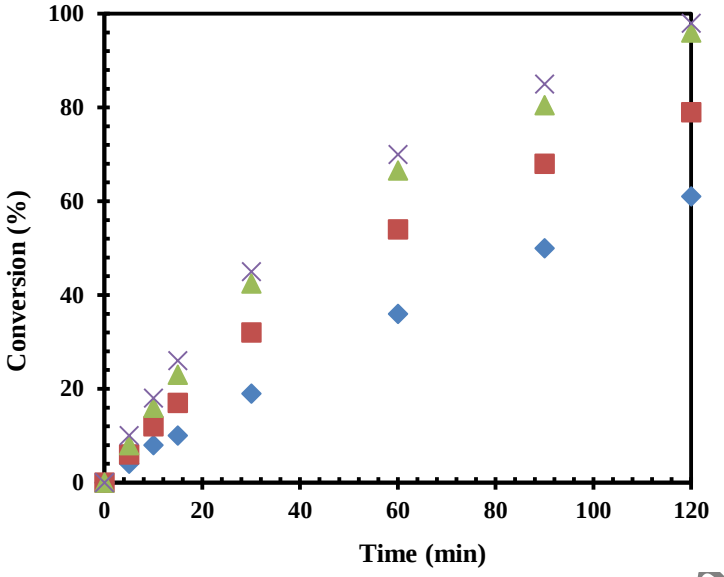

Figure 6.9 Effect of temperature on conversion of vanillin: vanillin 0.02 mol, DMC 0.3 mol, catalyst 2 % K La_2O_3-MgO, speed of agitation 800 rpm, total volume 30 cm^3, reaction time 2 h, catalyst loading 0.03 g/cm^3. (♦) 140 ºC, (■) 150 ºC, (▲) 160 ºC, (x) 170 ºC.

6.4.8 Reaction mechanism and mathematical model

The plausible O-methylation mechanism of vanillin with DMC on basic sites of 2 wt % K/ La_2O_3-MgO catalyst is depicted in Scheme 6.2. O-methylation of vanillin (A) with DMC (B) occurs by strong adsorption of vanillin on basic sites leading to the formation of veratraldehyde. The detail mathematical model was developed using LHHW mechanism as same reported in the recent literature [123,202].

The rate of reaction of Vanillin can be given as:

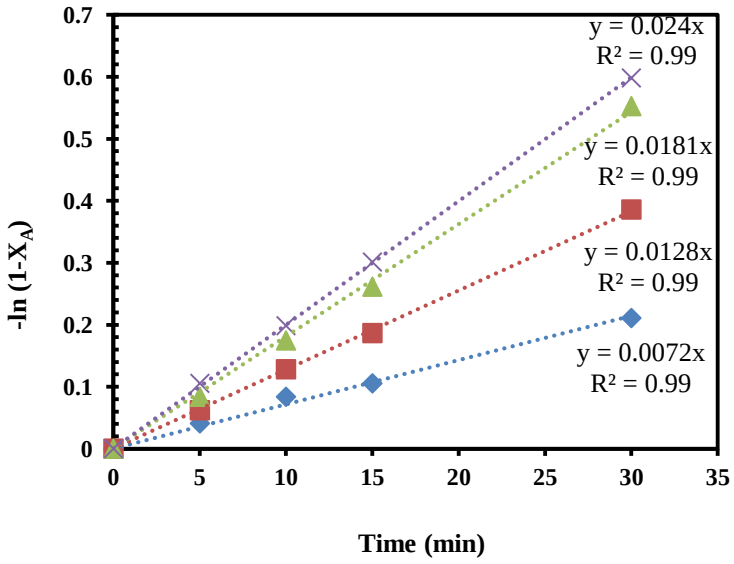

Figure 6.10 Kinetics plots for various temperatures: vanillin 0.02 mol, DMC 0.3 mol, catalyst 2 % K/ La_2O_3-MgO, speed of agitation 800 rpm, total volume 30 cm^3, reaction time 2 h, catalyst loading 0.03 g/cm^3. (♦) 140 ºC, (■) 150 ºC, (▲) 160 ºC, (x) 170 ºC.

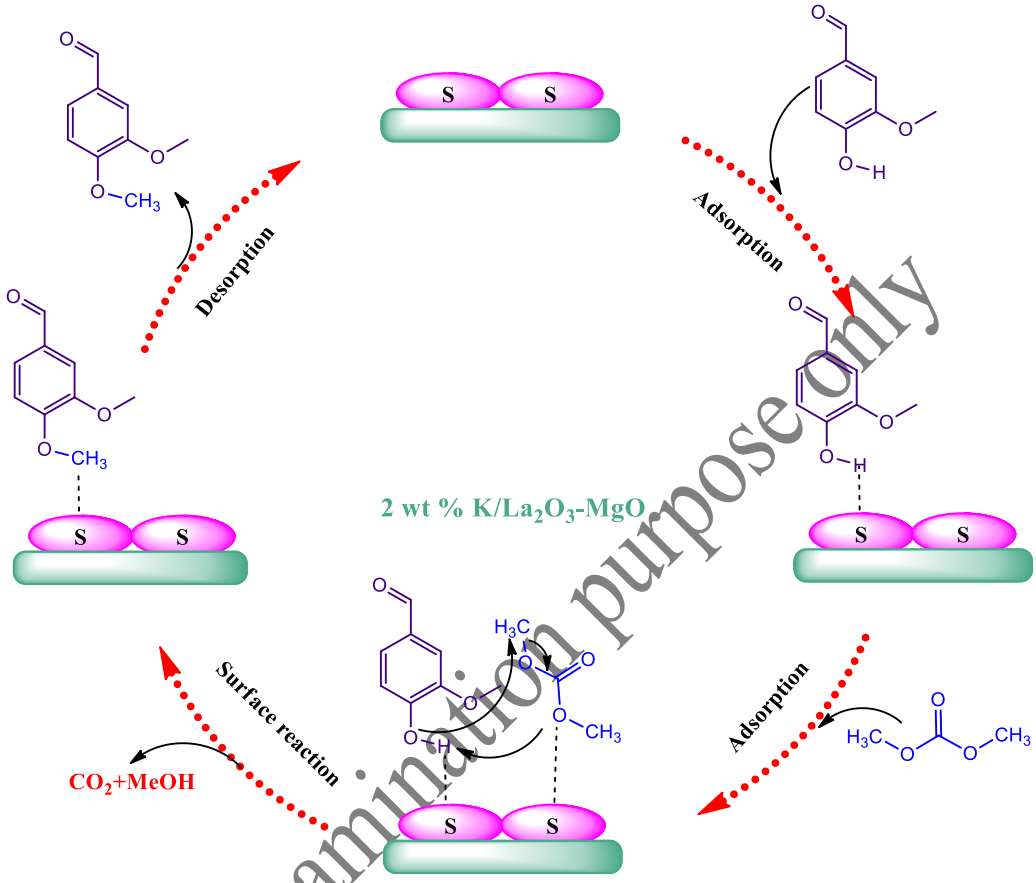

Scheme 6.2: Reaction mechanism of O-methylation of vanillin with DMC

Let A = Vanillin, B = DMC, ES = veratraldehyde, W= Methanol, S=vacant sites.

Chemisorption of A and B on vacant site S

Adsorption

Adsorption of vanillin (A) on a vacant site S is given by:

$$A + S \xleftrightarrow{K_A} AS \qquad (1)$$

Adsorption of DMC (B) on a vacant site S is given by:

$$B + S \xleftrightarrow{K_B} BS \qquad (2)$$

Surface reaction

Surface reaction of AS and BS in the vicinity of an active site, leading to the formation of ES and WS on the active

$$AS + BS \xleftrightarrow{K_2} ES + WS + CO_2 \quad (3)$$

Desorption of veratraldehyde (ES) and methanol (WS) is given by:

$$ES \xleftrightarrow{1/K_E} E + S \quad (4)$$

$$WS \xleftrightarrow{1/K_W} W + S \quad (5)$$

The total concentration of the sites, C_t expressed as,

$$C_t = C_S + C_{AS} + C_{BS} + C_{ES} + C_{WS} \quad (6)$$

Or

$$C_t = C_S + K_A C_A C_S + K_B C_B C_S + K_S C_E C_S + K_W C_W C_S \quad (7)$$

When the adsorption and desorption steps are assumed to be equilibrium,

The concentration of vacant sites can be written as,

$$C_S = \frac{C_t}{\left(1 + K_A C_A + K_B C_B + K_S C_E + K_W C_W\right)} \quad (8)$$

If the surface reaction controls the rate of reaction, then the rate of reaction of A is given by

$$-r_A = -\frac{dC_A}{dt} = k_2 C_{AS} C_{BS} - k_2 C_{ES} C_{WS} p_{CO_2}$$

$$-\frac{dC_A}{dt} = \frac{k_2 \left\{ K_A K_B C_A C_B - \frac{K_E K_W C_E C_W p_{CO_2}}{K_2} \right\} C_t^2}{\left(1 + K_A C_A + K_B C_B + K_S C_E + K_W C_W\right)^2} \quad (9)$$

When the reaction is far away from equilibrium

$$-\frac{dC_A}{dt} = \frac{k_2 C_t^2 K_A K_B C_A C_B}{\left(1 + \sum K_i C_i\right)^2} \quad (10)$$

$$-\frac{dC_A}{dt} = \frac{k_{R_2} w C_A C_B}{\left(1 + \sum K_i C_i\right)^2} \quad (11)$$

Since $k_{R_2} w = k_2 C_t^2 K_A K_B$ where, w is catalyst loading. If the adsorption constants are small, then the above equation reduces to:

$$-\frac{dC_A}{dt} = C_{A_0} \frac{dX_A}{dt} = k_{R_2} w C_{A_0} \left(1 - X_A\right) C_{B_0} \quad (12)$$

DMC was taken in molar excess over vanillin ($C_{B_0} > C_{A_0}$), it becomes a pseudo-first order equation which can be integrated as follows:

$$-\ln\left(1 - X_A\right) = k_1 w t \quad (13)$$

Where, k_1 is the pseudo-first order constant.

A plot of –ln (1-X_A) against time was made at a various temperature to get excellent, there by supporting the model. This is an overall pseudo first order reaction (Figure 6.7). Energy of activation was calculated by plotting Arrhenius plot of lnk against time (Figure 6.8) and energy of activation was found to be 13.5 kcal/mol, which supports the fact that reaction is intrinsically kinetically controlled.

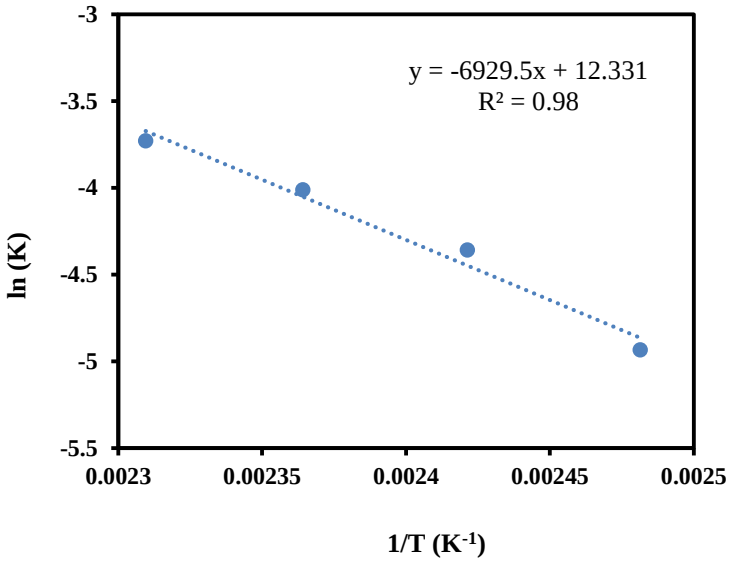

Figure 6.11 Arrhenius plot

6.4.9 Reusability of catalyst

The reusability of the 2 wt % K/ La_2O_3-MgO catalyst was tested four times in case of O-methylation of vanillin. After each reaction, the catalyst was separated by filtration and washed with methanol and then dried at 120 ºC. It was observed that 2 wt % K/ La_2O_3-MgO shows the very small difference activity after third time use. In the case of fourth time reuse, there is a 6 % conversion difference compare to fresh catalyst (Figure 6.9). These results clearly show the stability of 2 wt % K/ La_2O_3-MgO catalyst.

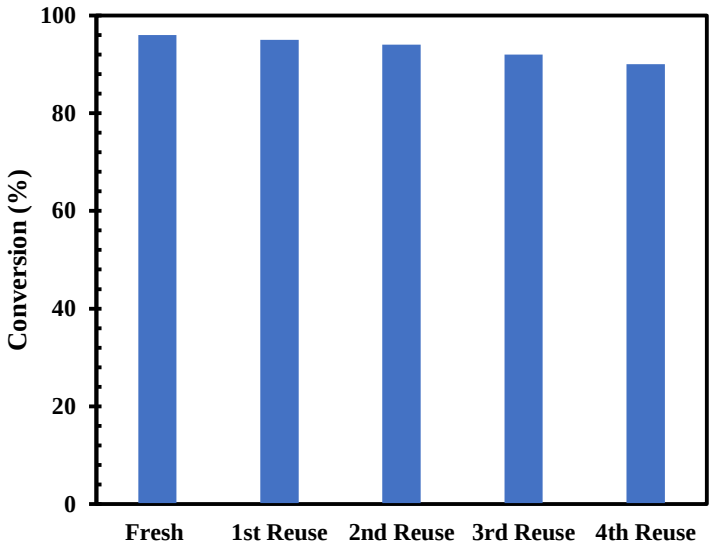

Figure 6.12 Catalyst reusability: vanillin 0.02 mol, DMC 0.3 mol, catalyst 2 % K/ La_2O_3-MgO, speed of agitation 800 rpm, temperature 160 ºC, total volume 30 cm^3, reaction time 2 h, catalyst loading 0.03 g/cm^3

6.5 Conclusion

Different loadings of potassium promoted on La_2O_3-MgO (1-4 wt %) catalysts were synthesized, characterized with various techniques. The activity of catalyst was demonstrated in the reaction vanillin with DMC for synthesis of veratraldehyde in compare with several other catalysts such as CHT, Li-HT, MgO, La_2O_3, La2O3-MgO, 1 wt % K/ La_2O_3-MgO, 2 wt % K/ La_2O_3-MgO, 3 wt % K/ La_2O_3-MgO and 4 wt % K/ La_2O_3-MgO. Potassium promoted mixed oxides showed much higher catalytic activity than the corresponding pure La_2O_3-MgO mixed oxide in the O-methylation of vanillin with DMC, due to increase in moderate, strong, super basic sites. Moreover, loading of potassium on La_2O_3-MgO changes the structural properties like pore volume and surface area, and it gives higher conversion towards the desired product. Two wt % K/ La_2O_3-MgO gives 96 % of conversion at a mole ratio of 1:15 of vanillin to DMC and 0.03 g/cm^3 catalyst loading at 160 °C. By using this catalyst, we studied various parameters studied systematically to establish kinetics. The catalyst is reusable up to four cycles. The energy of activation for O-methylation of vanillin was found to be 13.5 kcal/mol.

CHAPTER 7

SOLVENT-FREE SYNTHESIS OF METHYL SALICYLATE USING COMBUSTION SYNTHESIZED NOVEL SULFATED IRON-ZIRCONIA CATALYST

J. Molleti, G.D. Yadav, Solvent-free synthesis of methyl salicylate using combustion synthesized novel sulfated iron-zirconia catalyst, Appl. Catal., A. (Communicated)

7.1 Abstract

Sulfated Fe_2O_3-ZrO_2 catalyst with different iron loadings has been, for the first time, prepared by combustion technique. The activity of sulfated Fe_2O_3-ZrO_2 was evaluated for the esterification of salicylic acid with dimethyl carbonate. The product methyl salicylate is extensively used in the food and pharma industries. Catalyst with different loadings of iron on zirconia (5, 10, 15, 20 wt %) was synthesized and activity of the catalyst was compared with the solid acid catalysts such as ZrO_2, sulfated zirconia. The introduction of iron, considerably increases salicylic acid conversion. The activity of the catalysts increases after the loading of iron on zirconia and 10 wt % iron gave the highest acidity and best catalytic for the synthesis of methyl salicylate (oil of wintergreen). These catalysts were characterized by using different techniques such as SEM, XRD, FTIR, TGA, NH_3-TPD and BET surface area analysis. Ten wt % sulfated Fe_2O_3-ZrO_2 catalyst demonstrated 95 % conversion of salicylic acid with 100 % selectivity of methyl salicylate at 120 °C after 150 min at a 1:10 molar ratio of salicylic acid to dimethyl carbonate and catalyst loading of 0.03 g/cm^3. Effect of various kinetic parameters on the rate of esterification of salicylic acid was studied for the kinetics of the reaction. The activation energy for this reaction was found to be 13.82 kcal/mol.

7.2 Introduction

Methyl salicylate is extensively used in the synthesis of solvents, perfumes, cosmetics, food preservatives, chiral auxiliaries, plasticizers, drugs, and pharmaceuticals [223]. Esterification reactions are reported with various homogeneous catalysts such as HCl, H_2SO_4, HF, and H_3PO_4. But, these methods have drawbacks such as generation of undesired inorganic salts, hazardous conditions, difficulty in catalyst recovery and reuse [224]. During the past few years, heterogeneous catalysts such as mesoporous materials, acidic clays, zeolites, ion-exchangeable resins, heteropolyacids (HPA) supported on clays, and sulfated mixed oxides have been replaced with the conventional mineral acids [225–230]. Although, heterogeneous catalysts such as ion-exchangeable resins have some drawbacks such as poor reusability, less surface area and thermal stability of ion exchange resins [231]. Thus, it is important to design a heterogeneous catalytic system for the synthesis of methyl esters that involves the use of safe, active and reusable catalysts.

Methyl salicylate synthesis is an industrially important reaction [232]. The conventional esterification reaction using acid and alcohol results in the formation of water as a co-product and leads to leaching of active sites in many liquid phase reactions, which decreases the activity of catalyst [233]. Hence, there is a need to substitute the alkylating agent.

Dimethyl carbonate (DMC), which is a safe, green, and cheap reagent has been reported as a potential methylating agent [182]. In recent years methylating activity of DMC has been studied extensively [180,234,235]. Using DMC as a methylating agent in reaction results in methanol as a by-product, which can be recovered for the generation of DMC [236].

Very few reports are published on the synthesis of methyl salicylate by esterification of salicylic acid with DMC. Shimizu and Lee [234] demonstrated the esterification of mycophenolic acid with DMC by using cesium carbonate as a catalyst. But, in this reaction, both the groups are alkylated. Sreekumar et al. [235] reported salicylic acid with DMC using zeolite, in this case, mono methylation was observed. Narayanan et al. [236] demonstrated 90 % conversion of salicylic acid and 95 % selectivity of methyl salicylate with DMC over zeolites for 4 h at 135 °C. Yuhan et al. [237] reported 98 % conversion and 96 % selectivity with DMC over AlSBA-15-SO_3H catalyst for 8 h at 200 °C and 99 % conversion of salicylic acid and 77 % selectivity to methyl salicylate with DMC over mesoporous aluminosilicate [238]. Recently, Li et al. [239] reported 93 % conversion and 99 % selectivity with methanol using Ce^{4+} modified cation-exchange resins for 12 h at 95 °C. However, these reports are not favorable due to harsh condition and long reaction time. Thus, the development of highly stable, active and recyclable catalyst for the efficient synthesis of methyl salicylate is highly desirable.

Combustion synthesis is an alternative material synthesis. It does not involve multistep synthesis, highly reproducible and it takes very less time when compared with other methods. In this synthesis nitrates of metals are used as oxidizers and carbon-based compounds containing reducible functional groups are used as fuels [240,241]. Different metal oxides and mixed metal oxides are synthesized by solution combustion method [242]. Sulfated zirconia (SZ) has been reported as a better catalyst as well as support due to its surface chemical properties, versatile structures and good thermal stability [107,243,244]. SZ has been reported for the preparation of aspirin, esterification of acids with acids, protection of carbonyl compounds and Friedel-Crafts acylation [245–249]. The acid strength of SZ depends on parameters like amount of surface exposed, preparation conditions, nature of crystalline phase of zirconia and sulfate density [250,251]. The activity of SZ can be improved by doping of transition metal on zirconia and following sulfate grafting or by supporting noble metals on the SZ. Chen et al. reported after the introduction of transition metal ions like Cu, Al, Fe, Cr, Mo and Co into the zirconia lattice increase the activity and stability of sulfated metal oxide [251]. The tetragonal phase of zirconia stabilizes with the existence of promoters like Fe and Mn, making promoted catalysts much more stable through treatment and storage [252].

Based on the above knowledge, we have prepared sulfated bimetallic oxide by the combustion method for the first time. The effect of Fe_2O_3 loading on the zirconia was successfully investigated. The current work describes highly selective esterification of salicylic acid with DMC over sulfated bimetallic oxide (Scheme 1). The fresh and spent catalysts were characterized by different techniques. The effects of various parameters such as speed of agitation, mole ratio, catalyst loading, and temperature were examined to establish kinetics and mechanism.

7.3 Experimental Section

7.3.1 Materials

Salicylic acid, methanol, 1, 2-dichloroethane, chlorosulfonic acid and n-dodecane were procured from SD Fine chemicals limited, Mumbai. Zirconyl nitrate hexahydrate, iron nitrate nonahydrate and glycine were purchased from Thomas Baker Chemicals, Mumbai.

7.3.2 Preparation of catalysts

Fe_2O_3/ZrO_2 was synthesized by combustion technique. In a typical synthesis, $ZrO(NO_3)_2$. 6 H_2O, $Fe(NO_3)_3$. 9 H_2O as precursor salts and glycine as fuel. To this solution, the predetermined quantities of salts and fuel were dissolved in a minimum quantity of water. The mixture was taken in a crucible and heated to form a viscous material. This material was shifted into a muffle furnace for combustion at 350 °C to obtain the Fe_2O_3-ZrO_2 composite catalyst. The material was brown coloured fluffy powder. Sulphonation was done as described in our laboratory [253]. It was washed with ethylene dichloride and acidified with 15 cm^3/g of 1 M chlorosulfonic acid under nitrogen gas to avoid moisture absorption on the powder. The resultant solid was dried at 120 °C for 24 h. The sulfated Fe_2O_3-ZrO_2 was activated by calcination at 650 °C for 4 h. By using this method, sulphated Fe_2O_3-ZrO_2 catalysts with Fe_2O_3 contents 5, 10, 15, 20 wt % were prepared. The sulphated Fe_2O_3-ZrO_2 are referred as SFZ-x in the text, where x denotes the wt % of the Fe_2O_3 present in the mixed oxide.

7.3.3 Characterization methodology

The detailed methodology is given in Chapter 5 (Section 5.2.3).

7.3.4 General procedure for esterification of salicylic acid

All experiments were done in 100 ml Amar (Mumbai, India) autoclave with pitched blade turbine impeller and controllers for pressure and temperature. In a standard experiment, 0.075 mol salicylic acid, 0.75 mol DMC and 0.2 mL n-decane as an internal standard with a catalyst loading of 0.03 g/ cm^3 against the total volume (40 cm^3) of the liquid. The reaction mass was heated at 120 °C and 1000 rpm for 150 min. Sampling was done at regular intervals of time for analysis.

7.3.5 Method of analysis

Samples were analyzed by GC equipped with a capillary column BP-1 (length 30 m and inner diameter 0.32 mm) and FID detector. Product confirmation was carried out by GC-MS from Perkin Elmer, Clarius model 500 on an Elite-1 capillary column of length 30 m and inner diameter 0.25 mm. The conversions were based on the decrease in the conversion of the limiting reagent, salicylic acid.

7.4 Result and Discussion

7.4.1 XRD

X-ray diffraction patterns of the SZ, SFZ-5, SFZ-10, SFZ-15, SFZ-20 and reused SFZ-10 catalysts prepared by combustion method are shown in Figure 7.1. Sulfated zirconia (Figure 7.1(a)) shows characteristic reflections at 2θ values of 30.2°, 35.98°, 50.4° and 60.6° corresponding to the presence of tetragonal phase of zirconia (JCPDS:14-0534). No diffraction peaks corresponding to the presence of monoclinic phases are observed in combustion synthesized SZ, which suggests the selective stabilization of tetragonal phase of zirconia in current process [254]. For catalytic applications, tetragonal phase of SFZ-x catalyst is essential instead of monoclinic phase [255]. XRD patterns of SFZ-x catalysts show less intense peaks than the SZ which is due to the inhibition and intergrowth of the grains of ZrO_2 and Fe_2O_3 during combustion method. Iron loading of 15 and 20 % samples show no crystalline peaks of ZrO_2 (Figure 7.1 (d) and (f)). It is due to the transformation of zirconia from a crystalline phase to an amorphous state. The XRD pattern of SFZ-10 and reused catalysts were compared to find that they were almost the same which confirmed that the prepared catalyst was stable.

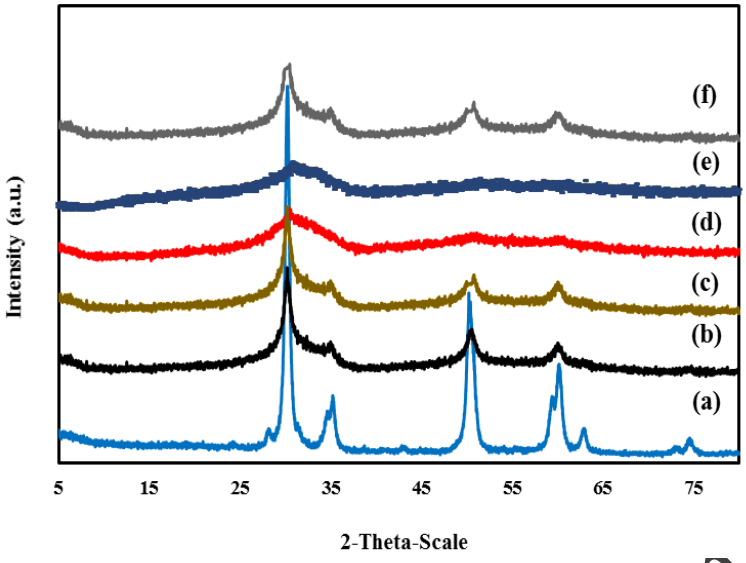

Figure 7.1 XRD of (a) SZ; (b) SFZ-5; (c) SFZ-10; (d) SFZ-15; (e) SFZ-20 and (f) reused SFZ-10

7.4.2 FT-IR

FT-IR analysis of SZ, SFZ-5, SFZ-10, SFZ-15, SFZ-20 and reused SFZ-10 catalysts are shown in Figure 7.2. All the catalysts show a strong peak at 3440 cm^{-1} which is attributed to the stretching mode of -OH group associated with zirconia, whereas the mild peak at 1635 cm^{-1} is attributed to the presence of water molecule associated with sulfate group [256,257]. Samples showed the characteristic peaks at 1340, 1240, 1140, 1014 and 997 cm^{-1} related to the chelating bidentate sulfate ion, which is assigned to the S=O or S-O bonds [258]. The peak at 754 cm^{-1} is due to stretching mode of Zr-O, which is related to the zirconium oxide phase. The virgin and reused catalyst showed no change in spectra, which confirms the stability and reusability.

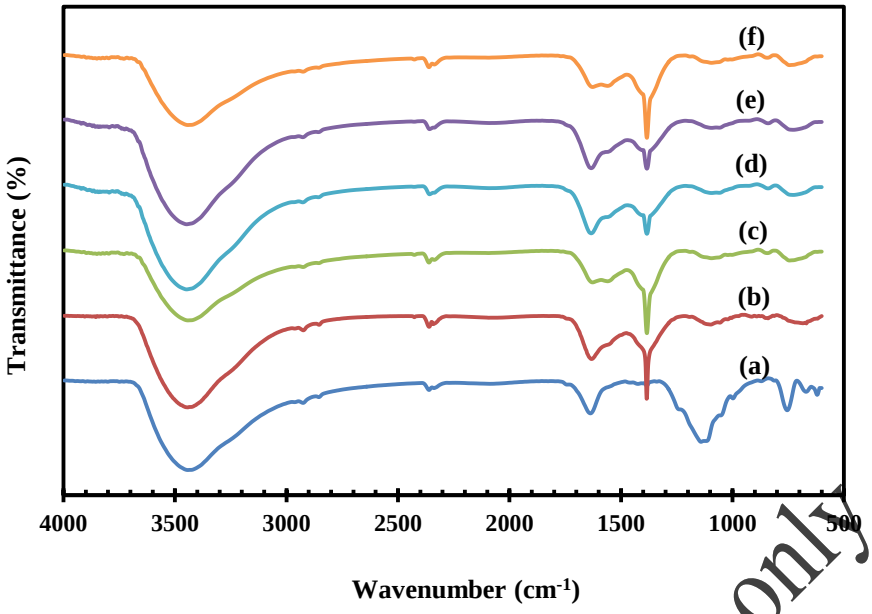

Figure 7.2 FT-IR analysis of (a) SZ, (b) SFZ-5, (c) SFZ-10, (d) SFZ-15, (e) SFZ-20 and (f) reused SFZ-10

7.4.3 Surface area and pore size analysis

N_2 adsorption/desorption isotherms of SZ, SFZ-5, SFZ-10, SFZ-15 and SFZ-20 are shown in Figure 7.3. All the catalysts show isotherms of type IV and type H3 hysteresis loop, which indicates that the materials are mesoporous. Physical properties: surface area, average pore diameter and pore volume of SZ catalysts are 6 $m^2 g^{-1}$, 30 nm and 0.09 $cm^3 g^{-1}$, respectively (Table 7.1). The surface area gradually increases with lower loading (5, 10 wt %) of Fe_2O_3, but it decreases at the higher loading (15, 20 wt %) of Fe_2O_3, which could be due to the blockage of the pores of Fe_2O_3 on the surface of ZrO_2.

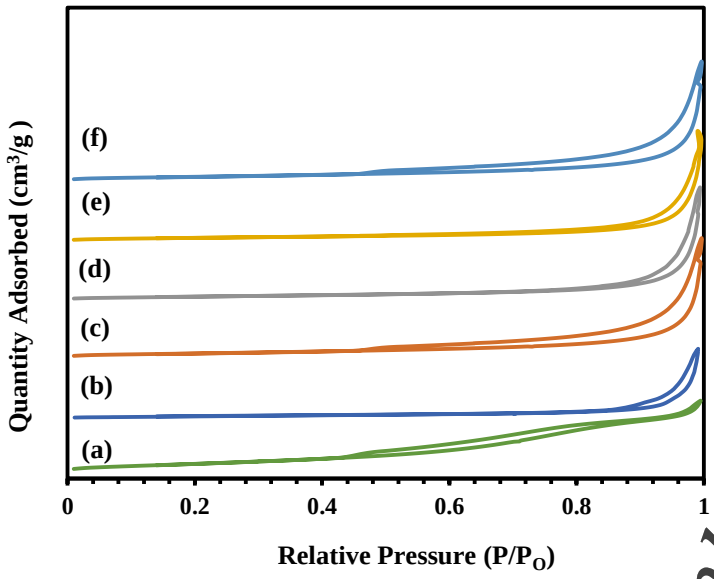

Figure 7.3 N_2 adsorption-desorption plot for the catalysts: (a) SZ; (b) SFZ-5; (c) SFZ-10; (d) SFZ-15; (e) SFZ-20; (f) reused SFZ-10

Table 7.1 Surface area analysis of catalysts

Catalysts	BET surface area (m^2/g)	Average pore diameter (nm)	BJH pore volume (cm^3/g)
SZ	6	30	0.09
SFZ-5	10	25	0.08
SFZ-10	22	18	0.10
SFZ-15	16	26	0.10
SFZ-20	12	24	0.09
Reused SFZ-10	21	18	0.10

7.4.4 TGA

TGA of optimized SFZ-10 catalyst was studied to measure the weight loss with respect to temperature (Figure 7.4). Two thermal losses were observed in the SFZ-10 catalyst. The first weight loss was observed at 0-150 °C which was due to loss of moisture content of the catalyst. Second weight loss was observed at 550-650 °C which was due to change of hydroxide phase into oxide phase. Overall, SFZ-10 catalyst showed a weight loss up to 10.8 %. Above 650 °C temperature, significant weight loss is not observed, which shows the catalyst is thermally stable.

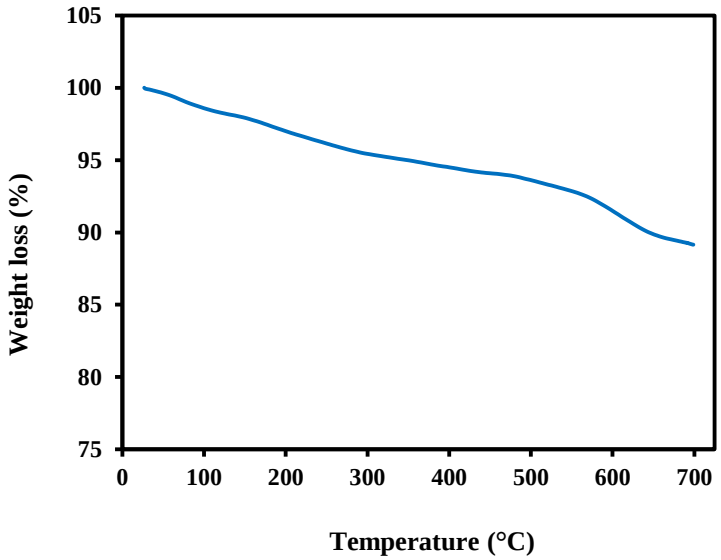

Figure 7.4 TGA analysis of SFZ-10

7.4.5 Ammonia-TPD

Ammonia-TPD analysis of SZ, SFZ-5, SFZ-10, SFZ-15 and SFZ-20 catalysts are given in Table 7.2. NH_3-TPD analysis of SFZ-10 catalyst is depicted in Figure 7.5 which shows the acidity of the catalyst. NH_3 desorption peaks observed at 230 and 550 °C correspond to moderate and strong basic sites, and the amount of desorbed NH_3 was 0.35 and 0.43 $mmolg^{-1}$ respectively. Acid strength of the catalyst is depending on the desorption temperature[259]. By comparison of all the catalysts, the area of the peaks for weak, moderate and strong acid sites of SFZ-10 are found to be higher (0.78 $mmolg^{-1}$). Higher desorption temperatures of SFZ-x catalysts showed higher acidity than the SZ, which indicated that the incorporation of iron can effectively improve the acid strength of sulfated zirconium oxide.

Table 7.2 NH_3-TPD analysis of catalysts

Catalysts	NH_3 TPD analysis
	Acidity (mmol g^{-1})
	Moderate/strong
SZ	0.60
SFZ-5	0.65
SFZ-10	0.78

SFZ-15	0.72
SFZ-20	0.68
Reused SFZ-10	0.77

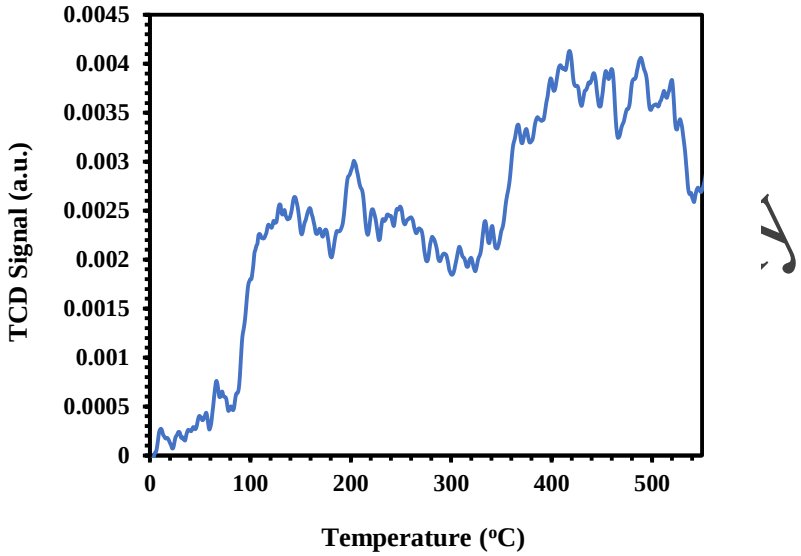

Figure 7.5 NH_3-TPD pattern of SFZ-10 catalyst

7.4.6 SEM

The scanning electron micrograph of the SZ and SFZ-10 catalysts depicted in Figure 7.5. Both catalysts are found to be highly porous and spongy nature, it is due to the escaping of large amount gases during the combustion process.

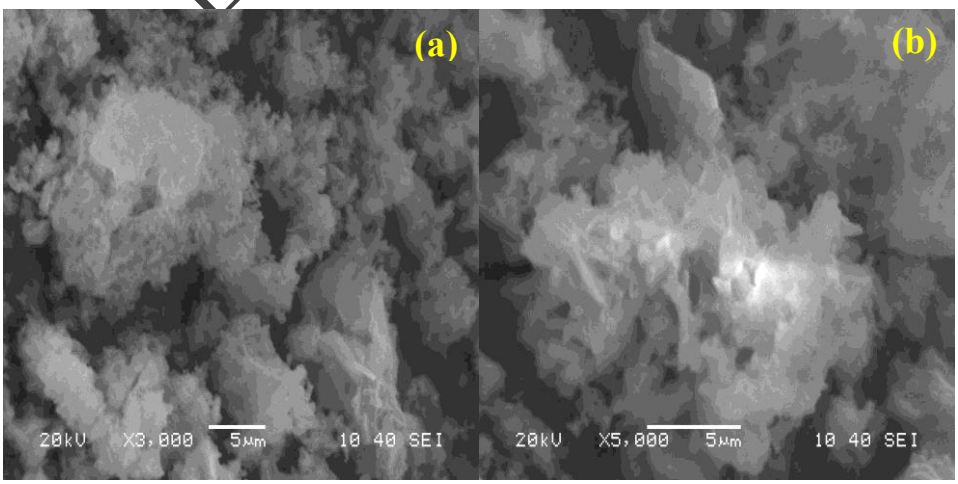

Figure 7.6 SEM images of (a) SZ; (b) SFZ-10

7.4.7 Catalytic reaction

The reaction of salicylic acid with dimethyl carbonate using SFZ-10 catalyst was given in Scheme 7.1.

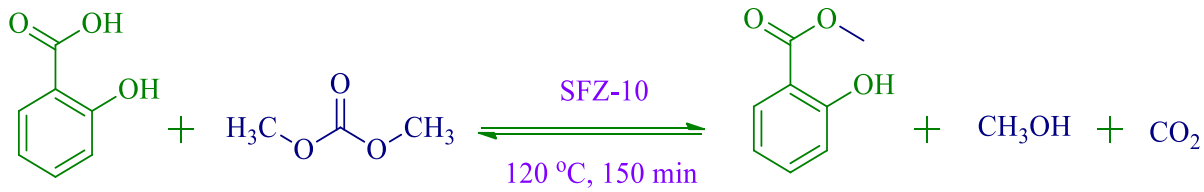

Scheme 7.1 Esterification of salicylic acid with DMC

7.4.8 Efficacy of various catalyst

Figure 7.7 shows the conversion of salicylic acid by esterification with DMC using SZ, SFZ-5, SFZ-10, SFZ-15 and SFZ-20 catalysts. All the catalysts showed conversion of salicylic acid in the range 68-95 %. The order of conversion was as follows: SFZ-10 (95 %) > SFZ-15 (87 %) > SFZ-20 (82 %) > SFZ-5 (76 %) > SZ (68 %). TPD-NH_3 and surface analysis of SFZ-x catalysts showed higher values of acidity and surface area in comparison with the SZ catalyst. The higher catalytic activity of SFZ-x catalysts is due to the presence of iron oxide, which is responsible for the increase in the number of acidic sites of the SFX-x catalysts [260]. SFZ-10 catalyst showed higher activity when compared with the other catalysts due to its higher acidity and surface area. Therefore, SFZ-10 catalyst was found to be the best for esterification of salicylic acid to methyl salicylate.

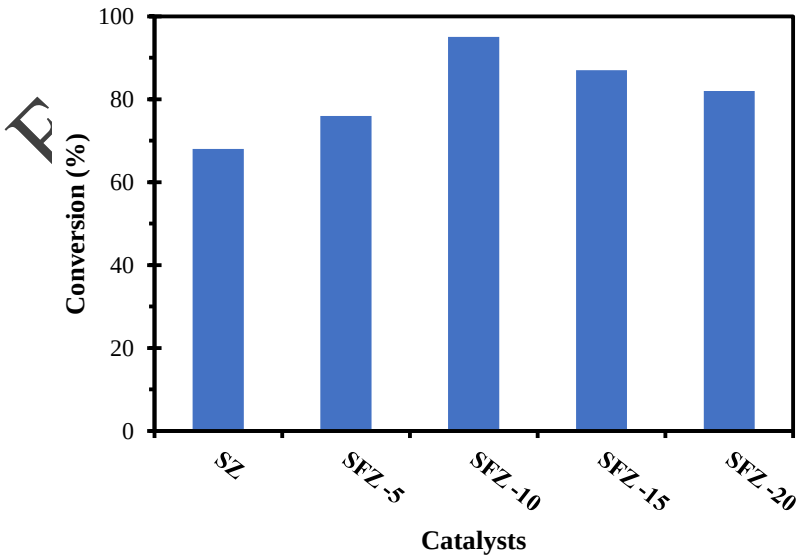

Figure 7.7 Effect of various catalysts on salicylic acid: Salicylic acid 0.075 mol, methanol 0.75 mol, speed of agitation 800 rpm, temperature 120 ºC, total volume 40 cm^3, reaction time 150 min, catalyst loading 0.03 g/cm^3

7.4.9 Effect of speed of agitation

The effect of external mass transfer resistance on the conversion of salicylic acid was studied from 400 to 1000 rpm at 120 °C for a catalyst loading of 0.03 g/cm^3 (Figure 7.8). The conversion of salicylic acid was found to be practically the same beyond 800 rpm, which shows the absence of external mass transfer resistance in the reaction. Therefore, all further experiments were carried out at 800 rpm.

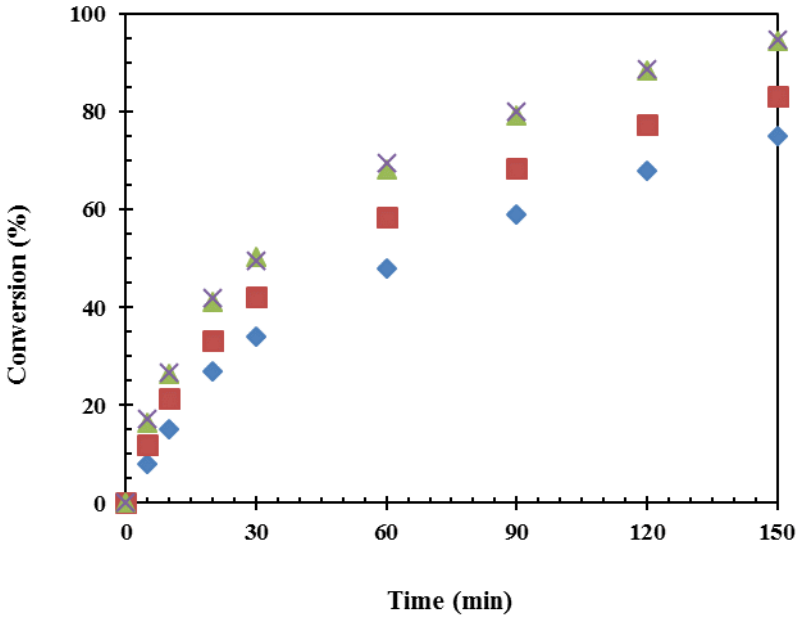

Figure 7.8 Effect of speed of agitation on conversion of Salicylic acid: Salicylic acid 0.075 mol, methanol 0.75 mol, catalyst SFZ-10, temperature 120 ºC, total volume 40 cm^3, reaction time 150 min, catalyst loading 0.03 g/cm^3. (♦) 400 rpm, (■) 600 rpm, (▲) 800 rpm, (x) 1000 rpm

7.4.10 Effect of catalyst loading

Effect of catalyst loading was studied from 0.01 to 0.04 g/cm^3 (Figure 7.9). The conversion increases with increase in the catalyst amount up to 0.03 g/cm^3, which is due to the linear increase in the number of active sites. When SFZ-10 catalyst loading was increased from 0.03 to 0.04 g/cm^3, there was no significant change observed within the experimental error. Therefore, further reactions were carried out at 0.03 g/cm^3. Figure 7.10 depicts that the initial

rate of reaction increases linearly with catalyst loading which confirms that mass transfer resistance is absent.

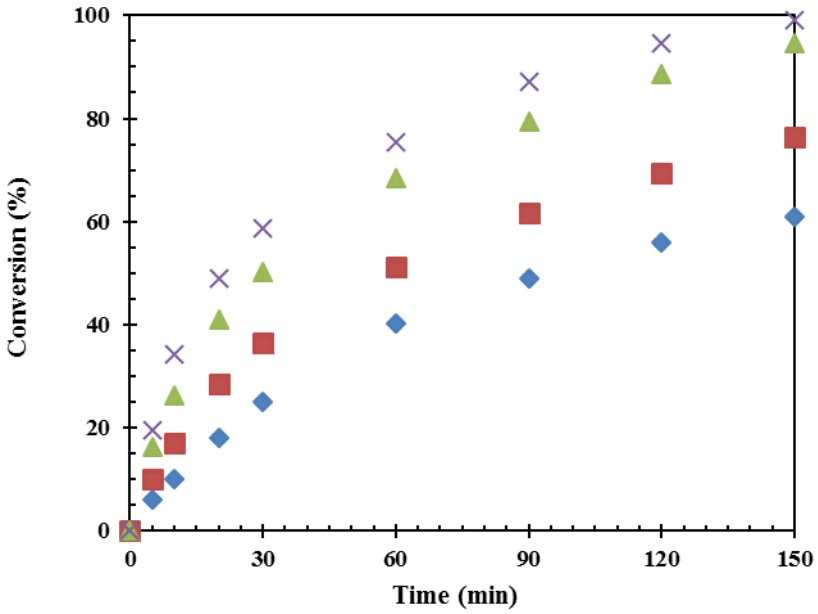

Figure 7.9 Effect of catalyst loading on conversion of Salicylic acid: Salicylic acid 0.075 mol, methanol 0.75 mol, catalyst SFZ-10, temparature-120 ºC, total volume 40cm^3, reaction time 150 min, speed of agitation 800 rpm. (◆) 0.01 g/cm^3, (■) 0.02 g/cm^3, (▲) 0.03 g/cm^3, (x) 0.04 g/cm^3

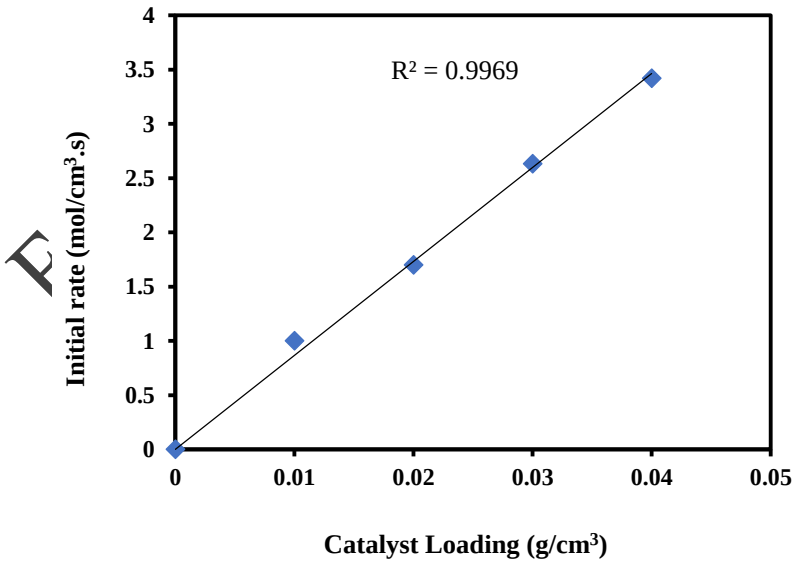

Figure 7.10 Plot of initial rate on conversion of Salicylic acid: Salicylic acid 0.075 mol, methanol 0.75 mol, catalyst SFZ-10, temparature-120 ºC, total volume 40 cm^3, reaction time 150 min, speed of agitation 800 rpm.

7.4.11 Effect of mole ratio

Salicylic acid to DMC mole ratio was varied from 1: 2 to 1: 15 under the similar conditions by keeping the total volume constant (Figure 7.11). The increase in conversion of salicylic acid was observed due to increase in a number of moles of DMC with respect to salicylic acid. However, 1:10 mole ratio was taken for further experiments.

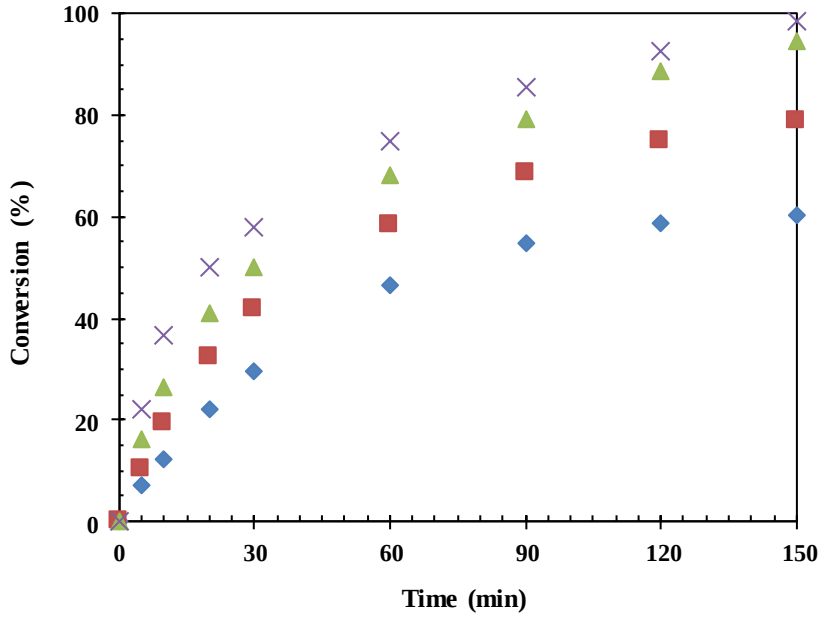

Figure 7.11 Effect of mole ratio on conversion of Salicylic acid: Salicylic acid 0.075 mol, catalyst SFZ-10, temparature-120 °C, total volume 40 cm^3, reaction time 150 min, speed of agitation 800 rpm. (♦) 1:2, (■) 1:5, (▲) 1:10, (x) 1:15.

7.4.12 Effect of temperature

SFZ-10 catalyst was employed for esterification of salicylic acid over a period of 150 min at four different temperatures ranging from 100 to 130 °C (Figure 7.12) under the similar conditions. The conversion increased from 58 % at 100 °C to 95 % at 130 °C. The increase in conversion of salicylic acid with an increase in temperature revealed that the reaction was kinetically controlled.

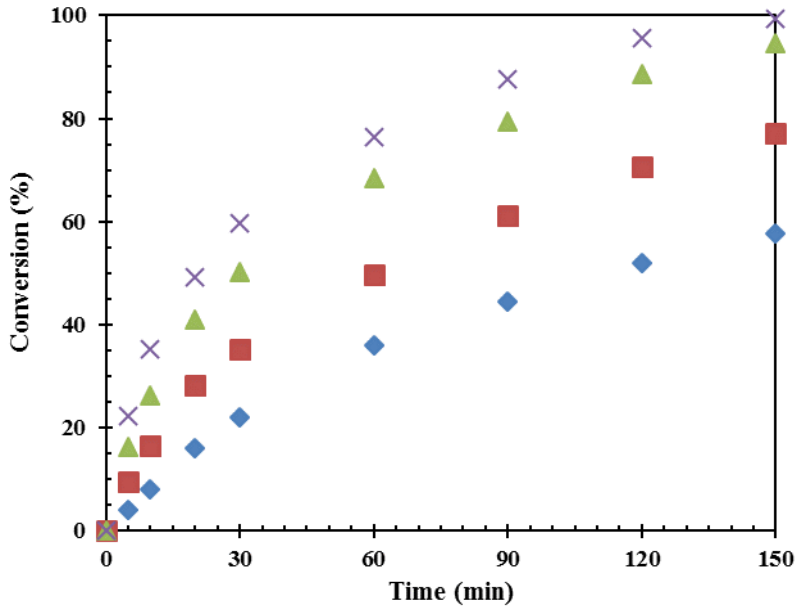

Figure 7.12 Effect of temperature on conversion of Salicylic acid: Salicylic acid 0.075 mol, methanol 0.75 mol, catalyst SFZ-10, speed of agitation 800 rpm, total volume 40 cm^3, reaction time 150 min, catalyst loading 0.03 g/cm^3. (♦) 100 ºC, (■) 110 ºC, (▲) 120 ºC, (x) 130 ºC

7.4.13 Reaction mechanism and mathematical model

Reaction mechanism of esterification of salicylic acid on SFZ-10 is shown in Scheme 7.2. SFZ-10 consists of Brønsted acidic sites. Initially, salicylic acid gets adsorbed on the surface of SFZ-10. The adsorbed species reacts with DMC to give intermediate. This intermediate rearranges to form methyl salicylate, methanol and carbon dioxide. Methyl salicylate gets desorbed from the catalytic sites into the reaction mixture. The catalyst gets regenerated at the end of the cycle.

In the absence of any mass transfer resistance and intra particle diffusion limitation, the reaction is controlled by intrinsic kinetics and a model can be developed for the same. The detailed mathematical model was developed using LHHW mechanism which is the same as reported in the recent literature [261]. The preliminary analysis of data suggested that there was a weak adsorption of all spices. Therefore a power law model with second order kinetics was used as given below.

Let A = Salicylic acid, B = DMC, ES = Methyl salicylate, W= Methanol, S=vacant sites.

Chemisorption of A and B on vacant site S

Adsorption

Adsorption of salicylic acid (A) on a vacant site S is given by:

$$A + S \xleftrightarrow{K_A} AS \qquad (1)$$

Adsorption of DMC (B) on a vacant site S is given by:

$$B + S \xleftrightarrow{K_B} BS \qquad (2)$$

Surface reaction

Surface reaction of AS and BS in the vicinity of an active site, leading to the formation of ES and WS on the active

$$AS + BS \xleftrightarrow{K_2} ES + WS + CO_2 \qquad (3)$$

Desorption of methyl salicylate (ES) and methanol (WS) is given by:

$$ES \xleftrightarrow{1/K_E} E + S \qquad (4)$$

$$WS \xleftrightarrow{1/K_W} W + S \qquad (5)$$

The total concentration of the sites, C_t expressed as,

$$C_t = C_S + C_{AS} + C_{BS} + C_{ES} + C_{WS} \qquad (6)$$

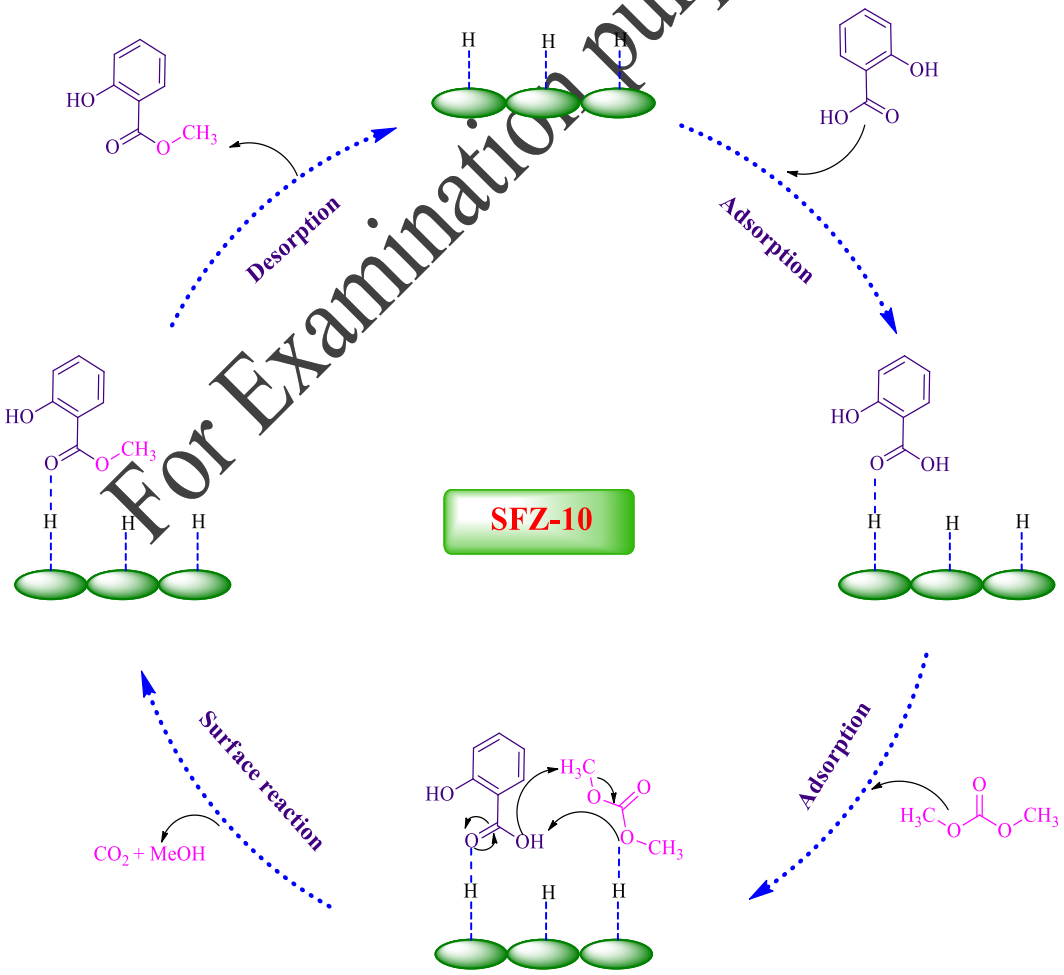

Scheme 7.2 Catalytic cycle for esterification of salicylic acid with DMC over SFZ-10

Or

$$C_t = C_S + K_A C_A C_S + K_B C_B C_S + K_S C_E C_S + K_W C_W C_S \quad (7)$$

When the adsorption and desorption steps are assumed to be equilibrium,

The concentration of vacant sites can be written as,

$$C_S = \frac{C_t}{\left(1 + K_A C_A + K_B C_B + K_S C_E + K_W C_W\right)} \quad (8)$$

If the surface reaction controls the rate of reaction, then the rate of reaction of A is given by

$$-r_A = -\frac{dC_A}{dt} = k_2 C_{AS} C_{BS} - k_2 C_{ES} C_{WS} p_{CO_2}$$

$$-\frac{dC_A}{dt} = \frac{k_2 \left\{ K_A K_B C_A C_B - \frac{K_E K_W C_E C_W p_{CO_2}}{K_2} \right\} C_t^2}{\left(1 + K_A C_A + K_B C_B + K_S C_E + K_W C_W\right)^2} \quad (9)$$

When the reaction is far away from equilibrium

$$-\frac{dC_A}{dt} = \frac{k_2 C_t^2 K_A K_B C_A C_B}{\left(1 + \sum K_i C_i\right)^2} \quad (10)$$

$$-\frac{dC_A}{dt} = \frac{k_{R_2} w C_A C_B}{\left(1 + \sum K_i C_i\right)^2} \quad (11)$$

Where $k_{R_2} w = k_2 K_A K_B C_t^2$ and w is catalyst loading.

If adsorption constants are very small then above equation is reduces to

$$\frac{dC_A}{dt} = k_{R_1} w C_A C_B \quad (12)$$

Let $C_{B_o} / C_{A_o} = M$, the molar ratio of salicylic acid at t=0. Then the above equation

$$\frac{dX_A}{dt} = k_{R1} w C_{Ao} \left(1 - X_A\right)\left(M - X_A\right) \quad (13)$$

$$\frac{dX_A}{dt} = k_1 C_{Ao} \left(1 - X_A\right)\left(M - X_B\right) \quad (14)$$

Integrating above equation

$$\ln\left\{\left(\frac{M - X_A}{M\left(1 - X_A\right)}\right)\right\} = k_1 C_{Ao} \left(M - 1\right) t \quad (15)$$

The plot of $\ln\left\{\frac{(M - X_A)}{M(1 - X_A)}\right\}$ against *t* (Figure 7.13) was made at different temperature to get an excellent fit, there by supporting the model. The reaction is intrinsically kinetically controlled and second order with an activation energy was calculated as 13.8 kcal/mol (Figure 7.14).

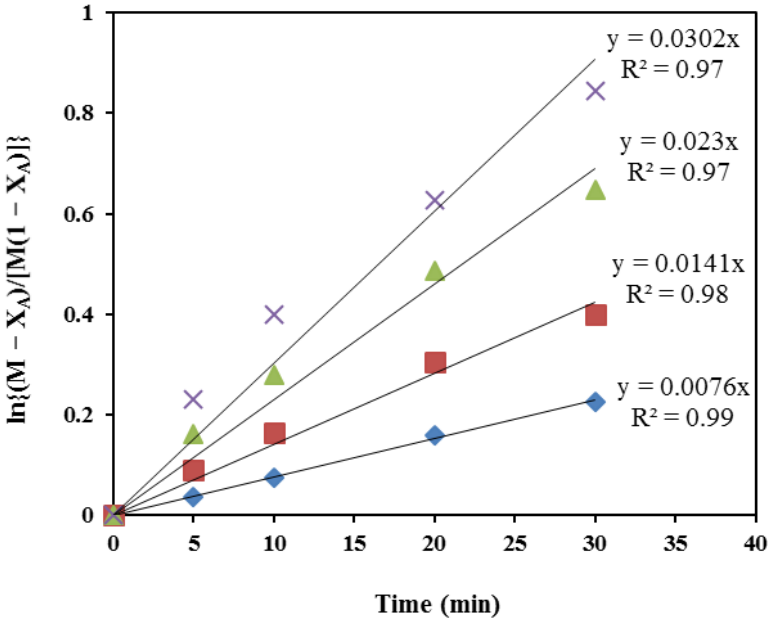

Figure 7.13 Kinetics plots for various temperatures: Salicylic acid 0.075 mol, methanol 0.75 mol, catalyst SFZ-10, speed of agitation 800 rpm, total volume 40 cm^3, reaction time 150 min, catalyst loading 0.03 g/cm^3, (◆) 100 ºC, (■) 110 ºC, (▲) 120 ºC, (x) 130 ºC

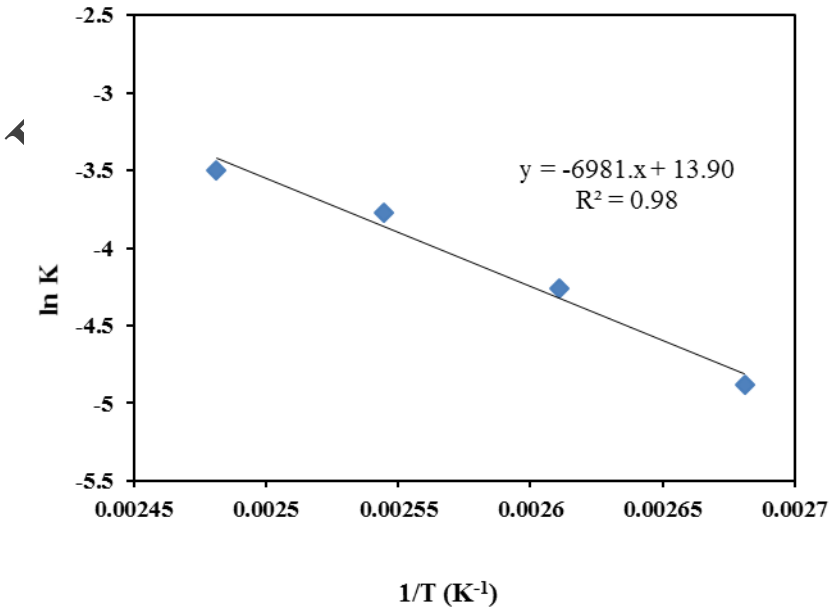

Figure 7.14 Arrhenius plot

7.4.14 Reusability of catalyst

The reusability of SFZ-10 catalyst (Figure 7.15) was carried out to find its stability under the optimized conditions (catalyst loading 0.03g/cm^3 temperature 120 °C, time 150 min). After each reaction, the catalyst was recovered and refluxed in methanol to eliminate the absorbed material from the surface and pores of SFZ-10 catalyst. It was dried for 12 h at 120 °C. It was detected that there was a marginal decrease in total conversion. Reused catalyst was characterized to see if there were any changes occurred in the catalyst. XRD, NH_3-TPD, FTIR and surface area analysis confirmed that there were no significant changes in the morphology and structure of catalyst after reuse. Thus, the prepared catalyst is stable. Further, the hot filtration test was also conducted to study leaching of active sites, if any. Reaction was stopped after 30 min and the catalyst filtered. The reactor was washed to get rid of any traces of catalyst. The reaction was continued further for 150 min. The conversion was noticed from 50 to 52 % which can be an experimental error. SFZ-10 catalyst was found stable up to four runs without significant loss of activity.

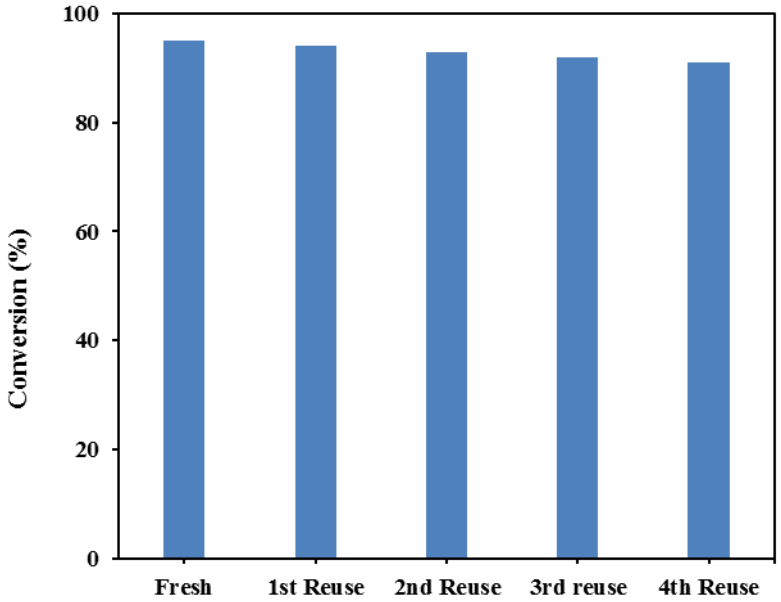

Figure 7.15 Catalyst reusability: Salicylic acid 0.075 mol, methanol 0.75 mol, catalyst SFZ-10, speed of agitation 800 rpm, temperature 120 ºC, total volume 40 cm^3, reaction time 150 min, catalyst loading 0.03 g/cm^3

7.5 Conclusion

Esterification of salicylic acid with DMC under solvent-free condition was screened using sulfated Fe_2O_3-ZrO_2 with different loadings of Fe (0, 5, 10, 15, and 20 wt %). Among

which 10 wt % SFZ was the most active catalyst. Iron promoted ZrO_2 showed much more catalytic activity than the corresponding sulfated ZrO_2 in the esterification of salicylic acid, which is due to increase in acidic sites. The highest salicylic acid conversion of 95 % with 100 % selectivity was obtained with a mole ratio of 1:10 of salicylic acid to DMC at 120 °C for 150 min at a catalyst loading of 0.03 g/cm^3. The catalyst can be reused four times with insignificant changes in the catalytic activity. Various parameters such as catalyst loading, speed of agitation, mole ratio of salicylic acid to DMC were studied to establish the reaction kinetics.

CHAPTER 8

CONCLUSION

8.1 Accomplishment

The focus of the current work was on the synthesis of safer chemicals by using various heterogeneous catalysts. It includes the use of heterogeneous acid, base metal oxides and the combination of both to make multifunctional catalytic system. Different catalysts were synthesized by using methods developed in our laboratory and reported elsewhere in the literature. Different sophisticated instruments were used for characterization of prepared catalysts. Further, the processes were optimized to get maximum conversion and selectivity of desired product.

8.1.1 Selectivity engineering in hydroxyalkoxylation of phenol by ethylene carbonate using calcined hydrotalcite

The high consumption of mono-ethylene glycol phenyl ether in various sectors requires clean and green synthesis. Herein we report an efficient, selective and green route of hydroxylation using calcined hydrotalcite for the preparation of mono-ethylene glycol phenyl ether. Various types of solid base catalysts were prepared and well characterized by TGA-DSC, FT-IR, XRD, CO_2-TPD, NH_3-TPD, SEM, and BET surface area. The catalyst possesses very high activity for hydroxyalkoxylation of phenol and ethylene glycol with 96 % conversion at 180 °C in 2 h with a catalyst loading of 0.03 g/cm^3. The insight of reaction reveals that it is kinetically controlled with second order reaction and follows power law model. The apparent activation energy for the reaction is 21.3 kcal/mol. The catalyst is highly reusable and shows green chemistry prospective and gives excellent results up to four runs.

8.1.2 Novel synthesis of Ru supported on OMS by solvent-free method: Highly active catalyst for selective hydrogenation of levulinic acid to γ-valerolactone in aqueous medium

γ-Valerolactone (GVL) is an important biomass molecule for the sustainable production of value-added chemicals and fuels. Here we are reporting the synthesis of ruthenium supported on manganese oxide octahedral molecular sieve (OMS-2) catalysts prepared by different methods for the selective hydrogenation of biomass-derived levulinic acid (LA) to GVL using molecular hydrogen in an aqueous medium. Three different methods i.e. reflux, hydrothermal and solvent less were used for preparation of OMS-2. Among which solventless synthesized OMS (OMS-2_s) is energy efficient, rapid and economical way of synthesis. Among three different catalysts, Ru supported on solventless OMS-2 i.e.1 wt% Ru/OMS-2_S catalyst showed

LA conversion of 99.9% and selectivity of 100 % towards GVL at mild conditions (100º C, 30 atm H_2). The specific textural and chemical properties of catalysts were characterized by XRD, FT-IR, NH_3-TPD, H_2-pulse chemisorption, FESEM, EDXS, nitrogen sorption and TEM. Moreover, 1 wt % Ru/OMS-2_S catalyst is reusable up to four times without significant loss of activity and is very stable. By studying the effects of different process parameter kinetic model was developed based on LHHW type of mechanism. The apparent activation energy for LA hydrogenation to GVL is 11.75 kcal/mol.

8.1.3 Potassium modified La-Mg mixed oxide: selective mono-methylation of phenylacetonitrile with dimethyl carbonate

Herein, we report wet impregnation of potassium on lanthanum-magnesium oxide. It is used first time for the selective mono-methylation of phenylacetonitrile to 2-phenyl propionitrile with dimethyl carbonate as a methylating agent. The catalyst with different loadings of potassium (1 to 4 wt %) on La_2O_3-MgO was prepared and the activity of catalyst verify for the methylation of phenylacetonitrile with dimethyl carbonate. Two wt % K/ La_2O_3-MgO catalyst showed 100 % of conversion of phenylacetonitrile and 100 % selectivity of 2-phenyl propionitrile at 150 ºC after 2 h. The characterization of 2 wt % K/ La_2O_3-MgO was done using different techniques such as FTIR, SEM, EDXA, TGA-DSC, XRD, and BET surface area analysis. Two wt % K/ La_2O_3-MgO catalyst used to study the reaction mechanism, and a kinetic model was using LHHW type of mechanism. The apparent activation for methylation of phenylacetonitrile to 2-phenyl propionitrile is found to be 13.77 kcal/mol.

8.1.4 Green synthesis of veratraldehyde using a novel potassium promoted lanthanum-magnesium mixed oxide catalyst

The industrially important veratraldehyde was synthesized from the O-alkylation of the vanillin with the environmentally benign reagent, dimethyl carbonate. A series of potassium loaded La_2O_3-MgO were prepared by incipient wetness impregnation method. All the catalysts were characterized by N_2 adsorption/desorption, XRD, TGA-DSC, FT-IR, CO_2-TPD and SEM techniques. Effects of different loadings (1-4 wt %) of potassium on La_2O_3-MgO was studied and 2 wt % loading showed the best results. 2 wt % k/La_2O_3-MgO catalyst showed better activity as compared to La_2O_3-MgO catalyst, it is due to high dispersion of potassium and high basicity as revealed in characterization. The optimized 2 wt % k/ La_2O_3-MgO catalyst was used for O-methylation of vanillin with dimethyl carbonate (DMC), and activity was found to be

closely associated with basicity. Various parameters were studied to achieve maximum yield of the desired product. The maximum conversion was found with a catalyst loading of 0.03 g/cm^3 at 160 °C in 2 h. The reaction follows pseudo first order kinetics for the O-methylation of vanillin. The energy of activation was found to be 13.5 kcal/mol.

8.1.5 Novel combustion synthesized sulfated iron-zirconia catalyst: Esterification of salicylic acid with dimethyl carbonate under solvent free condition

Sulfated Fe_2O_3-ZrO_2 catalyst with different Fe_2O_3 loadings have been first time prepared by combustion technique. The catalytic activity of sulfated Fe_2O_3-ZrO_2 was estimated for the esterification of salicylic acid with dimethyl carbonate. The catalyst with different loadings of Fe on zirconia (5, 10, 15, 20 wt %) was synthesized and activity of the catalyst was compared with the acid catalysts such as ZrO_2, sulfated zirconia for the esterification of salicylic acid with dimethyl carbonate. The introduction of Fe_2O_3 considerably increases salicylic acid conversion. The activity of the catalysts increases after the loading of metal and 10 wt % of Fe_2O_3 gave the highest acidity and best catalytic for synthesis of methyl salicylate (oil of wintergreen). The prepared catalysts were characterized by using various techniques such as XRD, FTIR, TGA, SEM, EDX, NH_3-TPD and BET surface area analysis. The 10 wt % sulfated Fe_2O_3-ZrO_2 catalyst demonstrated 95 % conversion of salicylic acid with 100 % selectivity at 120 °C within 2-3 h at a 1:10 molar ratio of salicylic acid to dimethyl carbonate and a catalyst loading of 0.03 g/cm^3. Effect of different kinetic parameters on the rate of esterification of salicylic acid was studied to found the kinetics of the reaction. The apparent activation energy for this reaction was found to be 13.82 kcal/mol.

CHAPTER 9

FURTHER WORK

9.1 Further Work

The utilization of renewable resources for production of valuable chemicals and energy is one of the best approaches to solve the problem of energy and sustainable growth. The fine tuning of materials depends on their method of preparation, precursor used for synthesis and conditions applied for synthesis. Ruthenium supported on octahedral molecular sieve used in this study was found to be a very good catalyst. Different metals can be incorporated for selective engineering of various platform molecules into desired product. The potassium promoted La-Mg catalyst is super basic and can be used for various base catalyzed reactions. Sulfated iron-zirconia catalyst can be used for oxidation reactions.

CHAPTER 10

BIBLIOGRAPHY
AND
REFERENCES

[1] G.D. Yadav, M.S. Krishnan, Etherification of β-Naphthol with Alkanols Using Modified Clays and Sulfated Zirconia, Ind. Eng. Chem. Res. 37 (1998) 3358–3365.

[2] S.R. Kirumakki, N. Nagaraju, K.V.R. Chary, S. Narayanan, A facile O-alkylation of 2-naphthol over zeolites Hβ, HY, and HZSM5 using dimethyl carbonate and methanol, J. Catal. 221 (2004) 549–559.

[3] J.C. Anastas, P. T.; Warner, Green Chemistry Theory and Practice, Oxford University Press, New York, 1998.

[4] O. G.A., Friedel –Crafts chemistry, Wiley, New York, 1973.

[5] A. Corma, From Microporous to Mesoporous Molecular Sieve Materials and Their Use in Catalysis, Chem. Rev. 97 (1997) 2373–2420.

[6] J.C.W. P.T. Anastas, Green Chemistry: Theory and Practice, Oxford University Press, New York, 1998.

[7] P. Metivier, Fine Chemicals through Heterogeneous Catalysis, Wiley-VCH, Weinheim, 2001.

[8] J.A. Gladysz, Introduction: Recoverable Catalysts and ReagentsPerspective and Prospective, Chem. Rev. 102 (2002) 3215–3216.

[9] S. Schneider, W. Bannwarth, Repetitive Application of Perfluoro-Tagged Pd Complexes for Stille Couplings in a Fluorous Biphasic System, Angew. Chemie. 39 (2000) 4142–4145.

[10] M.J. Ingleson, M.F. Mahon, N.J. Patmore, G.D. Ruggiero, A.S. Weller, [(PPh3)Ag(HCB11Me11)]: A Complex with Intermolecular Ag···H3C Interactions, Angew. Chemie Int. Ed. 41 (2002) 3694–3697.

[11] C.C. Tzschucke, C. Markert, H. Glatz, W. Bannwarth, Fluorous Biphasic Catalysis without Perfluorinated Solvents: Application to Pd-Mediated Suzuki and Sonogashira Couplings, Angew. Chemie Int. Ed. 41 (2002) 4500–4503.

[12] Q.-H. Fan, Y.-M. Li, A.S.C. Chan, Recoverable Catalysts for Asymmetric Organic Synthesis, Chem. Rev. 102 (2002) 3385–3466.

[13] C.A. McNamara, M.J. Dixon, M. Bradley, Recoverable Catalysts and Reagents Using Recyclable Polystyrene-Based Supports, Chem. Rev. 102 (2002) 3275–3300.

[14] D.E. De Vos, M. Dams, B.F. Sels, P.A. Jacobs, Ordered Mesoporous and Microporous Molecular Sieves Functionalized with Transition Metal Complexes as Catalysts for Selective Organic Transformations, Chem. Rev. 102 (2002) 3615–3640.

[15] A.P. Wight, M.E. Davis, Design and Preparation of Organic−Inorganic Hybrid Catalysts, Chem. Rev. 102 (2002) 3589–3614.

[16] G.D. Yadav, N. Kirthivasan, Single-pot synthesis of methyl tert-butyl ether from tert-butyl alcohol and methanol: dodecatungstophosphoric acid supported on clay as an efficient catalyst, J. Chem. Soc. Chem. Commun. (1995) 203.

[17] G.D. Yadav, Y.B. Jadhav, Role of the Omega Phase in the Analysis and Intensification of Solid−Liquid Phase-Transfer-Catalyzed Reactions, Langmuir. 18 (2002) 5995–6002.

[18] G. Yadav, Cesium-substituted dodecatungstophosphoric acid on K-10 clay for benzoylation of anisole with benzoyl chloride, J. Catal. (2003).

[19] G.D. Yadav, N.S. Asthana, V.S. Kamble, Friedel–Crafts benzoylation of p-xylene over clay supported catalysts: novelty of cesium substituted dodecatungstophosphoric acid on K-10 clay, Appl. Catal. A Gen. 240 (2003) 53–69.

[20] G.D. Yadav, A.D. Murkute, Preparation of a novel catalyst UDCaT-5: enhancement in activity of acid-treated zirconia—effect of treatment with chlorosulfonic acid vis-à-vis sulfuric acid, J. Catal. 224 (2004) 218–223.

[21] G.D. Yadav, Insight into Green Phase Transfer Catalysis, Top. Catal. 29 (2004) 145–161.

[22] A. Corma, H. García, Lewis Acids as Catalysts in Oxidation Reactions: From Homogeneous to Heterogeneous Systems, Chem. Rev. 102 (2002) 3837–3892.

[23] A. Corma, H. García, Lewis Acids: From Conventional Homogeneous to Green Homogeneous and Heterogeneous Catalysis, Chem. Rev. 103 (2003) 4307–4366.

[24] K.U. and M.O. Y. Izumi, Zeolites, Clays and Heteropoly Acids, VCH Publishers Inc, London, 1992.

[25] G.D. Yadav, J.J. Nair, Sulfated zirconia and its modified versions as promising catalysts for industrial processes, Microporous Mesoporous Mater. 33 (1999) 1–48.

[26] B.M. Reddy, M.K. Patil, Organic Syntheses and Transformations Catalyzed by Sulfated Zirconia, Chem. Rev. 109 (2009) 2185–2208.

[27] B. Umansky, On the strength of solid acids, J. Catal. 127 (1991) 128–140.

[28] K.B. Fogash, G. Yaluris, M.R. Gonzlez, P. Ouraipryvan, D.A. Ward, E.I. Ko, J.A. Dumesic, Characterization and selective poisoning of acid sites on sulfated zirconia, Catal. Letters. 32 (1995) 241–251.

[29] T.K. Cheung, J.L. Ditri, B.C. Gates, Cracking of n-Butane Catalyzed by Iron- and Manganese-Promoted Sulfated Zirconia, J. Catal. 153 (1995) 344–349.

[30] R. Keogh, Pt-SO2−4-ZrO2 Catalysts: The Impact of Water on Their Activity for Hydrocarbon Conversion, J. Catal. 151 (1995) 292–299.

[31] H. Hattori, Heterogeneous Basic Catalysis, Chem. Rev. 95 (1995) 537–558.

[32] H. Hattori, Basic catalysts and fine chemicals, (1993) 35–49.

[33] F. Cavani, F. Trifirò, A. Vaccari, Hydrotalcite-type anionic clays: Preparation, properties and applications., Catal. Today. 11 (1991) 173–301.

[34] W. REICHLE, Catalytic reactions by thermally activated, synthetic, anionic clay minerals, J. Catal. 94 (1985) 547–557.

[35] J.L. Lemberton, M. Touzeyidio, M. Guisnet, Catalytic hydroprocessing of simulated coal tars, Appl. Catal. 54 (1989) 91–100.

[36] W. REICHLE, Catalytic reactions by thermally activated, synthetic, anionic clay minerals, J. Catal. 94 (1985) 547–557.

[37] E. Suzuki, Y. Ono, Aldol Condensation Reaction between Formaldehyde and Acetone over Heat-Treated Synthetic Hydrotalcite and Hydrotalcite-Like Compounds, Bull. Chem. Soc. Jpn. 61 (1988) 1008–1010.

[38] J.L. Lemberton, M. Touzeyidio, M. Guisnet, Catalytic hydroprocessing of simulated coal tars, Appl. Catal. 54 (1989) 91–100.

[39] A. CORMA, Determination of base properties of hydrotalcites: Condensation of benzaldehyde with ethyl acetoacetate, J. Catal. 134 (1992) 58–65.

[40] A. Takagaki, K. Iwatani, S. Nishimura, K. Ebitani, Synthesis of glycerol carbonate from glycerol and dialkyl carbonates using hydrotalcite as a reusable heterogeneous base catalyst, Green Chem. 12 (2010) 578.

[41] M. Malyaadri, K. Jagadeeswaraiah, P.S. Sai Prasad, N. Lingaiah, Synthesis of glycerol carbonate by transesterification of glycerol with dimethyl carbonate over Mg/Al/Zr catalysts, Appl. Catal. A Gen. 401 (2011) 153–157.

[42] V. Calvino-Casilda, G. Mul, J.F. Fernández, F. Rubio-Marcos, M.A. Bañares, Monitoring the catalytic synthesis of glycerol carbonate by real-time attenuated total reflection FTIR spectroscopy, Appl. Catal. A Gen. 409–410 (2011) 106–112.

[43] R. Bai, S. Wang, F. Mei, T. Li, G. Li, Synthesis of glycerol carbonate from glycerol and dimethyl carbonate catalyzed by KF modified hydroxyapatite, J. Ind. Eng. Chem. 17 (2011) 777–781.

[44] A. Desmartin-Chomel, B. Hamad, J. Palomeque, N. Essayem, G. Bergeret, F. Figueras, Basic properties of MgLaO mixed oxides as determined by microcalorimetry and kinetics, Catal. Today. 152 (2010) 110–114.

[45] M.L. Kantam, K.B.S. Kumar, V. Balasubramanyam, G.T. Venkanna, F. Figueras, One-pot Wittig reaction for the synthesis of α,β-unsaturated esters using highly basic magnesium/lanthanum mixed oxide, J. Mol. Catal. A Chem. 321 (2010) 10–14.

[46] N.S. Babu, R. Sree, P.S.S. Prasad, N. Lingaiah, Room-Temperature Transesterification of Edible and Nonedible Oils Using a Heterogeneous Strong Basic Mg/La Catalyst, Energy & Fuels. 22 (2008) 1965–1971.

[47] S. Yan, M. Kim, S.O. Salley, K.Y.S. Ng, Oil transesterification over calcium oxides modified with lanthanum, Appl. Catal. A Gen. 360 (2009) 163–170.

[48] J. Palomeque, J. Lopez, F. Figueras, Epoxydation of Activated Olefins by Solid Bases, J. Catal. 211 (2002) 150–156.

[49] F. Figueras, J. Lopez, J. Sanchezvalente, T. Vu, J. Clacens, J. Palomeque, Isophorone Isomerization as Model Reaction for the Characterization of Solid Bases: Application to the Determination of the Number of Sites, J. Catal. 211 (2002) 144–149.

[50] M.L. Kantam, H. Kochkar, J.-M. Clacens, B. Veldurthy, A. Garcia-Ruiz, F. Figueras, MgLa mixed oxides as highly active and selective heterogeneous catalysts for Wadsworth–Emmons reactions, Appl. Catal. B Environ. 55 (2005) 177–183.

[51] B. Veldurthy, F. Figueras, An efficient synthesis of organic carbonates: atom economic protocol with a new catalytic system, Chem. Commun. (2004) 734.

[52] F.S.H. Simanjuntak, V.T. Widyaya, C.S. Kim, B.S. Ahn, Y.J. Kim, H. Lee, Synthesis of glycerol carbonate from glycerol and dimethyl carbonate using magnesium–lanthanum mixed oxide catalyst, Chem. Eng. Sci. 94 (2013) 265–270.

[53] B. Veldurthy, J.M. Clacens, F. Figueras, Magnesium-Lanthanum Mixed Metal Oxide: a Strong Solid Base for the Michael Addition Reaction, Adv. Synth. Catal. 347 (2005) 767–771.

[54] J. Palomeque, Epoxydation of Activated Olefins by Solid Bases, J. Catal. 211 (2002) 150–156.

[55] C.S. MacLeod, A.P. Harvey, A.F. Lee, K. Wilson, Evaluation of the activity and stability of alkali-doped metal oxide catalysts for application to an intensified method of biodiesel production, Chem. Eng. J. 135 (2008) 63–70.

[56] G. Suppes, Transesterification of soybean oil with zeolite and metal catalysts, Appl. Catal. A Gen. 257 (2004) 213–223.

[57] G. Arzamendi, I. Campo, E. Arguiñarena, M. Sánchez, M. Montes, L.M. Gandía, Synthesis of biodiesel with heterogeneous NaOH/alumina catalysts: Comparison with homogeneous NaOH, Chem. Eng. J. 134 (2007) 123–130.

[58] W. Xie, H. Li, Alumina-supported potassium iodide as a heterogeneous catalyst for biodiesel production from soybean oil, J. Mol. Catal. A Chem. 255 (2006) 1–9.

[59] C.S. MacLeod, A.P. Harvey, A.F. Lee, K. Wilson, Evaluation of the activity and stability

of alkali-doped metal oxide catalysts for application to an intensified method of biodiesel production, Chem. Eng. J. 135 (2008) 63–70.

[60] G. Suppes, Transesterification of soybean oil with zeolite and metal catalysts, Appl. Catal. A Gen. 257 (2004) 213–223.

[61] D.M. Alonso, R. Mariscal, R. Moreno-Tost, M.D.Z. Poves, M.L. Granados, Potassium leaching during triglyceride transesterification using K/γ-Al2O3 catalysts, Catal. Commun. 8 (2007) 2074–2080.

[62] K. Tanabe M. Misono H. Hattori Y. Ono, New Solid Acids and Bases, Their Catalytic Properties, Tokya, 1990.

[63] J. Hua Zhu, Y. Wang, Y. Chun, X. Shu Wang, Dispersion of potassium nitrate and the resulting basicity on alumina and zeolite NaY, J. Chem. Soc. Faraday Trans. 94 (1998) 1163–1169.

[64] L.B. Sun, J. Yang, J.H. Kou, F.N. Gu, Y. Chun, Y. Wang, J.H. Zhu, Z.G. Zou, One-Pot Synthesis of Potassium-Functionalized Mesoporous γ-Alumina: A Solid Superbase, Angew. Chemie Int. Ed. 47 (2008) 3418–3421.

[65] X. Li, G. Lu, Y. Guo, Y. Guo, Y. Wang, Z. Zhang, X. Liu, Y. Wang, A novel solid superbase of Eu2O3/Al2O3 and its catalytic performance for the transesterification of soybean oil to biodiesel, Catal. Commun. 8 (2007) 1969–1972.

[66] Y. Wang, W.Y. Huang, Z. Wu, Y. Chun, J.H. Zhu, Superbase derived from zirconia-supported potassium nitrate, Mater. Lett. 46 (2000) 198–204.

[67] Y. Wang, W.Y. Huang, Y. Chun, J.R. Xia, J.H. Zhu, Dispersion of Potassium Nitrate and the Resulting Strong Basicity on Zirconia, Chem. Mater. 13 (2001) 670–677.

[68] S.-F. Yin, B.-Q. Xu, S.-J. Wang, C.-T. Au, Nanosized Ru on high-surface-area superbasic ZrO2-KOH for efficient generation of hydrogen via ammonia decomposition, Appl. Catal. A Gen. 301 (2006) 202–210.

[69] A.M. Ferrari, G. Pacchioni, Electronic Structure of F and V Centers on the MgO Surface, J. Phys. Chem. 99 (1995) 17010–17018.

[70] N. Sun, K.J. Klabunde, High Activity Solid Super Base Catalysts Employing Nanocrystals of Metal Oxides: Isomerization and Alkylation Catalysis, Including Conversion of Propylene-Ethylene Mixtures to Pentenes and Heptenes, J. Catal. 185 (1999) 506–512.

[71] J.H. Zhu, Y. Chun, Y. Wang, Q.H. Xu, New unusually strong solid basic material derived from KL zeolite impregnated with KNO3, Mater. Lett. 33 (1997) 207–210.

[72] L.B. Sun, J.H. Kou, Y. Chun, J. Yang, F.N. Gu, Y. Wang, J.H. Zhu, Z.G. Zou, New

Attempt at Directly Generating Superbasicity on Mesoporous Silica SBA-15, Inorg. Chem. 47 (2008) 4199–4208.

[73] Y. Wei, S. Zhang, S. Yin, C. Zhao, S. Luo, C. Au, Solid superbase derived from lanthanum–magnesium composite oxide and its catalytic performance in the knoevenagel condensation under solvent-free condition, Catal. Commun. 12 (2011) 1333–1338.

[74] J. Zhao, J. Xie, C.-T. Au, S.-F. Yin, Novel and versatile solid superbases derived from magnesium–zirconium composite oxide and their catalytic applications, RSC Adv. 4 (2014) 6159.

[75] T. Montanari, L. Castoldi, L. Lietti, G. Busca, Basic catalysis and catalysis assisted by basicity: FT-IR and TPD characterization of potassium-doped alumina, Appl. Catal. A Gen. 400 (2011) 61–69.

[76] T. Yuzhakova, V. Rakić, C. Guimon, A. Auroux, Preparation and Characterization of Me 2 O 3 −CeO 2 (Me = B, Al, Ga, In) Mixed-Oxide Catalysts, Chem. Mater. 19 (2007) 2970–2981.

[77] A.S. Ivanova, Structure, Texture, and Acid-Base Properties of Alkaline Earth Oxides, Rare Earth Oxides, and Binary Oxide Systems, Kinet. Catal. 46 (2005) 620–633.

[78] A.S. Ivanova, B.L. Moroz, E.M. Moroz, Y.V. Larichev, E. a. Paukshtis, V.I. Bukhtiyarov, New binary systems Mg–M–O (M=Y, La, Ce): Synthesis and physico-chemical characterization, J. Solid State Chem. 178 (2005) 3265–3274.

[79] J. Clacens, D. Genuit, L. Delmotte, A. Garcia-Ruiz, G. Bergeret, R. Montiel, J. Lopez, F. Figueras, Effect of the support on the basic and catalytic properties of KF, J. Catal. 221 (2004) 483–490.

[80] Y.-H. Sun, L.-B. Sun, T.-T. Li, X.-Q. Liu, Modulating the Host Nature by Coating Alumina: A Strategy to Promote Potassium Nitrate Decomposition and Superbasicity Generation on Mesoporous Silica SBA-15, J. Phys. Chem. C. 114 (2010) 18988–18995.

[81] Y. Wang, W.Y. Huang, Y. Chun, J.R. Xia, J.H. Zhu, Dispersion of Potassium Nitrate and the Resulting Strong Basicity on Zirconia, Chem. Mater. 13 (2001) 670–677.

[82] P. Qiu, B. Yang, C. Yi, S. Qi, Characterization of KF/γ-Al2O3 Catalyst for the Synthesis of Diethyl Carbonate by Transesterification of Ethylene Carbonate, Catal. Letters. 137 (2010) 232–238.

[83] C. Illenseer, H.-G. Löhmannsröben, Investigation of ion–molecule collisions with laser-based ion mobility spectrometry, Phys. Chem. Chem. Phys. 3 (2001) 2388–2393.

[84] R.L. Augustine, Catalytic Hydrogenation, Techniques and Applications in Organic

Synthesis, Marcel Dekker, New York, 1965.

[85] P.N. Rylander, Catalytic Hydrogenation in Organic Synthesis, Academic Press, New York, 1979.

[86] M. Freifelder, Catalytic Hydrogenation in Organic Synthesis: Procedures and Commentary, Wiley, New York, 1978.

[87] Reductions in Orgaic Chemistry, Ellis Horwood Limited, Chichester, 1984.

[88] H.S. Broadbent, T.G. Selin, Rhenium Catalysts. VI. Rhenium(IV) Oxide Hydrate 1, J. Org. Chem. 28 (1963) 2343–2345.

[89] P.K Goel, Catalysis in organic synthesis, UDCT Mumbai, 2001.

[90] J. Tan, J. Cui, T. Deng, X. Cui, G. Ding, Y. Zhu, Water-Promoted Hydrogenation of Levulinic Acid to γ-Valerolactone on Supported Ruthenium Catalyst, ChemCatChem. 3 (2015) 508–512.

[91] D. Richard, J. Ockelford, A. Giroir-Fendler, P. Gallezot, Composition and catalytic properties in cinnamaldehyde hydrogenation of charcoal-supported, platinum catalysts modified by FeCl2 additives, Catal. Letters. 3 (1989) 53–58.

[92] A. Corma, A. Iborra, S. Velty, Chemical Routes for the Transformation of Biomass into Chemicals , Chem. Rev. 107 (2007) 2411–2502.

[93] M.S.Davis, S. E.; Ide, R.J. Davis, Selective oxidation of alcohols and aldehydes over supported metal nanoparticles, Green Chem. 15 (2013) 17−45.

[94] J.S. Luterbacher, J.A. Martin-Alonso, D. Dumesic, Targeted chemical upgrading of lignocellulosic biomass to platform molecules, Green Chem. 16 (2014) 4816−4838.

[95] S.Y. Choi, S.; Song, C. W.; Shin, J. H. Lee, Biorefineries for the production of top building block chemicals and their derivatives. 2015, 28, 223−239., Metab. Eng. 28 (2015) 223–239.

[96] P. Gallezot, Conversion of biomass to selected chemical products, Chem. Soc. Rev. 41 (2012) 1538−1558.

[97] A.K. Kinage, S.P. Gupte, R.K. Chaturvedi, R. V. Chaudhari, Highly selective synthesis of mono-ethylene glycol phenyl ethers via hydroxyalkoxylation of phenols by cyclic carbonates using large pore zeolites, Catal. Commun. 9 (2008) 1649–1655.

[98] C.L. Butler, A.G. Renfrew, Hydroxyalkyl Ethers of Basic Phenols. The Antipneumococcic Activity of Some 8-Quinolyl Ethers, J. Am. Chem. Soc. 60 (1938) 1582–1585.

[99] R.E. Rindfusz, syntheses of chromanes and coumaranes, J. Am. Chem. Soc. 41 (1919) 665–670.

[100] M.S. Morgan, L.H. Cretcher, Two 6-β-Hydroxyethoxy-8 diethylaminoalkylaminoquinolines, J. Am. Chem. Soc. 68 (1946) 781–784.

[101] W.W. Carlson, L.H. Cretcher, Hydroxyalkylation with Cyclic Alkylene Esters. I. Synthesis of Hydroxyethylapocupreine, J. Am. Chem. Soc. 69 (1947) 1952–1956.

[102] T. Yoshino, S. Inaba, Y. Ishido, Synthetic Studies by the Use of Carbonates. III. The Condensation Reactions of Ethylene Carbonate with a Variety of Phenols Catalyzed by Lithium Hydride or Tetraethylammonium Halides, Bull. Chem. Soc. Jpn. 46 (1973) 553–556.

[103] K.m.kem, Process of preparing organophosphorus compounds by phase transfer catalysis, 4,261,922, 1981.

[104] N. Hildeberto, Hydroxyalklylation of phenols, 5,679,871, 1997.

[105] J.P. Parrish, R.N. Salvatore, K.W. Jung, Perspectives on Alkyl Carbonates in Organic Synthesis, Tetrahedron. 56 (2000) 8207–8237.

[106] P. Ziosi, T. Tabanelli, G. Fornasari, S. Cocchi, F. Cavani, P. Righi, Carbonates as reactants for the production of fine chemicals: the synthesis of 2-phenoxyethanol, Catal. Sci. Technol. 4 (2014) 4386–4395.

[107] G.D. Yadav, J.J. Nair, Sulfated zirconia and its modified versions as promising catalysts for industrial processes, Microporous Mesoporous Mater. 33 (1999) 1–48.

[108] Cejka, Zeolites and Catalysis, Wiley-VCH Verlag GmbH & Co. KGaA, Weinheim, Germany, 2010.

[109] G.D. Yadav, Synergism of Clay and Heteropoly Acids as Nano-Catalysts for the Development of Green Processes with Potential Industrial Applications, Catal. Surv. from Asia. 9 (2005) 117–137.

[110] K. Tanabe, Industrial application of solid acid–base catalysts, Appl. Catal. A Gen. 181 (1999) 399–434.

[111] G.J. Kelly, F. King, M. Kett, Waste elimination in condensation reactions of industrial importance, Green Chem. 4 (2002) 392–399.

[112] A. Corma, H. García, Lewis Acids: From Conventional Homogeneous to Green Homogeneous and Heterogeneous Catalysis, Chem. Rev. 103 (2003) 4307–4366.

[113] H. van B. Roger Arthur Sheldon, Fine Chemicals through Heterogeneous Catalysis, 2001.

[114] J.A. van Bokhoven, J.C.A.A. Roelofs, K.P. de Jong, D.C. Koningsberger, Unique Structural Properties of the Mg-Al Hydrotalcite Solid Base Catalyst: An In Situ Study Using Mg and Al K-Edge XAFS during Calcination and Rehydration, Chemistry

(Easton). 7 (2001) 1258–1265.

[115] M.J. Hernandez, M.A. Ulibarri, J. Cornejo, M.J. Peña, C.J. Serna, Thermal stability of aluminium hydroxycarbonates with monovalent cations, Thermochim. Acta. 94 (1985) 257–266.

[116] M.L. Valcheva-Traykova, N.P. Davidova, A.H. Weiss, Thermal decomposition of Mg, Al-hydrotalcite material, J. Mater. Sci. 28 (1993) 2157–2162.

[117] G.W. Brindley, Thermal Behavior of Hydrotalcite and of Anion-Exchanged Forms of Hydrotalcite, Clays Clay Miner. 28 (1980) 87–91.

[118] T.M. Jyothi, T. Raja, M.B. Talawar, B.S. Rao, Selective O-methylation of catechol using dimethyl carbonate over calcined Mg□Al hydrotalcites, Appl. Catal. A Gen. 211 (2001) 41–46.

[119] M.J. Climent, A. Corma, S. Iborra, A. Velty, Activated hydrotalcites as catalysts for the synthesis of chalcones of pharmaceutical interest, J. Catal. 221 (2004) 474–482. [120] G.D. Yadav, P. Aduri, Aldol condensation of benzaldehyde with heptanal to jasminaldehyde over novel Mg–Al mixed oxide on hexagonal mesoporous silica, J. Mol. Catal. A Chem. 355 (2012) 142–154.

[121] F. Cavani, F. Trifirò, A. Vaccari, Hydrotalcite-type anionic clays: Preparation, properties and applications., Catal. Today. 11 (1991) 173–301.

[122] M.S. Tiwari, G.D. Yadav, Kinetics of Friedel-Crafts benzoylation of veratrole with benzoic anhydride using Cs2.5H0.5PW12O40/K-10 solid acid catalyst, Chem. Eng. J. 266 (2015) 64–73.

[123] M.S. Tiwari, G.D. Yadav, Novel aluminium exchanged dodecatungstophosphoric acid supported on K-10 clay as catalyst: benzoylation of diphenyloxide with benzoic anhydride, RSC Adv. 6 (2016) 49091–49100.

[124] C.-H. Zhou, X. Xia, C.-X. Lin, D.-S. Tong, J. Beltramini, Catalytic conversion of lignocellulosic biomass to fine chemicals and fuels, Chem. Soc. Rev. 40 (2011) 5588.doi:10.1039/c1cs15124j.

[125] S.C. Patankar, G.D. Yadav, Cascade Engineered Synthesis of γ-Valerolactone, 1,4-Pentanediol, and 2-Methyltetrahydrofuran from Levulinic Acid Using Pd–Cu/ZrO 2 Catalyst in Water as Solvent, ACS Sustain. Chem. Eng. 3 (2015) 2619–2630.

[126] A.B. Gawade, M.S. Tiwari, G.D. Yadav, Biobased Green Process: Selective Hydrogenation of 5-Hydroxymethylfurfural to 2,5-Dimethyl Furan under Mild Conditions Using Pd-Cs 2.5 H 0.5 PW 12 O 40 /K-10 Clay, ACS Sustain. Chem. Eng. 4 (2016) 4113–4123.

[127] Ragauskas, The Path Forward for Biofuels and Biomaterials, Science (80-.). 311 (2006) 484–489.

[128] F. Yang, J. Fu, J. Mo, X. Lu, Synergy of Lewis and Brønsted Acids on Catalytic Hydrothermal Decomposition of Hexose to Levulinic Acid, Energy & Fuels. 27 (2013) 6973–6978.

[129] H.J. Heeres, Experimental and Kinetic Modeling Studies on the Sulfuric Acid Catalyzed Conversion of, (2015).

[130] L. Bui, H. Luo, W.R. Gunther, Y. Román-Leshkov, Domino Reaction Catalyzed by Zeolites with Brønsted and Lewis Acid Sites for the Production of γ-Valerolactone from Furfural, Angew. Chemie Int. Ed. 52 (2013) 8022–8025.

[131] I.T. Horváth, H. Mehdi, V. Fábos, L. Boda, L.T. Mika, γ-Valerolactone—a sustainable liquid for energy and carbon-based chemicals, Green Chem. 10 (2008) 238–242.

[132] C. Xie, J. Song, B. Zhou, J. Hu, Z. Zhang, P. Zhang, Z. Jiang, B. Han, Porous Hafnium Phosphonate: Novel Heterogeneous Catalyst for Conversion of Levulinic Acid and Esters into γ - Valerolactone, (2016) 6–11.

[133] J. Zhang, J. Chen, Y. Guo, L. Chen, Effective Upgrade of Levulinic Acid into γ-Valerolactone over an Inexpensive and Magnetic Catalyst Derived from Hydrotalcite Precursor, ACS Sustain. Chem. Eng. 3 (2015) 1708–1714.

[134] H. Heeres, R. Handana, D. Chunai, C. Borromeus Rasrendra, B. Girisuta, H. Jan Heeres, Combined dehydration/(transfer)-hydrogenation of C6-sugars (D-glucose and D-fructose) to γ-valerolactone using ruthenium catalysts, Green Chem. 11 (2009) 1247.

[135] E.F. Mai, M. a. Machado, T.E. Davies, J. a. Lopez-Sanchez, V. Teixeira da Silva, Molybdenum carbide nanoparticles within carbon nanotubes as superior catalysts for γ-valerolactone production via levulinic acid hydrogenation, Green Chem. 16 (2014) 4092. doi:10.1039/C4GC00920G.

[136] A.M.R. Galletti, C. Antonetti, V. De Luise, M. Martinelli, A sustainable process for the production of γ-valerolactone by hydrogenation of biomass-derived levulinic acid, Green Chem. 14 (2012) 688.

[137] M. Chia, J. a. Dumesic, Liquid-phase catalytic transfer hydrogenation and cyclization of levulinic acid and its esters to γ-valerolactone over metal oxide catalysts, Chem. Commun. 47 (2011) 12233.

[138] W.R.H. Wright, R. Palkovits, Development of Heterogeneous Catalysts for the Conversion of Levulinic Acid to γ-Valerolactone, ChemSusChem. 5 (2012) 1657–1667.

[139] L. Deng, J. Li, D.-M. Lai, Y. Fu, Q.-X. Guo, Catalytic Conversion of Biomass-Derived

Carbohydrates into γ-Valerolactone without Using an External H 2 Supply, Angew. Chemie Int. Ed. 48 (2009) 6529–6532.

[140] X.-L. Du, L. He, S. Zhao, Y.-M. Liu, Y. Cao, H.-Y. He, K.-N. Fan, Hydrogen-Independent Reductive Transformation of Carbohydrate Biomass into γ-Valerolactone and Pyrrolidone Derivatives with Supported Gold Catalysts, Angew. Chemie Int. Ed. 50 (2011) 7815–7819.

[141] F.M.A. Geilen, B. Engendahl, A. Harwardt, W. Marquardt, J. Klankermayer, W. Leitner, Selective and Flexible Transformation of Biomass-Derived Platform Chemicals by a Multifunctional Catalytic System, Angew. Chemie Int. Ed. 49 (2010) 5510–5514.

[142] F.M.A. Geilen, B. Engendahl, M. Hölscher, J. Klankermayer, W. Leitner, Selective Homogeneous Hydrogenation of Biogenic Carboxylic Acids with [Ru(TriPhos)H] + : A Mechanistic Study, J. Am. Chem. Soc. 133 (2011) 14349–14358.

[143] H. Mehdi, V. Fábos, R. Tuba, A. Bodor, L.T. Mika, I.T. Horváth, Integration of Homogeneous and Heterogeneous Catalytic Processes for a Multi-step Conversion of Biomass: From Sucrose to Levulinic Acid, γ-Valerolactone, 1,4-Pentanediol, 2-Methyl-tetrahydrofuran, and Alkanes, Top. Catal. 48 (2008) 49–54.

[144] M.J. Climent, A. Corma, S. Iborra, Conversion of biomass platform molecules into fuel additives and liquid hydrocarbon fuels, Green Chem. 16 (2014) 516.

[145] P.P. Upare, J.-M. Lee, Y.K. Hwang, D.W. Hwang, J.-H. Lee, S.B. Halligudi, J.-S. Hwang, J.-S. Chang, Direct Hydrocyclization of Biomass-Derived Levulinic Acid to 2-Methyltetrahydrofuran over Nanocomposite Copper/Silica Catalysts, ChemSusChem. 4 (2011) 1749–1752.

[146] A.M. Hengne, C. V. Rode, Cu–ZrO2 nanocomposite catalyst for selective hydrogenation of levulinic acid and its ester to γ-valerolactone, Green Chem. 14 (2012) 1064.

[147] J. Yuan, S. Li, L. Yu, Y. Liu, Y. Cao, H. He, K.-N. Fan, Copper-based catalysts for the efficient conversion of carbohydrate biomass into γ-valerolactone in the absence of externally added hydrogen, Energy Environ. Sci. 6 (2013) 3308.

[148] K. Yan, A. Chen, Selective hydrogenation of furfural and levulinic acid to biofuels on the ecofriendly Cu–Fe catalyst, Fuel. 115 (2014) 101–108.

[149] K. Yan, A. Chen, Efficient hydrogenation of biomass-derived furfural and levulinic acid on the facilely synthesized noble-metal-free Cu–Cr catalyst, Energy. 58 (2013) 357–363.

[150] I. Obregón, E. Corro, U. Izquierdo, J. Requies, P.L. Arias, Levulinic acid hydrogenolysis

on Al2O3-based Ni-Cu bimetallic catalysts, Chinese J. Catal. 35 (2014) 656–662.

[151] K. Shimizu, S. Kanno, K. Kon, Hydrogenation of levulinic acid to γ-valerolactone by Ni and MoO x co-loaded carbon catalysts, Green Chem. 16 (2014) 3899.

[152] M.G. Al-Shaal, W.R.H. Wright, R. Palkovits, Exploring the ruthenium catalysed synthesis of γ-valerolactone in alcohols and utilisation of mild solvent-free reaction conditions, Green Chem. 14 (2012) 1260.

[153] C. Xiao, T.-W. Goh, Z. Qi, S. Goes, K. Brashler, C. Perez, W. Huang, Conversion of Levulinic Acid to γ-Valerolactone over Few-Layer Graphene-Supported Ruthenium Catalysts, ACS Catal. 6 (2016) 593–599.

[154] L. Deng, Y. Zhao, J. Li, Y. Fu, B. Liao, Q.-X. Guo, Conversion of Levulinic Acid and Formic Acid into γ-Valerolactone over Heterogeneous Catalysts, ChemSusChem. 3 (2010) 1172–1175.

[155] D. Kopetzki, M. Antonietti, Transfer hydrogenation of levulinic acid under hydrothermal conditions catalyzed by sulfate as a temperature-switchable base, Green Chem. 12 (2010) 656.

[156] W.K. Pang, V.K. Peterson, N. Sharma, C. Zhang, Z. Guo, Evidence of Solid-Solution Reaction upon Lithium Insertion into Cryptomelane K 0.25 Mn 2 O 4 Material, J. Phys. Chem. C. 118 (2014) 3976–3983.

[157] P.H. Ho, S.C. Lee, J. Kim, D. Lee, H.C. Woo, Properties of a manganese oxide octahedral molecular sieve (OMS-2) for adsorptive desulfurization of fuel gas for fuel cell applications, Fuel Process. Technol. 131 (2015) 238–246.

[158] G.D. Yadav, H.G. Manyar, Synthesis of a Novel Redox Material UDCaT-3: An Efficient and Versatile Catalyst for Selective Oxidation, Hydroxylation and Hydrogenation Reactions, Adv. Synth. Catal. 350 (2008) 2286–2294.

[159] G.D. Yadav, S. Subramanian, H.G. Manyar, Selective Oxidation of Methyl Diphenyl Methyl Mercapto Acetate to Methyl Diphenyl Methyl Sulfinyl Acetate Using a Novel Catalyst UDCaT-3 †, Org. Process Res. Dev. 14 (2010) 537–543.

[160] H.G. Manyar, B. Yang, H. Daly, H. Moor, S. McMonagle, Y. Tao, G.D. Yadav, A. Goguet, P. Hu, C. Hardacre, Selective Hydrogenation of α,β-Unsaturated Aldehydes and Ketones using Novel Manganese Oxide and Platinum Supported on Manganese Oxide Octahedral Molecular Sieves as Catalysts, ChemCatChem. 5 (2013) 506–512.

[161] G.D. Yadav, R.K. Mewada, Selective hydrogenation of acetophenone to 1-phenyl ethanol over nanofibrous Ag-OMS-2 catalysts, Catal. Today. 198 (2012) 330–337.

[162] G.D. Yadav, R.K. Mewada, Novelties of azobenzene synthesis via selective

hydrogenation of nitrobenzene over nano-fibrous Ag-OMS-2 – Mechanism and kinetics, Chem. Eng. J. 221 (2013) 500–511.

[163] I.J. McManus, H. Daly, H.G. Manyar, S.F.R. Taylor, J.M. Thompson, C. Hardacre, Selective hydrogenation of halogenated arenes using porous manganese oxide (OMS-2) and platinum supported OMS-2 catalysts, Faraday Discuss. 188 (2016) 451–466.

[164] Y. Ding, X. Shen, S. Sithambaram, S. Gomez, R. Kumar, V.M.B. Crisostomo, S.L. Suib, M. Aindow, Synthesis and Catalytic Activity of Cryptomelane-Type Manganese Dioxide Nanomaterials Produced by a Novel Solvent-Free Method, Chem. Mater. 17 (2005) 5382–5389.

[165] Y. Li, Z. Fan, J. Shi, Z. Liu, J. Zhou, W. Shangguan, Modified manganese oxide octahedral molecular sieves M′-OMS-2 (M′=Co,Ce,Cu) as catalysts in post plasma-catalysis for acetaldehyde degradation, Catal. Today. 256 (2015) 178–185.

[166] S. Liang, F. Teng, G. Bulgan, R. Zong, Y. Zhu, Effect of Phase Structure of MnO 2 Nanorod Catalyst on the Activity for CO Oxidation, J. Phys. Chem. C. 112 (2008) 5307–5315.

[167] F. Su, L. Lv, F.Y. Lee, T. Liu, A.I. Cooper, X.S. Zhao, Thermally Reduced Ruthenium Nanoparticles as a Highly Active Heterogeneous Catalyst for Hydrogenation of Monoaromatics, J. Am. Chem. Soc. 129 (2007) 14213–14223.

[168] L. Wang, C. Zhang, H. He, F. Liu, C. Wang, Effect of Doping Metals on OMS-2/γ-Al 2 O 3 Catalysts for Plasma-Catalytic Removal of o -Xylene, J. Phys. Chem. C. 120 (2016) 6136–6144.

[169] X. Meng, J. Zhang, B. Chen, Z. Jing, P. Zhao, Copper supported on H + -modified manganese oxide octahedral molecular sieves (Cu/H-OMS-2) as a heterogeneous biomimetic catalyst for the synthesis of imidazo[1,2-a]-N-heterocycles, Catal. Sci. Technol. 6 (2016) 890–896.

[170] K.S.W. Sing, Reporting physisorption data for gas/solid systems with special reference to the determination of surface area and porosity (Recommendations 1984), Pure Appl. Chem. 57 (1985) 2201–2218.

[171] L. Zhang, J. Tu, L. Lyu, C. Hu, Enhanced catalytic degradation of ciprofloxacin over Ce-doped OMS-2 microspheres, Appl. Catal. B Environ. 181 (2016) 561–569.

[172] P.A. Son, S. Nishimura, K. Ebitani, Production of γ-valerolactone from biomass-derived compounds using formic acid as a hydrogen source over supported metal catalysts in water solvent, RSC Adv. 4 (2014) 10525.

[173] M. Sudhakar, M. Lakshmi Kantam, V. Swarna Jaya, R. Kishore, K.V. Ramanujachary,

A. Venugopal, Hydroxyapatite as a novel support for Ru in the hydrogenation of levulinic acid to γ-valerolactone, Catal. Commun. 50 (2014) 101–104.

[174] C. Ortiz-Cervantes, J.J. García, Hydrogenation of levulinic acid to γ-valerolactone using ruthenium nanoparticles, Inorganica Chim. Acta. 397 (2013) 124–128.

[175] A.M. Ruppert, M. Jędrzejczyk, O. Sneka-Płatek, N. Keller, A.S. Dumon, C. Michel, P. Sautet, J. Grams, Ru catalysts for levulinic acid hydrogenation with formic acid as a hydrogen source, Green Chem. 18 (2016) 2014–2028.

[176] A.M. Ruppert, J. Grams, M. Jędrzejczyk, J. Matras-Michalska, N. Keller, K. Ostojska, P. Sautet, Titania-Supported Catalysts for Levulinic Acid Hydrogenation: Influence of Support and its Impact on γ-Valerolactone Yield, ChemSusChem. 8 (2015) 1538–1547.

[177] J. Tan, J. Cui, T. Deng, X. Cui, G. Ding, Y. Zhu, Y. Li, Water-Promoted Hydrogenation of Levulinic Acid to γ-Valerolactone on Supported Ruthenium Catalyst, ChemCatChem. 7 (2015) 508–512.

[178] A. Primo, P. Concepción, A. Corma, Synergy between the metal nanoparticles and the support for the hydrogenation of functionalized carboxylic acids to diols on Ru/TiO2, Chem. Commun. 47 (2011) 3613.

179] M.S. Tiwari, G.D. Yadav, F.T.T. Ng, Selective hydrogenation of 3,4-dimethoxybenzophenone in liquid phase over Pd/C catalyst in a slurry reactor, Can. J. Chem. Eng. 92 (2014) 2157–2165.

[180] D. Barthomuf, Basic Zeolites: Characterization and Uses in Adsorption and Catalysis, Catal. Rev. 38 (1996) 521–612.

[181] Y. Ono, Selective reactions over solid base catalysts, Catal. Today. 38 (1997) 321–337.

[182] R. Bal, K. Chaudhari, S. Sivasanker, Vapour phase O-methylation of 2-naphthol over the solid bases alkali-loaded silica and Cs-loaded MCM-41, Catal. Letters. 70 (2000) 75–78.

[183] P. Tundo, M. Selva, The Chemistry of Dimethyl Carbonate, Acc. Chem. Res. 35 (2002) 706–716.

[184] J.-P. Rieu, A. Boucherle, H. Cousse, G. Mouzin, Tetrahedron report number 205, Tetrahedron. 42 (1986) 4095–4131.

[185] A. Bomben, C. A. Marques, M. Selva, P. Tundo, A new synthesis of 2-aryloxypropionic acids derivatives via selective mono-c-methylation of methyl aryloxyacetates and aryloxyacetonitriles with dimethyl carbonate, Tetrahedron. 51 (1995) 11573–11580.

[186] W.G. Kenyon, E.M. Kaiser, C.R. Hauser, Mono- and Dialkylation of Phenylacetonitrile by Means of Sodamide and Sodium Hydride. Alkylation of Diphenylacetonitrile 1a, J.

Org. Chem. 30 (1965) 4135–4138.

[187] Z.L. Shen, X.Z. Jiang, Selective N,N-dimethylation of primary aromatic amines with dimethyl carbonate in the presence of diphenylammonium triflate, J. Mol. Catal. A Chem. 213 (2004) 193–198.

[188] P. Tundo, F. Trotta, G. Moragliob, Selective and continuous-flow mono-methylation of arylacetonitriles with dimethyl carbonate under gas-liquid phase-transfer catalysis conditions, J. Chem. Soc. Perkin Trans. 1. (1989) 1070.

[189] P. Tundo, G. Moraglio, F. Trotta, Gas-liquid phase-transfer catalysis: a new continuous-flow method in organic synthesis, Ind. Eng. Chem. Res. 28 (1989) 881–890.

[190] M. Selva, C.A. Marques, P. Tundo, Selective mono-methylation of arylacetonitriles and methyl arylacetates by dimethyl carbonate, J. Chem. Soc. Perkin Trans. 1. (1994) 1323.

[191] Z. Fu, Selective α-Monomethylation of Phenylacetonitrile with Dimethyl Carbonate or Methanol over Alkali-Exchanged Faujasites, J. Catal. 145 (1994) 166–170.

[192] C. Venkatesan, M. Chidambaram, A.P. Singh, 3-Aminopropyltriethoxysilyl functionalized Na-Al-MCM-41 solid base catalyst for selective preparation of 2-phenylpropionitrile from phenylacetonitrile, Appl. Catal. A Gen. 292 (2005) 344–353.

[193] K. Motokura, D. Nishimura, K. Mori, T. Mizugaki, K. Ebitani, K. Kaneda, A Ruthenium-Grafted Hydrotalcite as a Multifunctional Catalyst for Direct α-Alkylation of Nitriles with Primary Alcohols, J. Am. Chem. Soc. 126 (2004) 5662–5663.

[194] Y. Wang, J. Hua Zhu, W. Yu Huang, Synthesis and characterization of potassium-modified alumina superbases, Phys. Chem. Chem. Phys. 3 (2001) 2537–2543.

[195] H. Tsuji, H. Kabashima, H. Kita, H. Hattori, Thermal activation of KF/alumina catalyst for double bond isomerization and Michael addition, React. Kinet. Catal. Lett. 56 (1995) 363–369.

[196] K.B. Rasal, G.D. Yadav, La-Mg mixed oxide as highly basic water resistant catalyst for utilisation of CO2 in synthesis of quinazoline-2,4(1H,3H)-dione, RSC Adv. (2016).

[197] M. Ogawa, H. Kaiho, Homogeneous Precipitation of Uniform Hydrotalcite Particles, Langmuir. 18 (2002) 4240–4242.

[198] K. Noiroj, P. Intarapong, A. Luengnaruemitchai, S. Jai-In, A comparative study of KOH/Al2O3 and KOH/NaY catalysts for biodiesel production via transesterification from palm oil, Renew. Energy. 34 (2009) 1145–1150.

[199] W. Xie, H. Peng, L. Chen, Transesterification of soybean oil catalyzed by potassium loaded on alumina as a solid-base catalyst, Appl. Catal. A Gen. 300 (2006) 67–74.

[200] V. Díez, Acid–base properties and active site requirements for elimination reactions on

alkali-promoted MgO catalysts, Catal. Today. 63 (2000) 53–62.

[201] V.K. Díez, C.R. Apesteguía, J.I. Di Cosimo, Aldol condensation of citral with acetone on MgO and alkali-promoted MgO catalysts, J. Catal. 240 (2006) 235–244.

[202] M. Di Serio, M. Ledda, M. Cozzolino, G. Minutillo, R. Tesser, E. Santacesaria, Transesterification of Soybean Oil to Biodiesel by Using Heterogeneous Basic Catalysts, Ind. Eng. Chem. Res. 45 (2006) 3009–3014.

[203] M.S. Tiwari, G.D. Yadav, Kinetics of Friedel – Crafts benzoylation of veratrole with benzoic anhydride using Cs 2 . 5 H 0 . 5 PW 12 O 40 / K-10 solid acid catalyst, Chem. Eng. J. 266 (2015) 64–73.

[204] L. Appels, R. Dewil, Biomass valorization to energy and value added chemicals: The future of chemical industry, Resour. Conserv. Recycl. 59 (2012) 1–3.

[205] J.C. Serrano-Ruiz, J. a. Dumesic, Catalytic routes for the conversion of biomass into liquid hydrocarbon transportation fuels, Energy Environ. Sci. 4 (2011) 83–99.

[206] A. Gandini, The irruption of polymers from renewable resources on the scene of macromolecular science and technology, Green Chem. 13 (2011) 1061.

[207] R.G. Kalikar, R.S. Deshpande, S.B. Chandalia, Synthesis of vanillin and 4-hydroxybenzaldehyde by a reaction scheme involving condensation of phenols with glyoxylic acid., J. Chem. Technol. Biotechnol. 36 (1986) 38–46.

[208] F. Zaera, Nanostructured materials for applications in heterogeneous catalysis, Chem. Soc. Rev. 2 (2013) 2746–2762.

[209] E. a. Dikusar, N. a. Zhukovskaya, K.L. Moiseichuk, E.G. Zalesskaya, P. V. Kurman, O.G. Vyglazov, Preparative synthesis of veratraldehyde and citral oxime esters, Russ. J. Appl. Chem. 81 (2008) 643–646.

[210] A.R. Massah, M. Mosharafian, A.R. Momeni, H. Aliyan, H.J. Naghash, M. Adibnejad, Solvent-Free Williamson Synthesis: An Efficient, Simple, and Convenient Method for Chemoselective Etherification of Phenols and Bisphenols, Synth. Commun. 37 (2007) 1807–1815.

[211] R.A.W. Johnstone, M.E. Rose, A rapid, simple, and mild procedure for alkylation of phenols, alcohols, amides and acids, Tetrahedron. 35 (1979) 2169–2173.

[212] A. Leggio, A. Liguori, A. Napoli, C. Siciliano, G. Sindona, Site selectivity in the synthesis of O-methylated hydroxamic acids with diazomethane, J. Org. Chem. 66 (2001) 2246–2250.

[213] F. Rajabi, M.R. Saidi, Microwave-Assisted Methylation of Carboxylic Acids and Phenolic Compounds with Dimethyl-Carbonate Under Solvent-Free Condition, Synth.

Commun. 34 (2004) 4179–4188.

[214] K. Wilberg, K. Saegebarth, Notes- An O 18 Tracer Study of the Acid-Catalyzed Formation of Enol Ethers, J. Org. Chem. 25 (1960) 832–833.

[215] F. Aricò, P. Tundo, Dimethyl carbonate as a modern green reagent and solvent, Russ. Chem. Rev. 79 (2010) 479–489.

[216] W. Shieh, S. Dell, O. Repic, and Microwave-Accelerated Green Chemistry in Methylation of Phenols , Indoles , and Benzimidazoles with Dimethyl Carbonate, (2001) 2000–2002.

[217] X. Jiang, A. Tiwari, M. Thompson, Z. Chen, T.P. Cleary, T.B.K. Lee, A Practical Method for *N* -Methylation of Indoles Using Dimethyl Carbonate, Org. Process Res. Dev. 5 (2001) 604–608.

[218] M. Selva, P. Tundo, A. Perosa, Reaction of Functionalized Anilines with Dimethyl Carbonate over NaY Faujasite. 3. Chemoselectivity toward Mono- N -methylation, J. Org. Chem. 68 (2003) 7374–7378.

[219] M. Selva, C.A. Marques, P. Tundo, Selective mono-methylation of arylacetonitriles and methyl arylacetates by dimethyl carbonate, J. Chem. Soc. Perkin Trans. 1. 1 (1994) 1323.

[220] W.C. Shieh, S. Dell, A. Bach, O. Repič, T.J. Blacklock, Dual nucleophilic catalysis with DABCO for the N-methylation of indoles, J. Org. Chem. 68 (2003) 1954–1957.

[221] P. Tundo, L. Rossi, A. Loris, Dimethyl carbonate as an ambident electrophile, J. Org. Chem. 70 (2005) 2219–2224.

[222] M. Selva, A. Perosa, M. Fabris, Sequential coupling of the transesterification of cyclic carbonates with the selective N-methylation of anilines catalysed by faujasites, Green Chem. 10 (2008) 1068.

[223] M.Y. Lui, A.K.L. Yuen, A.F. Masters, T. Maschmeyer, Masked *N* -Heterocyclic Carbene-Catalyzed Alkylation of Phenols with Organic Carbonates, ChemSusChem. 9 (2016) 2312–2316.

[224] M.A. Ogliaruso, J.F. Wolfe, S. Patai, Z. Rappoport, Synthesis of Carboxylic Acids, Esters and Their Derivatives (1991), John Wiley & Sons, Inc., Chichester, UK, 1991.

[225] H. Shi, W. Zhu, H. Li, H. Liu, M. Zhang, Y. Yan, Z. Wang, Microwave-accelerated esterification of salicylic acid using Brönsted acidic ionic liquids as catalysts, Catal. Commun. 11 (2010) 588–591.

[226] M. Bejblová, D. Procházková, J. Čejka, Acylation reactions over zeolites and mesoporous catalysts, ChemSusChem. 2 (2009) 486–499.

[227] M.A. Harmer, W.E. Farneth, Q. Sun, High surface area nafion resin/silica nanocomposites: A new class of solid acid catalyst, J. Am. Chem. Soc. 118 (1996) 7708–7715.

[228] W.F. Hoelderich, Nafion resin – silica nano- composite solid acid catalysts . Microstructure – processing – property correlations, Green Chem. (2000) 7–14.

[229] G. Yadav, Cesium-substituted dodecatungstophosphoric acid on K-10 clay for benzoylation of anisole with benzoyl chloride, J. Catal. 217 (2003) 88–99.

[230] B.M. Reddy, M.K. Patil, K.N. Rao, G.K. Reddy, An easy-to-use heterogeneous promoted zirconia catalyst for Knoevenagel condensation in liquid phase under solvent-free conditions, J. Mol. Catal. A Chem. 258 (2006) 302–307.

[231] G.D. Yadav, A.D. Murkute, Preparation of a novel catalyst UDCaT-5: Enhancement in activity of acid-treated zirconia - Effect of treatment with chlorosulfonic acid vis-??-vis sulfuric acid, J. Catal. 224 (2004) 218–223.

[232] K. Kaur, R.K. Wanchoo, A.P. Toor, Sulfated iron oxide: A proficient catalyst for esterification of butanoic acid with glycerol, Ind. Eng. Chem. Res. 54 (2015) 3285–3292.

[233] S.R. Kirumakki, N. Nagaraju, K.V.R. Chary, S. Narayanan, Kinetics of esterification of aromatic carboxylic acids over zeolites Hβ and HZSM5 using dimethyl carbonate, Appl. Catal. A Gen. 248 (2003) 161–167.

[234] S.E. Sen, S.M. Smith, K.A. Sullivan, Organic transformations using zeolites and zeotype materials, Tetrahedron. 55 (1999) 12657–12698.

[235] Y. Ono, Catalysis in the production and reactions of dimethyl carbonate, an environmentally benign building block, Appl. Catal. A Gen. 155 (1997) 133–166.

[236] K. Sreekumar, T.M. Jyothi, T. Mathew, M.B. Talawar, S. Sugunan, B.S. Rao, Selective N-methylation of aniline with dimethyl carbonate over Zn(1-x)Co(x)Fe2O4 (x = 0, 0.2, 0.5, 0.8 and 1.0) type systems, J. Mol. Catal. A Chem. 159 (2000) 327–334.

[237] S.R. Kirumakki, N. Nagaraju, K. V. Murthy, S. Narayanan, Esterification of salicylic acid over zeolites using dimethyl carbonate, Appl. Catal. A Gen. 226 (2002) 175–182.

[238] Y. Zheng, J. Li, N. Zhao, W. Wei, Y. Sun, One-pot synthesis of mesostructured AlSBA-15-SO3H effective catalysts for the esterification of salicylic acid with dimethyl carbonate, Microporous Mesoporous Mater. 92 (2006) 195–200.

[239] X. Su, J. Li, F. Xiao, W. Wei, Y. Sun, Esterification of Salicylic Acid with Dimethyl Carbonate over Mesoporous Aluminosilicate, Ind. Eng. Chem. Res. 48 (2009) 3685–3691.

[240] M. Zhang, W.S. Zhu, H.M. Li, H. Shi, Y.S. Yan, Z.G. Wang, Esterification of salicylic acid using Ce4+ modified cation-exchange resin as catalyst, J. Chil. Chem. Soc. 57 (2012) 1477–1481.

[241] A.G. Merzhanov, The chemistry of self-propagating high-temperature synthesis, J. Mater. Chem. 14 (2004) 1779–1786.

[242] K.C. Patil, S.T. Aruna, T. Mimani, Combustion synthesis: An update, Curr. Opin. Solid State Mater. Sci. 6 (2002) 507–512.

[243] H. Teterycz, R. Klimkiewicz, M. Łaniecki, The role of Lewis acidic centers in stabilized zirconium dioxide, Appl. Catal. A Gen. 249 (2003) 313–326.

[244] G.D. Yadav, A.D. Murkute, Novel efficient mesoporous solid acid catalyst UDCaT-4: Dehydration of 2-propanol and alkylation of mesitylene, Langmuir. 20 (2004) 11607–11619.

[245] T. Yamaguchi, Application of ZrO2 as a catalyst and a catalyst support, Catal. Today. 20 (1994) 199–217.

[246] B.M. Reddy, M.K. Patil, Organic Syntheses and Transformations Catalyzed by Sulfated Zirconia, Chem. Rev. 109 (2009) 2185–2208. doi:10.1021/cr900008m.

[247] K. Arata, Organic syntheses catalyzed by superacidic metal oxides: sulfated zirconia and related compounds, Green Chem. 11 (2009) 1719–1728.

[248] A.S. Khder, E.A. El-Sharkawy, S.A. El-Hakam, A.I. Ahmed, Surface characterization and catalytic activity of sulfated tin oxide catalyst, Catal. Commun. 9 (2008) 769–777.

[249] B. Tyagi, M.K. Mishra, R.V. Jasra, Solvent free synthesis of acetyl salicylic acid over nano-crystalline sulfated zirconia solid acid catalyst, J. Mol. Catal. A Chem. 317 (2010) 41–45.

[250] A. Sinhamahapatra, N. Sutradhar, M. Ghosh, H.C. Bajaj, A.B. Panda, Mesoporous sulfated zirconia mediated acetalization reactions, Appl. Catal. A Gen. 402 (2011) 87–93.

[251] M.K. Mishra, B. Tyagi, R. V Jasra, Effect of Synthetic Parameters on Structural, Textural, and Catalytic Properties of Nanocrystalline Sulfated Zirconia Prepared by Sol-Gel Technique, Ind. Eng. Chem. Res. 42 (2003) 5727–5736.

[252] F. Chen, S. Yu, X. Dong, S. Zhang, Environmentally friendly efficient one-pot electrochemical synthesis of 2,4-dimethylanisole by selective oxidation of m-xylene in methanol with metals promoted sulfated zirconia, Ind. Eng. Chem. Res. 50 (2011) 13650–13654.

[253] B.S. Klose-Schubert, R.E. Jentoft, F.C. Jentoft, The Balance Between Reactivity and

Stability of Modified Oxide Surfaces Illustrated by the Behavior of Sulfated Zirconia Catalysts, Top. Catal. 54 (2011) 398–414.

[254] G.D. Yadav, B.A. Gawade, Novelties of combustion synthesized and functionalized solid superacid catalysts in selective isomerization of styrene oxide to 2-phenyl acetaldehyde, Catal. Today. 207 (2013) 145–152.

[255] S. Samantaray, B.G. Mishra, Combustion synthesis, characterization and catalytic application of MoO3-ZrO2 nanocomposite oxide towards one pot synthesis of octahydroquinazolinones, J. Mol. Catal. A Chem. 339 (2011) 92–98.

[256] Y.-Y. Huang, T.J. McCarthy, W.M.H. Sachtler, Preparation and catalytic testing of mesoporous sulfated zirconium dioxide with partially tetragonal wall structure, Appl. Catal. A Gen. 148 (1996) 135–154.

[257] K. Arata, H. Nakamura, M. Shouji, Friedel–Crafts acylation of toluene catalyzed by solid superacids, Appl. Catal. A Gen. 197 (2000) 213–219.

[258] P. Salas, J.G. Hernández, J.A. Montoya, J. Navarrete, J. Salmones, I. Schifter, J. Morales, Effect of tin content on silica mixed oxides: Sulfated and unsulfated catalysts, J. Mol. Catal. A Chem. 123 (1997) 149–154.

[259] T. Yamaguchi, T. Jin, K. Tanabe, Structure of acid sites on sulfur-promoted iron oxide, J. Phys. Chem. 90 (1986) 3148–3152.

[260] A.K. Dalai, R. Sethuraman, S.P.R. Katikaneni, R.O. Idem, Synthesis and characterization of sulfated titania solid acid catalysts, Ind. Eng. Chem. Res. 37 (1998) 3869–3878.

[261] S. Samantaray, P. Kar, G. Hota, B.G. Mishra, Sulfate Grafted Iron Stabilized Zirconia Nanoparticles as Efficient Heterogenous Catalysts for Solvent-Free Synthesis of Xanthenediones under Microwave Irradiation, Ind. Eng. Chem. Res. 52 (2013) 5862–5870.

[262] G.D. Yadav, A.R. Yadav, Selective liquid phase oxidation of secondary alcohols into ketones by tert-butyl hydroperoxide on nano-fibrous Ag-OMS-2 catalyst, J. Mol. Catal. A Chem. 380 (2013) 70–77.

Synopsis Summary

Name of student	Jayaram Narasimha Molleti
Basic qualification	M.Sc. (Organic Chemistry)
Previous institute/college	Vaggdevi PG college
Previous university	Kakatiya University
Name of degree	Ph.D. (Sci.) - Chemistry
Department/Centre	Department of Chemical Engineering
Name Of Guide	Prof. Ganapati D Yadav
Guide ORCHID ID	0000-0002-8603-3959
Department/Center	Department of Chemical Engineering
Name of co-guide (if any)	
Co-Guide ORCHID ID	
Co-Guide Department/Center	
Student ORCID ID	0000-0003-2534-9957
Registration No	11 CHY 4011
Date of registration	Sep 19, 2011
Title of thesis at the time of registration	Design and synthesis of safer chemicals by benign green routes
Title of thesis (Revised and final)	Design and synthesis of safer chemicals by benign green routes
Classification	Heterogeneous catalysis, Sustainability, Green Chemistry
Keywords	Esterification, Catalyst support, Kinetics, o-methylation, Hydrotalcite, Fine chemicals

INSTITUTE OF CHEMICAL TECHNOLOGY

(University under Section -3 of the UGC Act 1956)

Maharashtra Govt's Elite Status and Centre of Excellence Matunga, Mumbai – 400019

Design and synthesis of safer chemicals by benign green routes

A SYNOPSIS OF THE THESIS TO BE SUBMITTED TO

THE INSTITUTE OF CHEMICAL TECHNOLOGY

FOR THE DEGREE OF

Ph.D. (Sci.) - Chemistry

Submitted by

Jayaram Narasimha Molleti

Under Supervision of

Prof. Ganapati D Yadav

Department of Chemical Engineering

Introduction:

Catalysis is an important interdisciplinary scientific and technological area for the development of environmentally benign chemical processes. Homogeneous catalysis is conventionally used in the chemical and fine chemicals manufacturing. Homogeneous catalysts are very selective and comparatively cheaper. But the drawbacks associated with them such as product contamination and product separation make them unappealing. Also a very few reactor configurations are available with homogeneous catalysis as compared to heterogeneous catalysis. Homogeneous catalysts are used in stiochiometric quantities at times difficult to handle, corrosive in nature, which increase the capital and processing cost and decrease the process equipment life. There is no control on the reaction, byproduct formation; also reusability and regeneration of catalyst are major concerns. It decreases the process efficacy. The effluent stream containing harmful acids and heavy metals make post processing difficult, cumbersome and costly. A possible answer is immobilization of the catalytic material and efforts are being taken to heterogenize the homogeneous catalysts [1, 2].

One of the most important challenges facing chemists and engineers is the successful development of new products, materials and chemical processes that satisfy the social and economic requirements of the world's ever-increasing population. The recent heightened awareness of environmental impacts associated with many established chemical processes has led to considerable pressures on chemical industry, both legislative and consumer driven, to adopt a cleaner and greener approach. Thus Green Chemistry has become a thrust area of research due to economic benefits, societal obligation and environmental crisis. The aim of Green Chemistry is waste minimization by reducing hazardous products and/or processes and increasing selectivity towards the desired product thus reducing energy consumption associated with the separation of byproducts [3].

In recent years, classical organic transformations using solid acid-base catalysts continue to attract considerable attention in both industrial and academic laboratories because of the potential of such technology to simplify processing and improving the economics of such reactions, thus converting them into green processes [4].

Objectives:

Owing to the growing importance of heterogeneous catalysts in organic synthesis, it was thought worthwhile to study synthesize various heterogeneous catalysts and their suitable applications in fine chemical and intermediates synthesis. Therefore, the synthesis and

characterization of catalysts, both reported and new, was considered to be an area of immense potential.

Thus, a general theme with the following specific objectives was planned, under the aegis of the current work.

1) Selectivity engineering in hydroxyalkoxylation of phenol by ethylene carbonate using calcined hydrotalcite [5].
2) Novel synthesis of Ru supported on OMS by solvent-free method as a catalyst for selective hydrogenation of levulinic acid to -valerolactone in aqueous medium and kinetic modelling.
3) Potassium modified La-Mg mixed oxide as active and selective catalyst for mono-methylation of phenylacetonitrile with dimethyl carbonate [6].
4) Green synthesis of veratraldehyde using novel potassium promoted lanthanum-magnesium mixed oxide catalyst [7].
5) Solvent-free synthesis of methyl salicylate using combustion synthesized novel sulfated iron-zirconia catalyst.

Materials and Methods:

All reactions were carried out in a 100 mL autoclave (Amar Equipments, Mumbai). Phenol, ethylene carbonate, levulinic acid, phenyl acetonitrile, vanillin, salicylic acid, dimethyl carbonate, tetrahydrofuran, magnesium nitrate hexahydrate, aluminium nitrate nonahydrate, sodium hydroxide, lanthanum nitrate, urea, ruthenium chloride were purchased from Thomas Baker, S. D. Fine chem. Ltd., Hi Media Chem. Ltd. and Aldrich. GC yields were obtained using capillary column BPX-50 (0.25 mm diameter and 30 m length), BP-1 (length 30 m and inner diameter 0.32 mm) and FID detector. All products were confirmed by GC-MS (Perkin Elmer, Clarus 500 with Elite-1 capillary column).

Result and Discussion:

1. Selectivity engineering in hydroxyalkoxylation of phenol by ethylene carbonate using calcined hydrotalcite

Phenoxyethanol is a typical organic solvent extensively used in solvents and personal care products such as soaps and detergents, fragrance, cosmetics, toiletries and antiseptic, preservatives and, pharmaceuticals. A green, efficient and selective process for the synthesis of mono-ethylene phenyl glycol ether (MEPGE) by hydroxyalkoxylation of phenol with

ethylene carbonate. Different catalysts such as Al_2O_3, MgO, CHT/HMS, CHT (1:1), CHT (2:1), CHT (3:1), CHT (4:1) and CHT (5:1) were prepared out of CHT (3:1) was active and reusable. It possesses high catalytic activity for the hydroxyalkoxylation of phenol with 96 % conversion at 180 °C in 2 h with a catalyst loading of 0.03 g/cm^3. The apparent energy of activation for the reaction is 21.3 kcal/mol (Scheme 1).

2. Novel synthesis of Ru supported on OMS by solvent-free method as a catalyst for selective hydrogenation of levulinic acid to -valerolactone in aqueous medium and kinetic modelling

Gamma -valerolactone (GVL) is an important biomass-derived molecule for the sustainable production of value-added chemicals and fuels. Ruthenium supported on manganese oxide octahedral molecular sieve (K-OMS-2) were prepared as catalysts for the aqueous phase hydrogenation of biomass-derived levulinic acid (LA) to GVL using molecular hydrogen. Three different methods i.e. reflux (R), hydrothermal (H) and solvent less (S) were used for preparation of OMS-2. Among which solventless synthesized OMS (OMS-2S) is energy efficient, rapid and economical way of synthesis. Among three different catalyst, Ru supported on solventless OMS-2 i.e.1 wt% Ru/OMS-2_S catalyst showed LA conversion of 99.9% and selectivity of 100 % towards GVL at mild conditions (100º C, 30 atm H_2). Moreover, 1 wt % Ru/OMS-2_S catalyst is very stable and reusable up to five times without significant loss of activity. Effects of various parameters were studied systematically and a kinetic model was developed using LHHW type of mechanism. The apparent activation energy of hydrogenation of LA to GVL was 11.75 kcal/mol (Scheme 2).

3. Potassium modified La-Mg mixed oxide as active and selective for mono-methylation of phenylacetonitrile with dimethyl carbonate

Selective mono-methylation of phenyl acetonitrile to 2-phenylpropionitrile by dimethyl carbonate as an alkylating agent was studied for the first time using hydrothermally prepared 2 wt % K/ La_2O_3-MgO as a catalyst. The monomethylation of phenyl acetonitrile is a very important step for the synthesis of the aryl acetic acid moieties, using drugs, natural products. etc. Different loadings of potassium (1 %, 2 %, 3 % and 4 % wt) promoted on La_2O_3-MgO catalysts were synthesized, characterized with various techniques and screened. In which 2 wt % K/ La_2O_3-MgO catalyst possesses high catalytic activity for the alkylation of phenylacetonitrile with 100% conversion at 150 °C in 2 h with a catalyst loading of 0.03 g/cm^3. Effects of various parameters were studied using 2 % K/ La_2O_3-MgO catalyst to establish

mechanism and kinetics. The apparent activation for methylation of phenylacetonitrile to 2-phenyl propionitrile was found to be 13.77 kcal/mol. The catalyst was reusable up to three runs without appreciable loss in its activity (Scheme 3).

4. Green synthesis of veratraldehyde using novel potassium promoted lanthanum-magnesium mixed oxide catalyst

O-Methylation of vanillin is a very important step for the synthesis of veratraldehyde which is widely used as a flavorant and odorant. Potassium promoted lanthanum-magnesium mixed oxide catalysts were prepared with different K loadings (1 %, 2 %, 3% and 4 % wt). In which 2 % K/ La_2O_3-MgO possesses high catalytic activity for the alkylation of vanillin with 100 % conversion at 160 °C in 2 h with a catalyst loading of 0.03 g/cm^3. Effects of various parameters were studied using 2 % K/ La_2O_3-MgO to establish mechanism and kinetics. The apparent activation for O-methylation of vanillin to veratraldehyde was 13.56 kcal/mol. The catalyst was reusable up to three runs without appreciable loss in its activity (Scheme 4).

5. Solvent-free synthesis of methyl salicylate using combustion synthesized novel sulfated iron-zirconia catalyst

Methyl esters of salicylic acid are widely used in fine chemicals, drugs, food preservatives, pharmaceuticals, solvents, perfumes, cosmetics, and chiral auxiliaries. The catalyst with different loadings of Fe_2O_3 on zirconia (5, 10, 15, 20 wt %) was synthesized and activity of catalyst was compared with the acid catalysts such as ZrO_2, sulfated zirconia for the esterification of salicylic acid with methanol. In which 10 wt % sulfated Fe_2O_3-ZrO_2 (SFZ-10) catalyst possesses high catalytic activity for the etherification of salicylic acid with 95 % conversion at 120 °C in 2 h with a catalyst loading of 0.03 g/cm^3. The catalyst was reusable up to three runs without appreciable loss in its activity. LHHW mechanism was used to find that all species are weakly adsorbed. The reaction is intrinsically kinetically controlled and follows zero order kinetics. The apparent energy of activation for the reaction is 13.8 kcal/mol (Scheme 5).

Conclusion:

This work dealt with the synthesis, characterization and application of novel catalysts. For the synthesis phenoxyethanol from phenol and ethylene carbonate, CHT (3:1) catalyst was found to highly active and robust. GVL was synthesized by the hydrogenation of LA using 1 wt %

Ru/ OMS-2_S. Selective monomethylation of phenylacetonitrile was catalyzed by 2 wt % K/ La-Mg mixed oxide. Veratraldehyde was synthesized from vanillin and DMC catalyzed by 2 wt % K/ La-Mg mixed oxide. SFZ-10 was used as a catalyst for esterification of salicylic acid. Detailed mechanistic and kinetic aspects have been discussed in all cases.

References:

1. G.D. Yadav, M.S. Krishnan, Etherification of 2-Naphthol with Alkanols Using Modified Clays and Sulfated Zirconia, Ind. Eng. Chem. Res. 37 (1998) 3358-3365.
2. S.R. Kirumakki, N. Nagaraju, K.V.R. Chary, S. Narayanan, A facile O-alkylation of 2-naphthol over zeolites Hbeta, HY, and HZSM5 using dimethyl carbonate and methanol, J. Catal. 221 (2004) 549559.
3. R.A. Sheldon, Atom efficiency and catalysis in organic synthesis, Pure Appl. Chem. 72 (2000)1233-1246.
4. A.Corma, From Microporous to Mesoporous Molecular Sieve Materials and Their Use in Catalysis, Chem. Rev. 97 (1997) 2373-2419.
5. J. Molleti, G.D. Yadav, Selectivity engineering in hydroxyalkoxylation of phenol by ethylene carbonate using calcined hydrotalcite, Clean Technol. Environ. Policy. 19 (2017) 1413-1422.
6. J. Molleti, G.D. Yadav, Potassium modified La-Mg mixed oxide as active and selective catalyst for mono-methylation of phenylacetonitrile with dimethyl carbonate, Mol. Catal. 438 (2017) 66-75.
7. J. Molleti, G.D. Yadav, Green Synthesis of Veratraldehyde Using Potassium Promoted Lanthanum-Magnesium Mixed Oxide Catalyst, Org. Process Res. Dev.21 (2017) 1012-1020.

Schemes/Figures/Schematics:

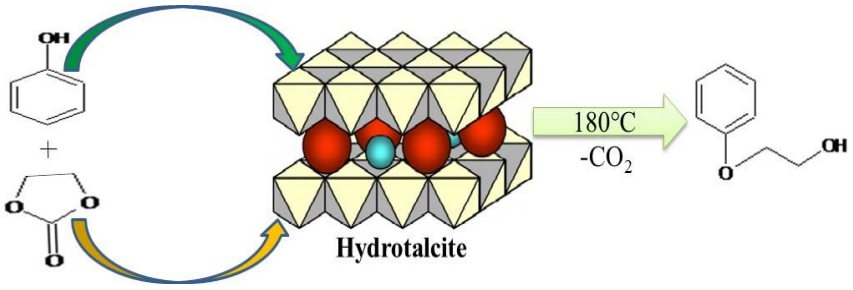

Scheme 1: Hydroxyalkoxylation of phenol by ethylene carbonate

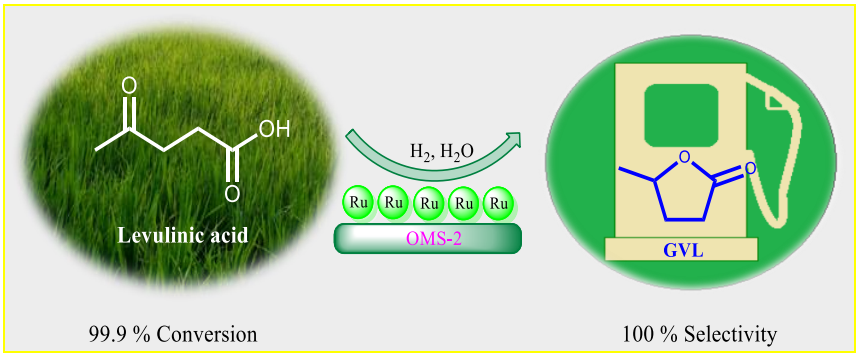

Scheme 2: Hydrogenation of Levulinic acid

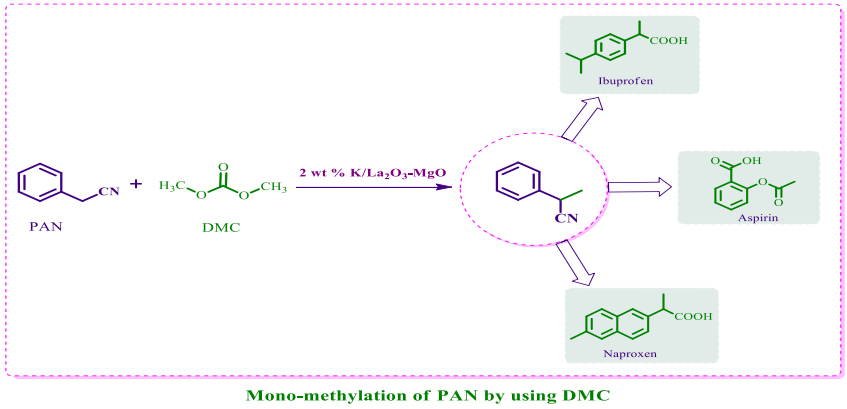

Scheme 3: Mono-methylation of Phenyl acetonitrile

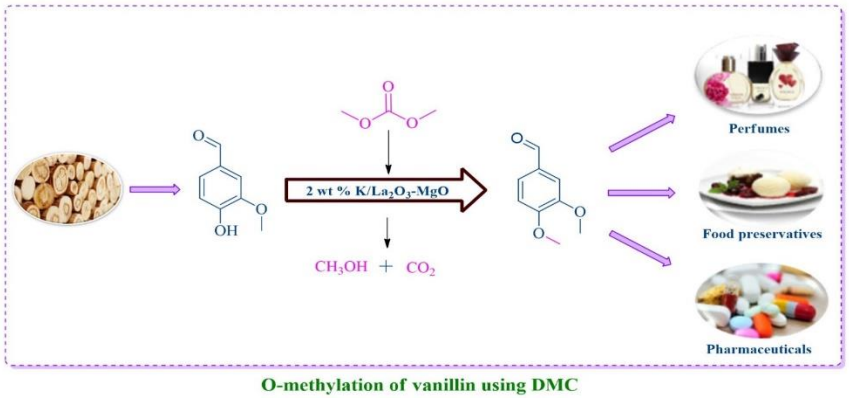

Scheme 4: O-methylation of Vanillin

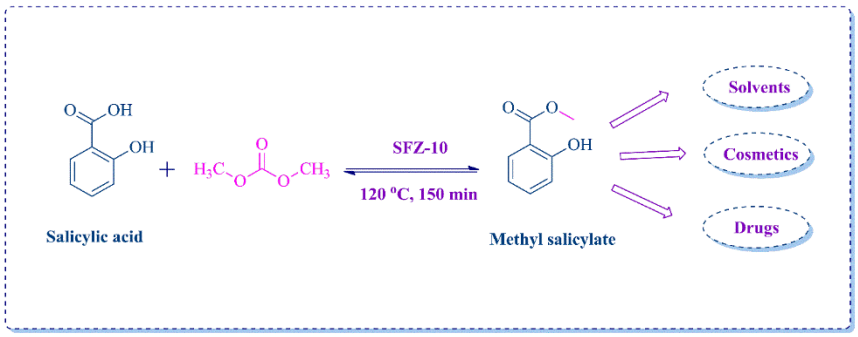

Esterification of salicylic acid

Scheme 5: Esterification of salicylic acid Tables:

List of Publications

The research papers published based on work presented in this thesis:

1. J. Molleti, G.D. Yadav, Selectivity engineering in hydroxyalkoxylation of phenol by ethylene carbonate using calcined hydrotalcite, Clean Technol. Environ. Policy. 19 (2017) 1413–1422.

2. J. Molleti, G.D. Yadav, Potassium modified La-Mg mixed oxide as active and selective catalyst for mono-methylation of phenylacetonitrile with dimethyl carbonate, Mol. Catal. 438 (2017) 66–75.

3. J. Molleti, G.D. Yadav, Green Synthesis of Veratraldehyde Using Potassium Promoted Lanthanum–Magnesium Mixed Oxide Catalyst, Org. Process Res. Dev. 21 (2017) 1012-1020.